Preface

"Static yield stress measurements on SCC, mortar and matrix" by M.Wirthova, K deWeerdt and S.Jacobsen

Summary

The static yield stress of fresh self-compacting concrete is a sensitive parameter both in terms of materials composition, ageing and measurement. We investigated its time dependency under different stress conditions in a slowly rotating ConTech4 viscometer. First we developed a measurement technique filtrating out inaccuracies in the BML ConTech4 rotation during the very slow rotation by analysis of the data logged in National Instruments lab View. Then we analyzed the difference in time dependent static yield stress in 5 different self-compacting mortars with a test cycle involving both static yield measurements starting from unconfined state as well as measurements in a confined state due to a residual stress after stop of the slow rotation. The confined yield stress increases with the same rate of change as the unconfined, though with an upwards parallel displacement due to the increased static yield stress under confined conditions. However, after removal of load and then applying new confinement the linear trend of increase of yield stress as function of time were independent of release/confinement repetition and the two lines (unconfined and confined) were parallel. We also observed increase of static shear moduli that gave useful quantification of the structural build up; also with a highly linear rate of change with time. Finally we investigated the static yield stress of the filler modified paste portion of the mortar in a Physica Paar parallel plate rheometer. First we observe the usual improved sensitivity of the static yield at very low increase of strain rate from zero giving exponential increase of time dependant stress (gel strength test) compared to static yield in the constant strain rate test. A very clear linear time dependant increase of shear modulus was found as for the mortar, though with much lower absolute values.

The rate of change of static yield stress of SCC and mortar varied in the range $0.014 - 0.25$ Pa/s in unconfined tests during the first 2,5 hours. This is a large range of variation (and then the very high results for S3 in ConTech have been exluded). In confined tests it is $0.2 - 0.41$ P/s. The only values at t = 0 are by linear regression and extrapolation, often giving values less than zero indicating some kind of non-linearity at early age although the increase after app 30 minutes seems linear both for unconfined an confined tests. The test principles in the four tests were: coaxial viscometer for mortar, static plate with continuous development, inclined plane and parallel plate for paste or matrix. The differences between the measurements, briefly, concern both the type of materials that can be used (SCC vs matrix) and the test principles and stress conditions during testing. Our materials were mortar with w/b ≈ 0.50, 40 volume % matrix and 8 mm maximum aggregate size, as well as matrix with similar composition as in the mortar. Apparently $\tau_{0,s}$ is very sensitive to both test method and how it is calculated. The confinement conditions in the coaxial viscometer seem to give higher values than in the plate- and inclined plane tests. From the summary table in section 4.3 it is seen that thixotropic structuration rate can vary by more than a factor of 10 x for one concrete depending on how it is measured and calculated. Based on this limited experience it is hard to give a definite answer but the confinement in the ConTech viscometer is possibly a good thing for simulation of concrete confined in a narrow tall wall. This is the geometry where yield stress build-up is of interest for formwork pressure. The inclined plane showed some weaknesses with larger aggregate particles loosening from the surface but might relate to aggregate segregation. The plate test also has its weaknesses with small roughness on the surface and should perhaps have been exchanged for geometry with vanes of some kind normal to the plate to get similar "grip" as the vanes of the viscometer. At present it is hard to use these experiences to recommend any of these tests. It should be mentioned that we were not able to get a sensitive vane-tool and we should like to include that in a later study. Clearly more work is needed to obtain a test. Possibly different tests are needed for yield stress for different purposes: related to formwork pressure, to casting joints and to stability of aggregate particle sinking. Therefore the main result of this report is not a recommendation of a test method but investigation of different measurement techniques. Observations of difficulties in static yield stress measurements and discussion of the magnitudes of these variations in various types of measurements will hopefully lead to more knowledge in this field.

Table of contents

1   Introduction

1.1   Principal objectives and scope

Measurements of static yield stress have received increased attention over the last years due to the important effect of this parameter on basic properties of fresh concrete, particularly Self compacting Concrete (SCC). Particularly formwork pressure, the ability of the concrete to start flowing under its own weight, seamless casting layers and its stability against segregation are affected by static yield stress. Static yield stress time dependency also describes the structural build-up and thixotropy of the concrete and thus is a fundamental property of fresh concrete.

This study was done during the Erasmus visit of PhD student Michaela Wirthova, BRNO University of Technology (BUT) at NTNU Department of Structural Engineering as part of her training on rheology of Self Compacting Concrete. Later, a return trip to Norway was made for COIN. The goal was to investigate static yield stress and its time dependancy with equipment available at the concrete laboratories at NTNU to establish measurement procedures in our laboratories for static yield stress and to explore its time dependency as well as sensitivity to test method Four different measurement methods for observing the static yield stress of fresh concrete, mortar and matrix were thus investigated as function of time to proceed in developing reliable static yield stress measurements and understanding its time dependancy.

First we made static yield stress measurements on self-compacting mortar with the ConTec 4 viscometer [1] Wallevik, Billberg [2] under various conditions. Here we attempted to detect the yield stress at slow rotation of the viscometer to capture the static yield stress and also to capture the stress-strain curve of the fresh concrete, also detecting thixotropic structure build-up rate. On this mortar we also performed some measurement with a more recent technique; the plate test developed in France by Amziane et al [3], a test originally intended for paste. Then we used the Physica parallel plate rheometer on matrix with similar composition as the matrix part of the mortar. (Matrix is assumed to consist of all fluid and particles finer than 125 microns as well as air voids and can be considered one of the two phases in the Particle Matrix model [4].) Finally, static yield stress measurements were made in conjunction with a full-scale concrete stability test of three different pumped concrete mixtures. Both the newly developed inclined-plane test [5] was used as well as the slow rotational Contech 4 viscometer for measurement of static yield stress on all 3 mixes.

1.2   Background

1.2.1   SCC

Awareness of self-compacting concrete (SCC) within the construction industry has grown year on year since it was developed in Japan in the late 1980s [6], and the quest for further understanding as to its capabilities and limitations has generated considerable interest in research worldwide.

SCC also known as self-consolidating concrete is a highly flowable concrete that can spread into place under its own weight and achieve good consolidation in the absence of vibration without exhibiting defects due to segregation and bleeding [7].

Feature/benefit analysis on the use of SCC would suggests that the following benefits should result [8]:
- increased productivity levels leading to shortened concrete construction time
- lower concrete construction costs
- improved working environment
- improvement in environmental loadings
- improved in-situ concrete quality in difficult casting conditions
- improved surface quality

Self-compacting concrete was developed to achieve durable concrete structures. The method for achieving self-compactibility involves not only high deformability of paste or mortar, but also

resistance to segregation between coarse aggregate and mortar when the concrete flows through the confined zone of reinforcing bars [9].

According to The European Guidelines for Self-Compacting Concrete the SCC [10] is classified (via properties of fresh SCC- slump flow, T500,...) into the following groups (Table 1 and Table 2). Slump-flow value describes the flowability of a fresh mix in unconfined conditions. It is a sensitive test that will normally be specified for all SCC, as the primary check that the fresh concrete consistence meets the specification.

The value of slump flow is related to the yield stress of fresh cement based materials [11,12], where the mini-cone was used for testing of fresh paste mixtures derived from SCC and evaluation of workability was done according to the formula:

$$\tau_0 = \frac{225g\rho V_c^2}{4\pi^2 D_f^5} \tag{1},$$

where ρ, g, V_f and D_f are the density, the gravity, the conical volume (in our case is 6 litres) and the final spread diameter respectively. Roussel et al. [12] showed that the model does not allow predicting low yield stresses because of surface effects. This means that small yield stress may be relevantly measured in this way by improving the wetting between the sample and the solid surface. Ideally, with a perfect wetting, infinitely small yield stress might be measured [13].

Table 1: classification of SCC according to [10] slump flow values

	Properties and applications
SF1 (550 - 650 mm)	Unreinforced or slightly reinforced concrete structures that are cast from the top with free displacement from the delivery point (e.g. housing slabs). Casting by a pump injection system (e.g. tunnel linings). Sections that are small enough to prevent long horizontal flow (e.g. piles and some deep foundations).
SF2 (660 - 750 mm)	Suitable for many normal applications (e.g. walls, columns).
SF3 (760 – 850 mm)	Typically produced with a small maximum size of aggregates (less than 16 mm) and is used for vertical applications in very congested structures, structures with complex shapes, or for filling under formwork.

Target values higher than 850 mm may be specified in some special cases but great care should be taken regarding segregation and the maximum size of aggregate should then normally be lower than 12 mm.

Viscosity can be assessed by the T_{500} time during the slump-flow test or assessed by the V-funnel flow time. The time value obtained does not measure the viscosity of SCC but is related to it by describing the rate of flow. Concrete with a low viscosity will have a very quick initial flow and then stop. Concrete with a high viscosity may continue to creep forward over an extended time. Viscosity (low or high) should be specified only in special cases such as those given below. It can be useful during mix development and it may be helpful to measure and record the T_{500} time while doing the slump-flow test as a way of confirming uniformity of the SCC from batch to batch.

Table 2: classification of SCC according to [10] T_{500} values

	Properties and applications
VS1/VF1 (T500 ≤ 2 s)	Good filling ability even with congested reinforcement. Capable of self-levelling. Generally the best surface finish. More likely to suffer from bleeding and segregation.
VS2/VF2 (T500 > 2 s)	No upper class limit but with increasing flow time it is more likely to exhibit thixotropic effects, which may be helpful in limiting the formwork pressure or improving segregation resistance. Negative effects may be experienced regarding surface finish (blow holes) and sensitivity to stoppages or delays between successive lifts.

1.2.2 Rhelogy

Rheology, defined as ,,the study of deformation and flow of matter", provides a measure between shear stress and rate of deformation. Concrete composed of cement particles, aggregates, water and air, can be characterized as suspended solid particles in viscous media. Numerous constitutive equations have been proposed to characterize the rheology of fresh concrete as suspensions, but only the Bingham model (2) and the Herschel-Bulkley model have received wide acceptance [14].

The validity of the Bingham equation has been verified [15] using different types of rheometers (BML, BTRHEOM, CEMAGREF-IMG, IBB, two-point) and different concrete compositions:

$$\tau = \tau_0 + \mu_{pl}\dot{\gamma} \tag{2}$$

Here τ is the shear stress [Pa], τ_0 the yield stress [Pa], μ_{pl} the plastic viscosity [Pa.s] and $\dot{\gamma}$ the shear strain rate. τ_0 and μ_{pl} are referred to as Bingham material properties with the first property providing a measure of shear stress required to initiate flow and the second one a measure of the material resistance to flow after the material begins to flow. These two rheological properties are therefore needed to quantitatively characterize the flow of fresh concrete [16].

In case of self compacting concrete, due to the addition of plasticizer or superplasticizer, it is known that the yield stress is much lower, compared to traditional concrete [17]. In order to maintain the stability of the concrete – to avoid segregation – the yield stress must be high enough, which can be achieved in several ways. It has been shown [18] that stability against particle sinking in concrete at rest is much more sensitive to changes in static yield stress than to changes in plastic viscosity. Due to the low yield stress, deviations from the Bingham model can occur, causing an apparent negative yield stress when using traditional rotational viscometry and resulting in a non-linear relationship between shear stress and shear rate. In Belgium and some surrounding countries, the shear thickening effect has been discussed. It has been claimed that the Bingham model is mostly not applicable in these cases [19]. In some cases such observations could be due to insufficient evaluation of the equilibrium Torque conditions during viscometer measurement [20], something that is not always reported.

Shear thickening is described in the literature as an increase in apparent viscosity with increasing shear rate [21]. Two possible theories are considered to be applicable on SCC. One is based on the formation of clusters and the other is based on grain inertia [22]. Generally in rheology such effects are also related to varying dilatancy as function of rate of shear.

Rheology is the logical tool to characterize and describe the flow behavior, thickening, workability loss, stability and even compactability of fresh cement based particle suspension such as cement paste, mortar and concrete. To apply this tool, one has to be able to evaluate and choose material parameters of importance (e.g. yield stress, plastic viscosity) and to be able to obtain information about them through testing. A great deal of effort has been spent on obtaining accurate and repeatable data on the rheological material parameters. Although the same trend and behavior is generally attained by different types of devices, the absolute value can however differ somewhat [1].

1.2.3 Dynamic and static yield stress

When discussing the rheology of concrete in its fresh state, the dynamic yield stress τ_0 (Pa), is normally referred to as the stress needed to make the concrete flow or, in other words, describing the concrete resistance to flow. However, since the dynamic yield stress is the equilibrium value for a concrete in motion it is probably even better to use this value as the limit of concrete flowability, i.e., the stress needed to stop the flow rather than the concrete resistance to flow. That is why the dynamic yield stress of a SCC in general correlates well to its slump-flow value [23].

Instead, a more correct value of the stress needed to make a concrete flow from a state of rest is static yield value. This is the stress level necessary to exceed in order to break the structure within a concrete at rest and go from elastic via visco-elastic, visco-plastic to plastic behaviour.

So, the dynamic yield stress is of interest when considering flow properties and planning of formwork filling, pumping etc. The static yield stress and how this develops in the concrete at rest, is instead important for issues such as form pressure, time between casting of concrete layers, the time a SCC can be left at rest in a skip before emptying it etc. [23]. As already briefly mentioned, static yield stress is also important for the stability at rest with respect to sinking of aggregate particles.

1.2.4   Thixotropic behavior and structural breakdown

The accepted definition of thixotropy is according to Barnes [21] a gradual decrease of the viscosity under shear stress followed by a gradual recovery of structure when the stress is removed. Additional definitions of thixotropy are given in [24].

The term structural breakdown was made by Tattersal in 1954. Because no recovery in torque was measured in the corresponding experiment, structural breakdown was considered to be a different phenomenon than thixotropic behavior. The mechanism of structural breakdown is attributed to the process of breaking certain linkages between the cement particles, which are assumed to be formed by the hydration process. The breaking of linkages was considered to be an irreversible process and thus non-thixotropic [25].

Thixotropy of cementitious materials is quantified by measuring the thixotropic loop, see Fig. 1. This method is based on the fact, that because of the transient nature of thixotropy and the dependency of specific rheological properties on the flow history, the stress/shear rate curves measured successively in a viscometer during increasing and decreasing sequences of applied shear rates will not superimpose. During the increasing shear rate ramp, de-flocculation occurs but not quickly enough to reach the steady state shear stress. The measured stress is thus always higher than what would be obtained if steady state was reached. On the other hand, during the decreasing shear rate ramp, flocculation occurs but here again not quickly enough for steady state to be reached and the measured stress stays lower than steady state. The area between the two curves is measured and is considered as representative of the work done per unit time and unit volume of the cement material to break some of the initially present linkages. It has to be noted that, in the case of a succession of shear rate steps, the loop appears only if the duration of the applied shear rate step is of course not sufficient for steady state to be reached [26].
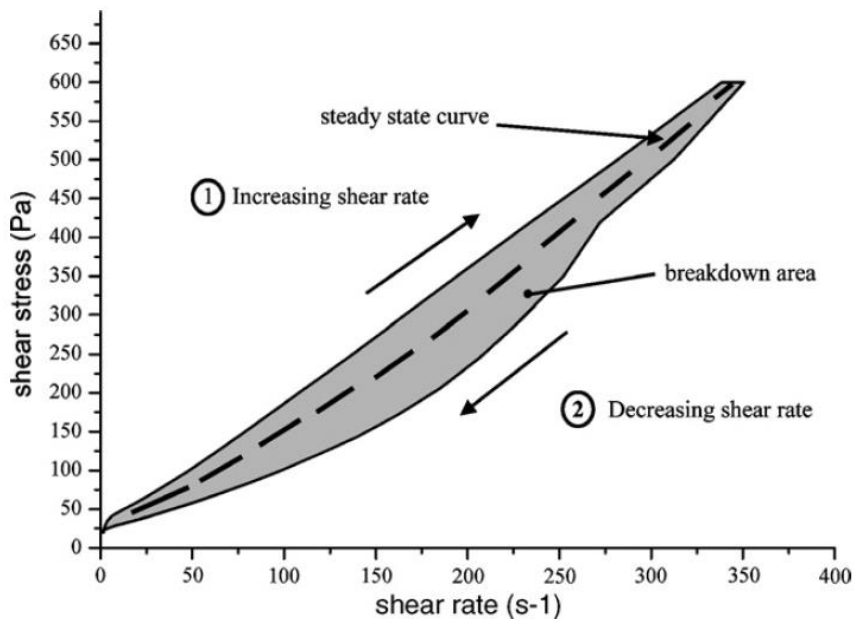

Fig. 1: Example of thixotropic loop obtained with a cement paste submitted successively to increasing and decreasing shear rate ramps [26]

2   Experiments

2.1.1   Mortar for part I (Con Tech and plate test)

Table 3 shows the composition of the mortar that was proportioned with a matrix volume fraction of 40 volume %. The mix design was the same as one of the mixes used in a study of flow conditions during form filling [27].

The materials used are:
- Cement: Norcem Standard FA, which is Portland cement type CEM II/A-V 42.5 R contains up to 20 % fly ash with typical Blaine value 450 m^2/kg
- Sand: Årdal 0/8 (low filler)
- Tau: NorStone Tau (rock type: quartz diorite)
- Superplasticizer (SP): ResconMapei SP-130 - Acrylic polymer with 30% dry solid, splitting type admixture, normal dosage = 0.3-1.2% of cement weight

Detailed information about the part materials (chemical composition, datasheets, sieve curves etc) are given in appendix I. The sand used for mixture I had moisture 2.2 % and for mixture II 1.3 %, adsorbed water is accounted for in water to cement ratio w/c. The volume of the mixtures: 40 litres

Table 3: materials and parameters

Material	Mixture I		Mixture II	
	Weight [kg]	kg/m^3	Weight [kg]	kg/m^3
Norcem Standard FA	17.285	432.1	17.285	432.1
Water	7.644	226.2	7.863	218.8
SP	0.110	2.8	0.110	2.8
Tau filler	2.273	56.8	2.273	56.8
Sand	63.771	1594.3	63.551	1588.8
	Moisture [%]	2.2	Moisture [%]	1.3
w/c	0.52		0.50	
SP [%]	0.6		0.6	

*w/c based on free water included moisture in sand

2.1.1.1   Mixing

The target mix design was the same for the two mixtures. At first the solid materials were mixed 1 minute (dry mix). Then the water and SP were added and mixed for 2 min (wet mix). After 2 min of rest the mixture was re-mixed for 1 min. A 50 litre flat-bottomed, horizontal plane rotating counter-current Eirich paddle mixer was used.

2.1.2   Basic properties of mortar

The rheological properties of fresh mortar were characterized by measurements of slump flow and T500 according to EN 12350-8. Density and air content were determined too regarding EN 12350-6 and EN 12350-7. All tests were done immediately after mixing in time less than 10 min after water addition.

2.1.3   Measurement with BML viscometer – SCC flow curves

The ConTech BML 3 coaxial viscometer used in this work has rotating outer cylinder and stationary inner cylinder measuring the torque. The rheological measurements consist of measuring torque T [Nm] as a function of rotational speed N [rps] and were also made within 10 minutes.

By plotting measured torque T as a function of rotational speed N obtained during the shear history shown in figures 1 and 2 the equation: $T = HN + G$, was obtained from linear regression of the flow curve. The value H is the slope of the line and G is the point of intersection with the ordinate. The equation used for converting H and G values into the dynamic yield stress $\tau_{0dynamic}$ and plastic viscosity

μ_{pl} respectively is known as the Reiner-Rivlin equation (3). These two parameters were calculated using the following equations (3,4) [16,28]:

$$\Omega = \frac{T}{4\pi\mu_{pl}h}\left(\frac{1}{R_i{}^2} - \frac{1}{R_o{}^2}\right) - \frac{\tau_{0dynamic}}{\mu_{pl}}\ln\frac{R_o}{R_i} \tag{3}$$

$$\mu_{pl} = \frac{H\left(\dfrac{1}{R_i^2} - \dfrac{1}{R_o^2}\right)}{4\pi h} \tag{4}$$

$$\tau_{0dynamic} = \frac{G\left(\dfrac{1}{R_i^2} - \dfrac{1}{R_o^2}\right)}{4\pi h \ln\dfrac{R_O}{R_i}} \tag{5}$$

where Ω is angular velocity of the outer cylinder [rad.s^{-1}] R_i is radius of inner cylinder [m], R_o is radius of outer cylinder [m] and h is height of inner cylinder [m]. The following values were used for the calculation of rheological parameters (Table 4):

Table 4: Dimensions of cylinders and height of immersed part of inner cylinder of BML viscometer

	Mixture I	Mixture II
R_i [m]	0.100	0.100
R_o [m]	0.145	0.145
h [m]	0.175	0.180

The shear histories shown in Fig. 2 and Fig. 3 show that equilibrium values were obtained at each rotational velocity. The Bingham regression is done on the equilibrium shear stresses at each deformation rate level on the down curve. From this technique dynamic, or Bingham, yield stress and plastic viscosity of the mixture at the given time are obtained.
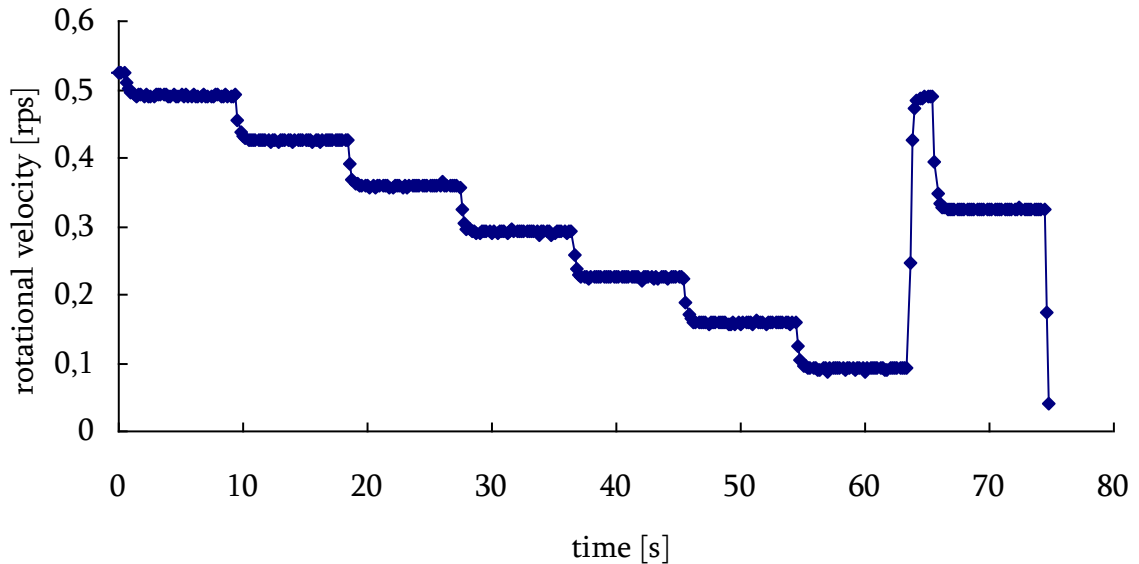

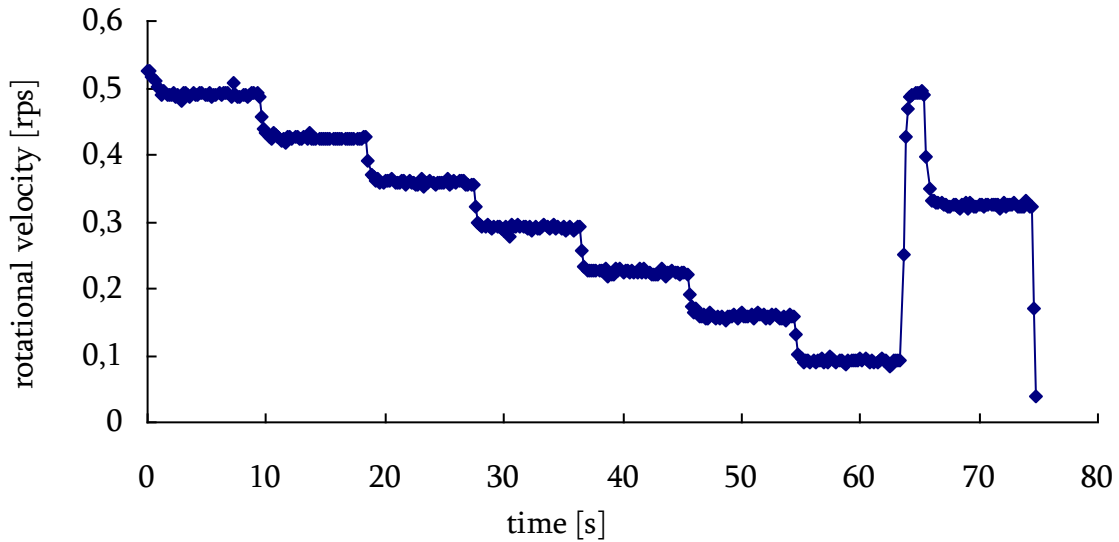Fig. 2: Shear history of measurement with BML viscometer – mixture I

Fig. 3: Shear history of measurement with BML viscometer – mixture II

2.1.4   Static yield stress measurements with ConTec4 viscometer measurements

Rheological measurements with the ConTec4 viscometer were performed in order to measure time development of torque T at very low, constant, rotational speed run in various test sequences. The obtained stress-rotation and then stress-strain curves were recalculated and the time-dependant development of yield stress value and structural build-up was found. Fig. 4 shows photos of the ConTec 4 instrument with computer and the actual container with 4 mm half-cylinder surface roughness and the static core that were used. The gap between the container and the cylinder was 18 mm.

Fig. 4: ConTec4 with rotating container and static core

2.1.4.1   Testing of mixture I

The first and the last test were done 18 minutes and 83 minutes after water addition, respectively. After the first two tests the inner cylinder was pulled up and the mixture was stirred lightly by hand, without using mixer. Then, two other measurements were done and the inner cylinder was kept immersed in the mixture between these measurements. Before the last test this was done after moving the inner cylinder up and down, i.e. still no mixing.

2.1.4.2   Testing of mixture II

The first and the last tests were done 32 minutes and 94 minutes after water addition respectively. Before the last test only motion up and down were made with the inner cylinder (it means no mixing) and then the whole measurement was repeated.

2.1.4.3   Static yield test conditions

In these tests we applied the rotational velocity N = 0.0015 rps (= 0.00942 rad/s), which is the slowest one with acceptable deviation. (It was found that with our ConTech 4 the deviation of speed control grows almost exponentially with decreasing velocity and for our purpose to catch the static yield stress the lowest rotational speed we used was 0.0015 rps with maximum deviation of about 35 %) This low speed makes it possible to follow changes of torque in real time and allows reaching the static yield stress and structural breakdown, which comes after that.

First we applied rotational speed 0.0015 rps for 200 seconds, then the rotation was stopped for 200 seconds (outer cylinder was static) and these two steps were repeated three times. After that the outer cylinder was ,,shaken" to relieve stress between the outer cylinder and the core to reach zero value of torque. The whole procedure was repeated two times again.

During the 200 seconds of measurement the cylinder turns 1.884 rad (0.00942·200 = 1.884 rad) which is 108° (alfa-deformation, see Fig. 5). So during one such measurement the cylinder turns less than a third of a whole revolution.

Before the second test only up- and down- movement with the inner cylinder was made (i.e. again no mixing) and then the whole measurement was repeated. This technique was applied in testing of mixture II.

In case of mixture I the duration of the applied rotation was changed. The last test with this mixture was carried out in a similar way, but after several stops of rotation the outer cylinder was ,,shook" to relieve residual stress between container and core to reach zero value of torque.

2.1.4.4   Analysis of measurement

The ConTec4 is, as described, a concentric cylinders viscometer. The outer cylinder is rotated a given velocity (N, ω) and the inner is stationary and includes a load-cell measuring the torque acting due to the drag from the fresh concrete. After some time of motion of the outer cylinder the point A goes to the point C as shown in Fig. 5.
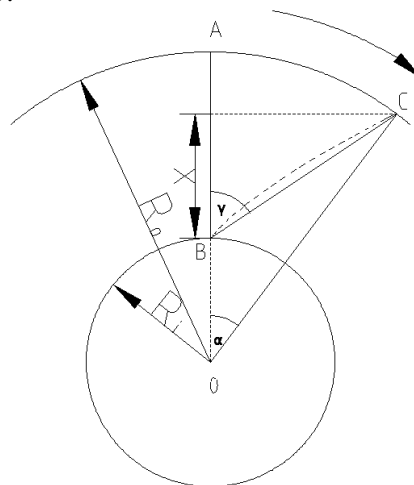

Fig. 5: Analysis of the angle gamma (γ) in thegap AB = $R_0 - R_i$ = 18 mm, figure after Billberg

For calculation of the angle gamma the following equation was deduced from Fig. 5 and some algebra:

$$\cos\gamma = \frac{R_0\cos\alpha - R_i}{\sqrt{R_i^2 + R_0^2 - 2R_0R_i\cos\alpha}} \tag{6}$$

where R_0 is 0.103 m and R_i is 0.085 m for the ConTec4 viscometer. This assumes a straight line BC which is probably not the case as pointed out by Billberg [2]. However, no effort was made to investigate to what extent the shear deformation between the inner and outer cylinder followed some other path, perhaps like indicated by the dotted curved line between B and C indicated in Fig. 5. This could perhaps have been done with some kind of color indicator sprinkled on the top surface. Still this would only reflect the surface shear and not what is going on inside the mortar where some other kind of shear detection would have to be used. Clearly Fig. 5 could be a simplification.

2.1.4.5   Conversion of measured torque to shear stress

For conversion of torque to shear stress we used the following relationship (7), where *r* is the radius where the shear stress acts and *h* is the height of the immersed part of the inner cylinder [16]:

$$\tau = \frac{T}{2\pi r^2 h} \tag{7}$$

The torque *T* is the same at all radii in a given time if we assume elastic constant shear modulus, G, (in addition to constant plastic viscosity) and the kind of linear shear-stress deformation angle ABC described in figure 4. Shear stress is inversely proportional to the square of the radius *r* – distance from the centre of symmetry. According to equation 7 the maximum shear stress is reached for maximum torque at the surface of the inner cylinder and minimum on the outer cylinder.

The yield stress is the minimum stress below which no flow occurs. According to eq. 7 the yield stress is first reached at the surface of the inner cylinder (and where later flow begins if high rotational speeds are applied). Then as the angular velocity is increased, the yield stress is reached at greater and greater radii from the inner cylinder until eventually it is reached at the surface of the outer cylinder. At sufficiently high rotational speed and assuming Bingham fluid behaviour plug flow is then assumed to be completely eliminated.

There was no visible motion in the whole mixture during measurement; only an area close to the outer cylinder could be seen moving. This motion was transferred via particle interactions and elastic and/or plastic and/or viscous type shear stress transfer through the whole mixture to the inner cylinder, which detected the value of the torque. That is the reason for using the radius of the inner cylinder R_i in eq. 7 instead of *r* for calculation of the yield stress. For calculation of shear stress the following dimensions of R_i, R_o and *h* were used (Table 5):

Table 5: Dimensions of cylinders and height of immersed part of inner cylinder of ConTec4 viscometer

Number of test	Mixture I	Mixture II
R_i [m]	0.085	0.085
R_o [m]	0.103	0.103
h [m]	0.138	0.139

The geometry and surfaces of the inner- and outer cylinders shown in Fig. 4 were designed to minimize end effects while giving maximum bond by Ø 4mm half-cylindrical roughness on the outer cylinder and vanes (or knifes) ensuring contact at the inner cylinder.

By alternating the applied rotational speed (0.0015 rps and 0 rps) during measurement with the ConTec4 viscometer the torque-time dependency was obtained. The maximum values of torque captured (see initial peaks after each start of rotation in Fig. 9, Fig. 15, Fig. 18, Fig. 22, Fig. 27, Fig. 28, Fig. 29, Fig. 31 and Fig. 33) were used for calculation of yield stress τ_0. When the rotation of the outer cylinder was stopped the torque surprisingly never reached zero value. The torque is maintained at a constant value when the rotation of the outer cylinder is stopped and these values of torques were used for calculation of stresses τ_{res} (according to the eq.7), which we called the residual stresses. The

explanation for the existence of residual stress seems to be some tension between particles which still persists in the mixture after stopping rotation and confining the mix between the inner and outer cylinder in some kind of state of permanent shear stress. The dynamic yield value τ_{dyn} was taken as the stress which was reached after overcoming the maximal yield stress.

The difference between τ_0 and τ_{res} was called the mobilized stress τ_{mob} and was calculated according eq.8:

$$\tau_{mob} = \tau_0 - \tau_{res} \tag{8}$$

To reach zero values of torque during stand still a light rotational ,,shaking'' by hand was applied on the outer cylinder of the viscometer. This is seen as the largest peaks in Fig. 18, Fig. 22 and Fig. 31. The yield stress reached immediately after ,,shaking'' is marked by * in Table 16, Table 20, Table 23, Table 24 and Table 27. If the yield value is reached directly after shaking, the stress is called fully mobilized τ_{fully} in

Table 18, Table 22 and Table 26..

2.1.5   The plate test

The plate test is based on the fact that the slight deformation of material under its own weight, evaporation and other causes of volumetric change that occur, allow to transfer a part of this load to the rough plate by the mobilization of a shear stress on the plate. This shear stress is equal to the maximum value physically acceptable, which is the yield stress [29]. It is important to note here that, as opposed to a penetrometer test (Vicat needle), the plate is perfectly static [3]. The test set up is shown in Fig. 6 with both plate with rough surface, container for paste and balance.

Fig. 6: Test set up for plate test

The shear stress acting on the surface of the plate was calculated from the measured apparent mass evolution using the following equation [30]:

$$\tau(t) = \frac{g \Delta M(t)}{2S} \tag{9}$$

where ΔM is the measured variation in the apparent mass of the plate and S is the immersed surface of the plate.

The structuration rate of the tested material is A_{thix} [Pa/s] [26]. It is the rate of increase in the static yield stress of material in Pa/s and also called structural build-up rate.

The structural build-up of micro mortar phase and SCC mixtures was intensively studied in Billberg's thesis [2]. Matrix is regarded as the continuous phase of concrete and thus incorporates all fine particles, water, air and chemical additives. In other words; matrix is what is left if all aggregate

having particle size greater than 0.125 mm is removed from the concrete. The results show that the time-dependent static yield stress ranges from 7.8 Pa/min for the densest paste (i.e. the lowest w/c = 0.34) down to 2.5 Pa/min for the leanest paste (highest w/c = 0.42) [2].

The SCC mixtures prepared and tested in Billberg`s work showed linear growth of static yield stress with time. The structural build-up ranged from 30 to 95 Pa/min. Common for all mixtures was the cement content equal to 320 kg/m^3, w/c ratio 0.58 and coarse aggregate (8-16 mm) equal to 30 % of total aggregate amount. From the results it is obvious, that an increased particle concentration increases the rate of structural build-up [2].

Roussel proposed the classification given in Table 6 according the author's own experience and other published results [26].

Table 6: Classification of SCC according to their flocculation rate [26]

Flocculation rate A_{thix} (Pa/s)	SCC type
Less than 0.1	Non-thixotropic SCC
Between 0.1 and 0.5	Thixotropic SCC
Higher than 0.5	Highly thixotropic SCC

2.1.5.1   Description of technique

The design of the plate test experimental device presented here was inspired from the device proposed by A. Perrot et all [29]. The vessel (cylindrical, with a diameter 190 mm and 220 mm in height) was filled with the mortar to a height of 200 mm. The plate was 3 mm thick, 75 mm wide and 102 mm long. It was covered with sand paper with average roughness of 200 μm. The sand paper was used to avoid any slippage between the mortar and the plate. The plate was rigidly attached to the vessel during filling. To ensure reproducibility vibration was applied for 10 s (vibrating table). The plate was then attached below a balance with accuracy of ± 0.01 g. The height H of the immersed portion of the plate was measured at the beginning and it was 69 mm and 67 mm for the first and second mixtures respectively. The whole testing was carried out under constant conditions in a climate room at 50 % RH and temperature 20 ˚C. The testing was started at time 14 min and 24 min after water addition for first and second mixture respectively.

2.2   Parallel plate rheometer

Following the mortar studies a series of matrices with the same binder composition and filler content were made and investigated with a MRC 300 rheometer produced by Paar Physica with parallel plate measuring system. The upper plate had a serrated surface to avoid slippage and the geometry of upper plate given by radius was 3 cm. The gap between the plates was set to 1.0 mm. The bottom plate was temperature controlled.

Proportioning of matrixes was varied so as to cover the composition of the matrices in the previously investigated mortar according to the particle-matrix model [4]. The matrix phase consists of water, chemical admixtures (SP) and all fines, including cement, pozzolanes and aggregate fines, i.e. particles < 0.125 mm. The mix composition is shown in Table 7 where matrix 1 corresponds to mortar tested previously (mixture II), matrix 2 had lower w/c ratio and matrix 3 had lower SP dosage to account for possible reductions in effective w/c and SP-dosage due to particles. The total matrix volume was approximately 200 ml.

Table 7: Proportioning of matrixes

Matrix	w/c ratio	SP [%]	Cement [g]	Filler* [g]	Tau [g]
M1	0.5	0.60	216.89	21.24	28.51
M2	0.4	0.60	243.27	23.82	31.98
M3	0.5	0.50	216.89	21.24	28.51

* particle size 0-0.125mm with the same material as used in the sand

All matrixes were blended in a high shear mixer Braun (MR5550CA). The blending was performed by adding solid materials to the water with SP. All mixtures were mixing for 30 seconds then resting for 5 minutes and blending again for 1 minute.

2.2.1 Testing

The following tests were performed on prepared matrixes (test I – III). All tests were started at time 10 min after water addition (age 10 min). Test I was done to obtain basic rheological properties like gel strength, yield stress and plastic viscosity. Tests II and III were performed for a detailed study of static yield stress and only done for matrix M1, which corresponded to the composition of the matrix phase of the mortar (mixture II).

2.2.1.1   Test I (Basic characterization)
It was used following test sequence:
1) 30 sec mixing with constant shear rate 60 s^{-1}
2) 1 min rest
3) shear rate – stress curve with logarithmic sweep of stress from 0.1 up to 100 Pa in 60 points lasting 5 second each to measure gel strength
4) 30 sec mixing with constant shear rate 60 s^{-1}
5) 1 min rest
6) 1 min with constant shear rate 0.01 s^{-1} to measure stress-strain curve in 60 measuring points lasting 1 second each
7) 30 sec mixing with constant shear rate 60 s^{-1}
8) 1 min rest
9) 3 min with constant shear rate 0.001 s^{-1} to measure stress-strain curve in 180 measuring points lasting 1 second each
10) 30 sec mixing with constant shear rate 60 s^{-1}
11) 1 min rest
12) 1 min with constant shear rate 0.01 s^{-1} to measure stress-strain curve in 30 measuring points lasting 2 seconds each
13) 30 sec mixing with constant shear rate 60 s^{-1}
14) 1 min rest
15) Shear rate – stress curve with logarithmic sweep of shear rate from 0.01 to 60 s^{-1} in 20 measuring points lasting 6 seconds each to measure flow curve
16) Shear rate – stress curve with logarithmic sweep of shear rate from 60 to 0.01 s^{-1} in 20 measuring points lasting 6 seconds each to measure flow curve

Total time was 31.5 min.

2.2.1.2   Test II
Test parameters:
1. 1 min mixing with constant shear rate 60 s^{-1}
2. 1 min rest
3. 1 min with constant shear rate 0.001 s^{-1} to measure stress-strain curve in 60 measuring points lasting 1 second each
4. 4 min rest
5. 1 min with constant shear rate 0.001 s^{-1} to measure stress-strain curve in 60 measuring points lasting 1 second each
6. 4 min rest
7. back to point 3.

Total: 21 steps and 10 resulting curves (total time 48 min)

2.2.1.3   Test III
Test parameters:
1. 1 min mixing with constant shear rate 60 s^{-1}
2. 1 min rest

3. 1 min with constant shear rate 0.01 s^{-1} to measure stress-strain curve in 60 measuring points lasting 1 second each
4. 4 min rest
5. 1 min with constant shear rate 0.01 s^{-1} to measure stress-strain curve in 60 measuring points lasting 1 second each
6. 4 min rest
7. back to point 3.

Total: 21 steps and 10 resulting curves (total time 48 min)

2.2.2 Evaluation of data from measurement with rheometer

The gel strength was determined first from the resulting curves in test I. Then the shear moduli (modulus of rigidity G) were calculated from the linear part of shear stress – strain curves according to Hookes law, equation (10) [21]:

$$\tau = G \cdot \gamma \tag{10}$$

G moduli were found at various ages of the matrixes, so rate of change of G (dG/dt) was determined too. Flow curves were evaluated using the Bingham model and the part of the down curve in range of shear rate 3 – 60 s^{-1} were used for this. All rheological parameters are related to their age (age 0 min is the moment of first contact of water with solid materials) at the start of measurement.

3 Results of part I – 5 months Erasmus

3.1 Basic properties of mortar

All mixtures were stable, distribution of coarse particles seemed to be homogeneous and no bleeding was observed. All measured parameters with testing times are shown in Table 8. The higher value of slump flow of mixture I compared to mixture II points out, that yield stress of mixture I is lower. As well a lower value of T$_{500}$ of mixture I predicts lower value of plastic viscosity. Air content of mixture I is a little bit lower than the value obtained for mixture II which corresponds with the density difference. Compared to Table 1 mixture I after 8 minutes correspond to class SF2 and at age 145 minutes is no longer self-compacting, whereas mixture II after 9 minutes corresponds to class SF1. According to the classification of SCC with regard to T500 values (Table 2) mixture I belongs to VS1/VF1 and mixture II VS2/VF2.

Table 8: Basic properties of fresh mixtures

Number of mixture	Time [min]	Fresh density [kg.m^{-3}]	Air content [%]	T$_{500}$ [sec]	Slump-flow [mm]	Predicted yield (eq.(1)) [Pa]	R [Pa/s]
I	8	2303	2.6	2.0	700	0.9	0.002
	145	-	-	-	485	5.4	0.001
II	9	2282	3.0	2.7	565	2.5	0.005

The measured slump-flow values were used in eq. 1 for predicting the yield stress (dynamic) of the mixtures (Table 8). If that value is connected with age of mixture, the rate of increasing of dynamic yield stress R [Pa/s] can be evaluated. The predicted yield stress for mixture I at age 8 min is 0.9 Pa, which corresponds to the rate 0.002 Pa/s. It should be noticed, that for the prediction of the yield stress at time 145 min the same value of density was used as in previous case (age 8 min). Mixture II showed lower slump-flow value which gave the predicted yield stress 2.5 Pa and rate of increasing 0.005 Pa/s.

3.2 Properties characterizing fresh mortar

Figures 7 and 8 show the flow curves of the two mortars based on the shear histories in figures Fig. 2 and Fig. 3, both indicating a shear thickening tendency often seen on self compacting concrete

[19,22]. That is, the Bingham model is not fitting the material behaviour perfectly as is also indicated by the correlation coefficients ≠ 1.
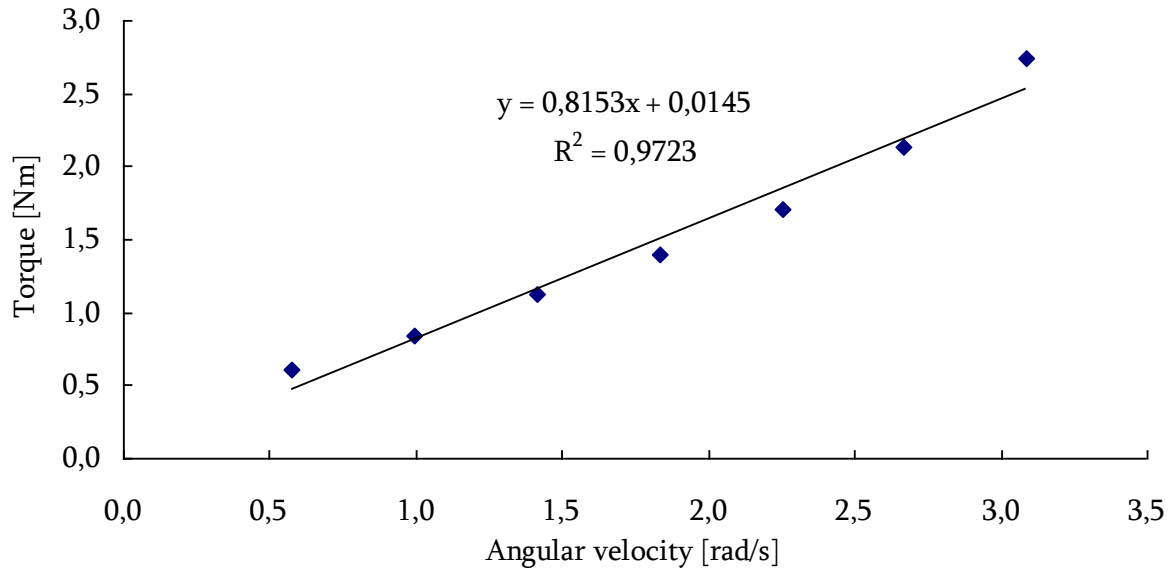

Fig. 7: Flow curve from measurement with BML viscometer of mixture I at time 11 min after water addition
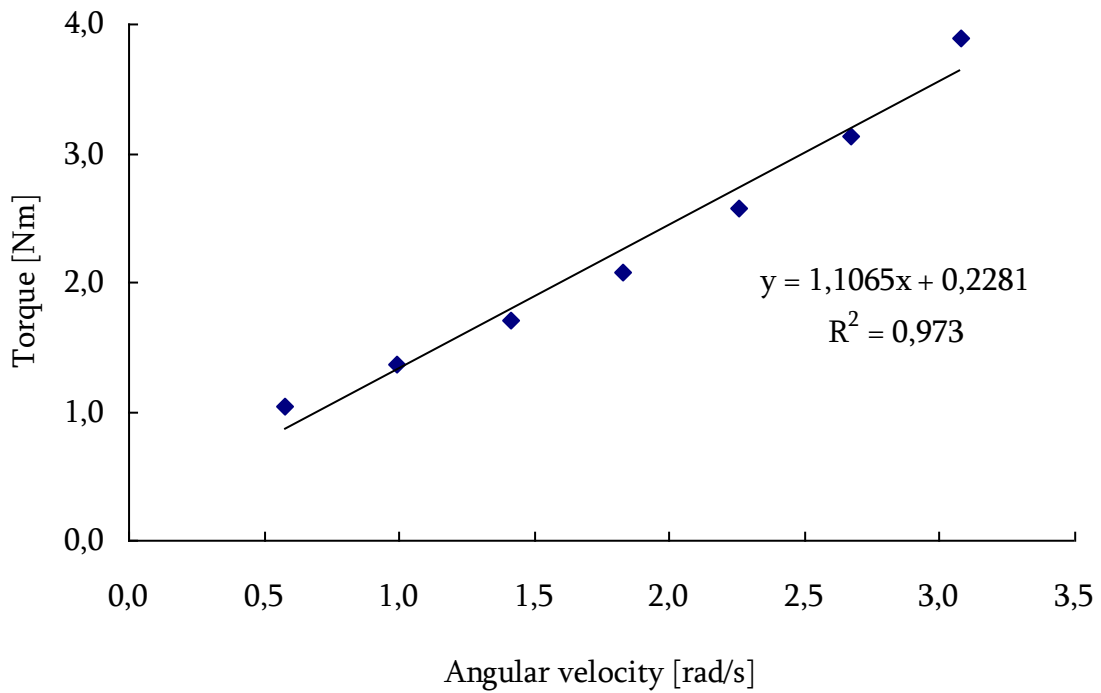

Fig. 8: Flow curve from measurement with BML viscometer of mixture II at time 20 min after water addition

Table 9: Results from measurement with BML viscometer

Number of mixture	Time [min]	$\tau_{0dynamic}$ [Pa]	μ_{pl} [Pas]	R [Pa/s]
I	11	0.9	19.4	0.001
II	20	14.2	25.7	0.012

Dynamic yield stress and plastic viscosity were obtained based on the flow curves in figure 7 and 8. Dynamic yield stress reached the value 0.9 Pa and plastic viscosity 19.4 Pas for first mixture and 14.2 Pa and 25.7 Pas for the second mixture. These differences correspond with results from the basic properties given in Table 8, where slump flow was 700 mm and 575 mm for first and second mixture, respectively. Plastic viscosity was a little bit different too also corresponding to that T_{500} was slightly higher for the second mixture.

The predicted yield stress of mixture I in Table 8 is in very good agreement with measured value in Table 9, where the rate of increasing of yield stress is 0.002 Pa/s and 0.001 Pa/s for predicted and measured values respectively. A little bit worse agreement is obtained in case of mixture II, where the rate of increasing of yield value is 0.005 Pa/s and 0.012 Pa/s for predicted (Table 8) and measured values (Table 9) respectively.

3.3 Static yield stress measurements with the ConTec4 viscometer

3.3.1 Mixture I

Figures 9, 11, 13, 15 and 18 show torque vs. time for the static tests of Mix I. Figures 10, 12, 14, 16 and 19 show the variation in rotational speed during the experiment. Fig. 17, Fig. 20 and Fig. 21 show the calculated yield stress values at different ages. Tables 10 – 18 show the parameters (static yield stress τ_0, structuration rate A_{thix} etc) determined from these results.
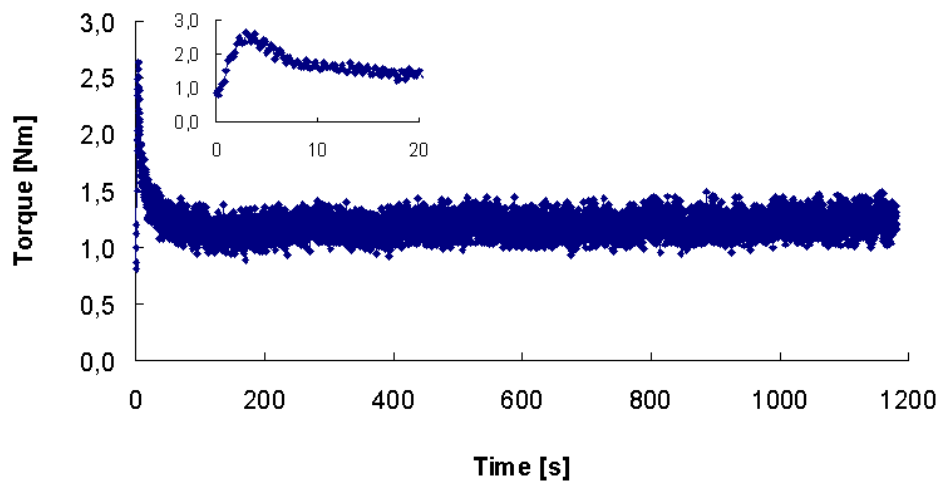
3.3.1.1   age of mixture I 18 min

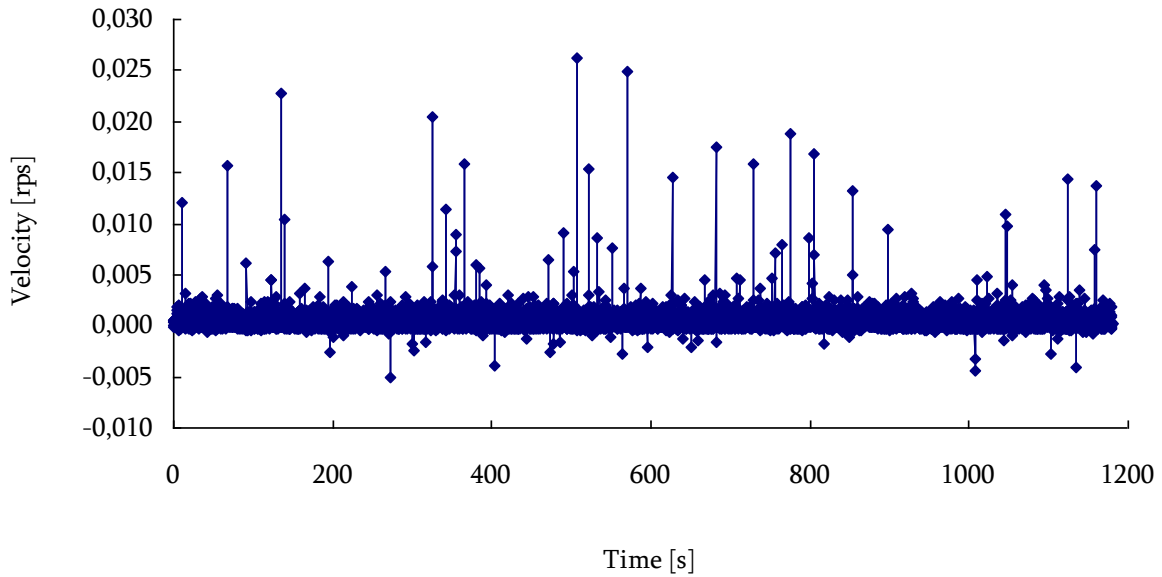Fig. 9: Torque-time dependence of mixture I at age 18 min on start of measurement at 0.0015 rps

Fig. 10: Velocity profile of measurement - average value of velocity [rps] = 0,00057

Table 10: Results for mixture I at age 18 min

Time [s]		Torque [Nm]	τ [Pa]		A_{thix} [Pa/s]
3		2.642506000	τ_0	421.8	0.389
100	200	1.136648489		181.4	-
200	300	1.182733650		188.8	-
300	400	1.162420285		185.6	-
400	500	1.183588132		188.9	-
500	600	1.199792970		191.5	-
600	700	1.166871088	τ_{dyn}	186.3	-
700	800	1.178676192		188.1	-
800	900	1.199375404		191.5	-
900	1000	1.205409036		192.4	-
1000	1100	1.215672964		194.1	-
1100	1180	1.232317125		196.7	-

In Fig. 9 the maximum value of torque is reached after 3 seconds, seen as a clear peak at the beginning of the experiment. Inserted in the figure is a higher resolution showing the linear nature of the deformation of the mortar before static yield is reached. The static yield stress takes the value 422 Pa and the succeeding average dynamic stress 181 Pa calculated from average torque reached in the interval 100 – 200 seconds. The following dynamic stresses and average torque for the given interval are shown in Table 10. The age of the concrete at the moment of reaching the yield stress was 18 min, so the structuration rate A_{thix} [Pa/s] is 0.389 Pa/s over these (18x60+3) seconds. Fig. 9 and Table 10 also show a tendency of slightly increasing dynamic stress during the experiment.

3.3.1.2   age of mixture 38 min
The next test was performed immediately after the previous one that means without remixing. Applied velocity was 0.002 rps instead of 0.0015 rps used in all tests. This was the only one exception, where the different rotational velocity was applied. Fig. 11 shows measured dependence for mixture I at the age 38 min and the velocity profile of the measurement is shown on Fig. 12.
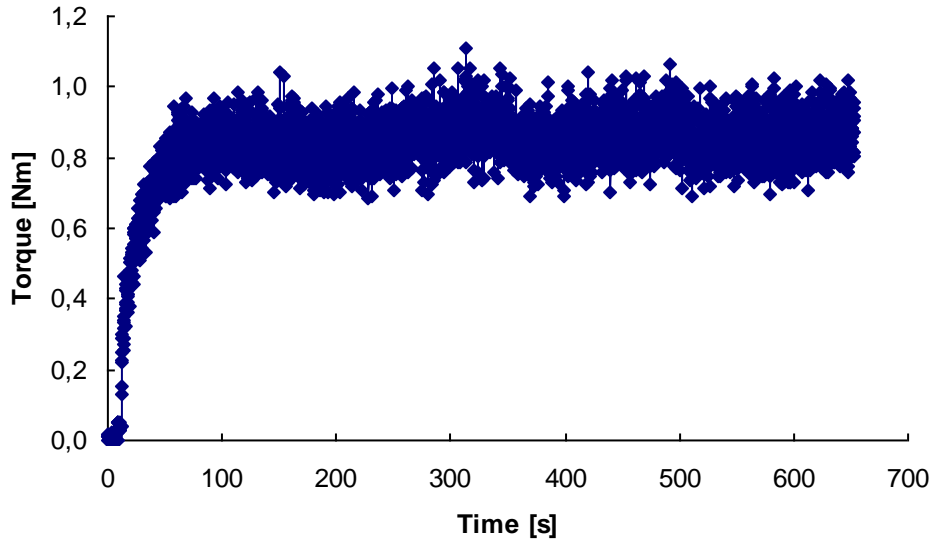
Fig. 11: Torque-time dependence of mixture I at age 38 min on start of measurement, where the rotational speed 0.002 rps was applied
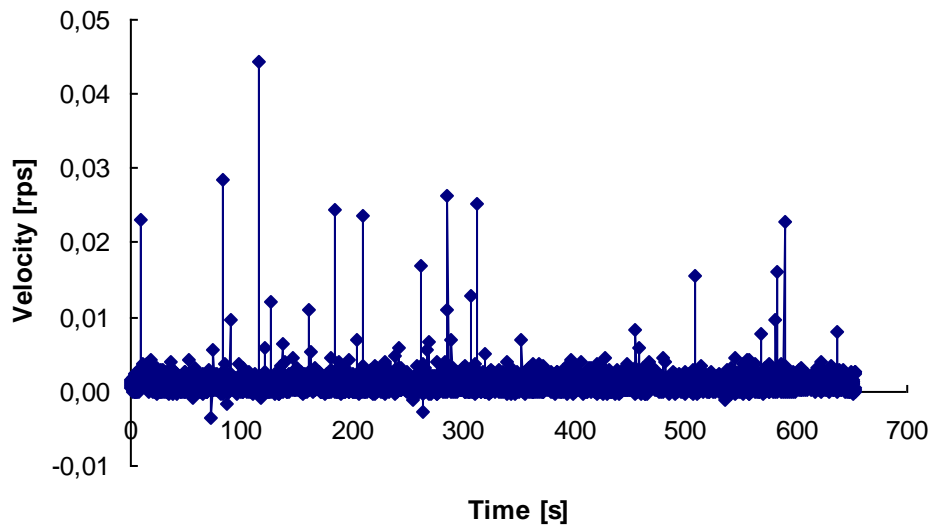

Fig. 12: Velocity profile of measurement - average value of velocity [rps] = 0,0012

Table 11: Results for mixture I at age 38 min

Time [s]		Torque [Nm]	τ_{dyn} [Pa]
50		0.806708	128.8
50	150	0.830709	132.6
150	250	0.835306	133.3
250	350	0.875266	139.7
350	450	0.852786	136.1
450	550	0.858647	137.1
550	650	0.859800	137.2

Fig. 11 shows torque-time dependence, where torque slowly increases during 50 seconds to the value of approximately 0.8 Nm which correspond to the stress 129 Pa. The absence of obvious yield stress is discussed in comments of measured curve in age 51.5 min (end of chapter 3.3.1.3.). The

dynamic yield stresses were calculated for every 100 seconds interval as shown in Table 11 and oscillated around value 136 Pa. The lower values of stresses (compared with values reached at age 18 min, where maximum value of stress was 197 Pa) are caused by the sensitivity of the Torque resistance in the sample on rotational velocity, which was in this case higher (0.002 rps instead of 0.0015 rps used in all other measurements) and caused larger destruction of the existing and forming structure.

3.3.1.3   age of mixture I 51.5 min

Fig. 13 and Fig. 14 show the torque – time – and velocity variation, respectively for the next experiment run on the same material, but where the mortar was hand mixed after lifting the stationary inner cylinder before the start of the experiment as described already.
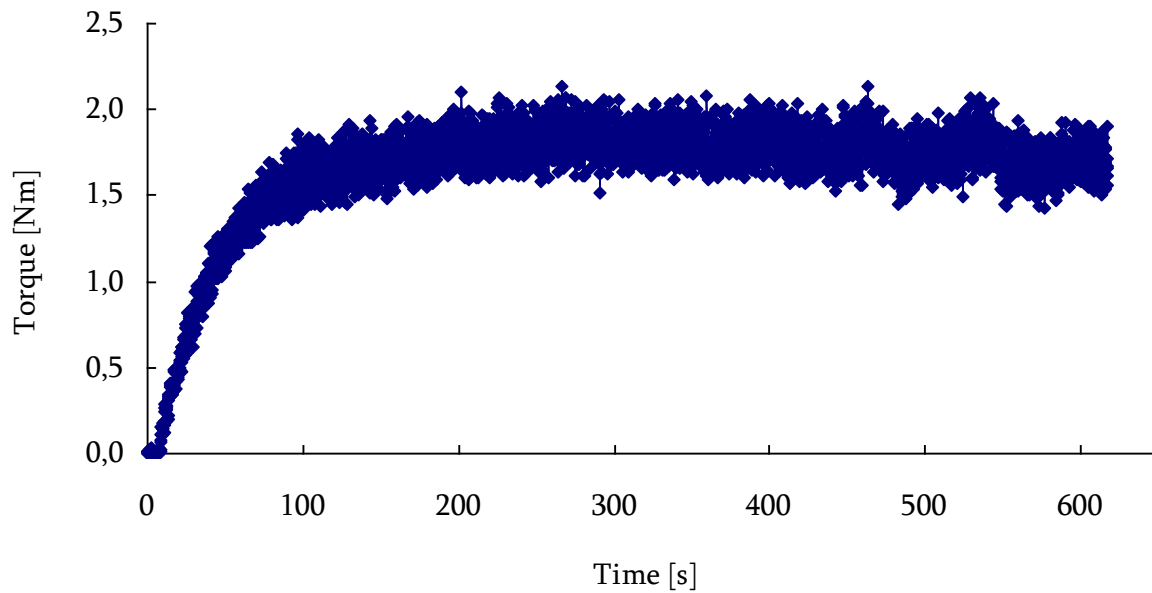

Fig. 13: Torque-time dependence of mixture I at age 51.5 min on start of measurement, 0.0015 rps
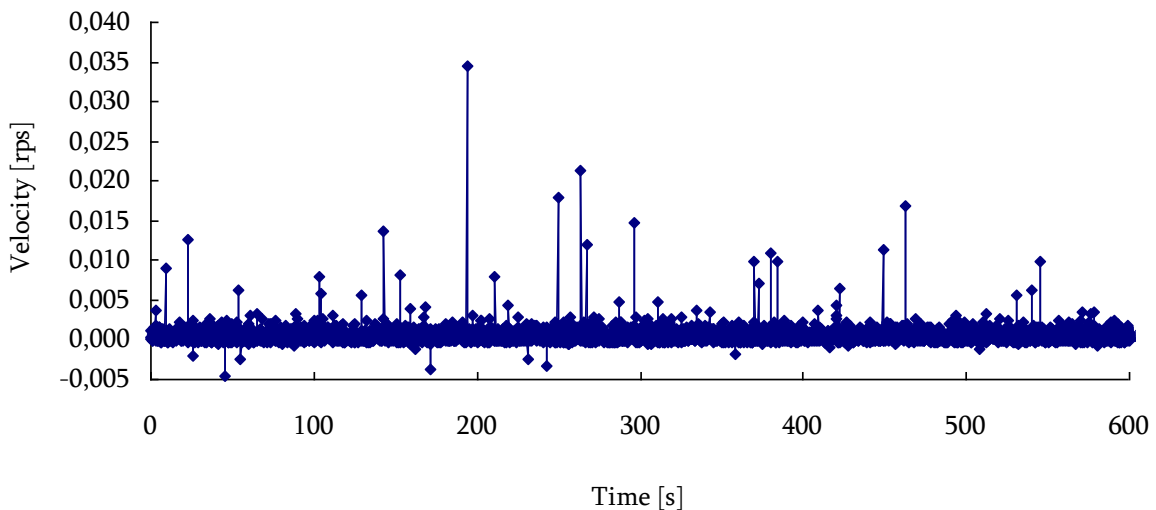

Fig. 14: Velocity profile of measurement - average value of velocity [rps] = 0.000599

Table 12: Results for mixture I at age 51.5 min

Time [s]		Torque [Nm]	τ_{dyn} [Pa]
100		1.787737	285.4
100	200	1.696747	270.8
200	300	1.811462	289.2
300	400	1.800362	287.4
400	500	1.771281	282.7
500	600	1.722679	275.0

Fig. 13 shows that the torque value slowly increased and then oscillated around the value 1.8 Nm, which corresponds to the stress 285 Pa. The evaluation of dynamic yield stresses were done in the same way as in figure 11 by dividing measured dependence on 100 seconds intervals as shown in Table 12. Again, there is no obvious yield stress (as in previous case – Fig. 11) and the reason for this can be in this case the hand-mixing just before testing, which breaks new bonds in the growing structure. However, the reason for the different kind of peaks at the beginning of Fig. 9 (sharp) and Fig. 11 and Fig. 13 (gradual) is not known. Apparently the gradual type happens when the test starts from an unconfined state immediately after pouring (see also figures Fig. 18, Fig. 22 and Fig. 31), whereas the steep rise and clear break are seen after start from rest in a more confined state (see the same figures). It does not appear to be a condition that the concrete must be subjected to the residual stress since the abrupt rise to clear peaks are also seen after the "shaking" in figures (see also figures Fig. 18, Fig. 22 and Fig. 31). Apparently, time at rest in the container is one factor affecting the features of the stress increase "peak" like in Fig. 9 or "gradual" like in Fig. 13. Another factor could be sensitivity to small variations in speed of rotation

3.3.1.4   age of mixture I 62 min

Fig. 15 shows the yield stress after repeated start/stop of mixture I. After the peaks ($\tau_{0static}$) a relatively steady value (τ_{dyn}) is maintained and as the viscometer rotation is stopped a residual stress (τ_{res}) remains as the viscometer is at rest. At new start a new, higher, peak is reached.
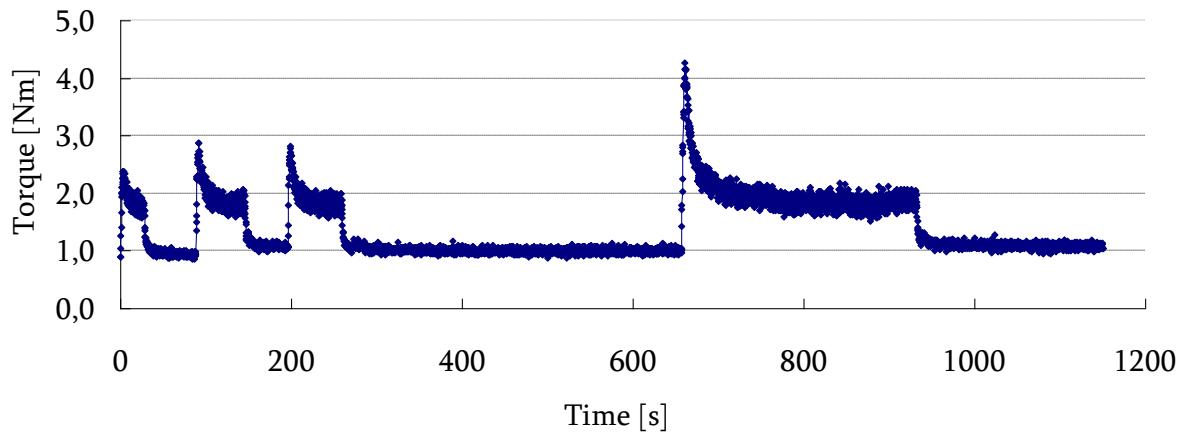

Fig. 15: Torque-time dependence of mixture I at age 62 min on start of measurement, 0.0015 rps
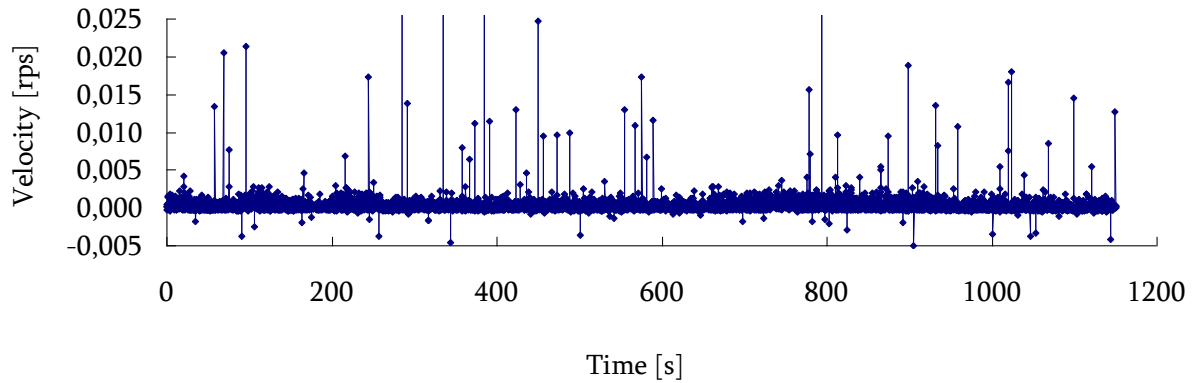
Fig. 16: Velocity profile of measurement

The evaluated stresses are shown in the following tables 13-15. There is a quite obvious increase of yield stress with time. The structuration rate calculated for these points grow from 0.10 Pa/s to 0.15 Pa/s (Table 13).

Table 13: Development of yield stresses τ_0 of mixture I

Age of SCC [s]	Age of SCC [min]	τ_0 [Pa]	A_{thix} [Pa/s]
3783	63	380.5	0.101
3872	65	458.7	0.118
3978	66	450.4	0.113
4440	74	664.9	0.150

Table 14: Development of residual stresses τ_{res} of mixture I

Age of SCC [s]	Age of SCC [min]	τ_{res} [Pa]
3868	64	146.3
3976	66	172.3
4436	74	159.6
4781	80	175.2

Table 15: Development of mobilized stresses τ_{mob} of mixture I

Age of SCC [s]	Age of SCC [min]	τ_{mob} [Pa]	A_{thix} [Pa/s]
3780	63	236.9	0.063
3868	64	312.4	0.081
3976	66	278.1	0.070
4436	74	505.3	0.114

All calculated stresses (τ_0, τ_{res} and τ_{mob}) and their time-development are shown in Fig. 17. The time development was calculated using linear regression, but the correlation coefficient is acceptable only for values of yield stress where $R^2 = 0.9659$. Interestingly, the linear regression in figure 17 shows a very different, higher, value of the structuration rate $A_{thix} = 0.412$ Pa/s. This value is in the order of 2 – 6 times higher than the values of tables 9-14 where all A_{thix} values are calculated based on their individual ages from addition of water, i.e. from birth including part of the time in a less confined state. The highest value from regression is based on structural build up when confined in the viscometer and apparently is higher. However, both ranges of values are within the ranges indicated in Table 6, though within different flocculation rate classes. The reason for the much higher structuration

rate in Fig. 17 thus is difficult to explain at present but possibly/probably the confinement plays an important role for A_{thix}. From figure 17 it seems that there is a constant difference between the confined (upper) and unconfined (middle) yield stress development regression lines. Of course remixing also plays a role, but the effect discussed above was obtained without remixing. The only factors were time and stress-state and the "shake" which rotated the container very little, less than 1/100th rotation, but enough to reduce the confinement.

Fig. 20 and Fig. 21 show that the yield stress is reduced by the stress release and that the time development of structural build-up probably is more complicated than the simple constant A_{thix} law indicates. This point was investigated in more detail on matrix based on the same cement, filler and SP in the Physica parallel plate viscometer presented later in this report, particularly the effect of deformation rate.
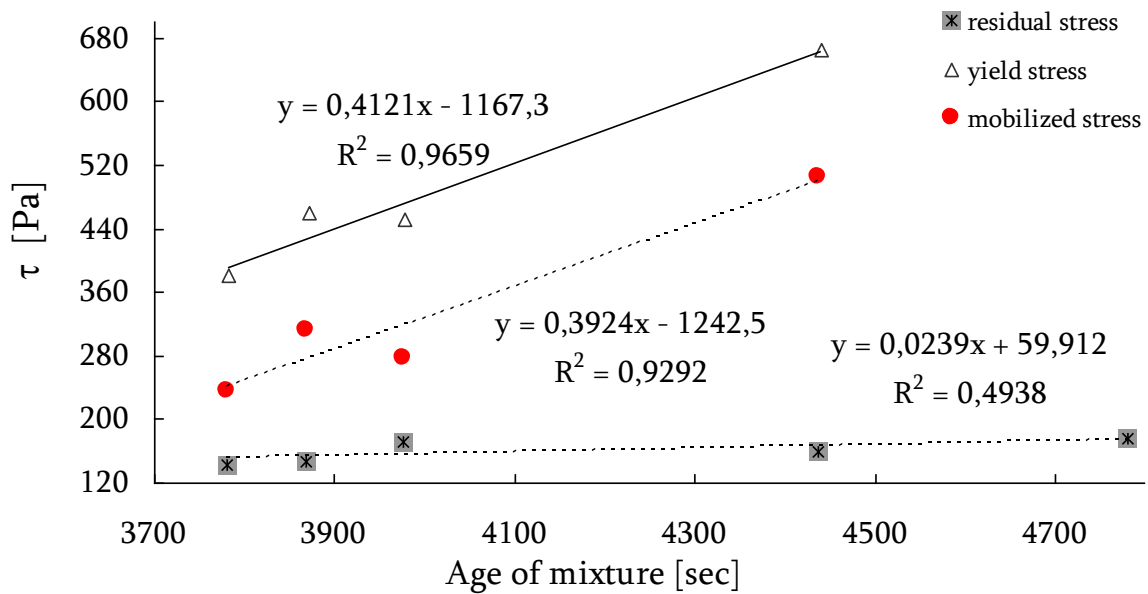

Fig. 17: Development of stresses in mixture I, no release of stress ("shaking")

3.3.1.5 age of mixture I 83 min

Fig. 18 shows the torque-time dependence of mixture I at age 83 min after water addition with applying „shaking" to reach zero value of torque. The evaluated stresses and values of structuration rate are shown in the 16-18.
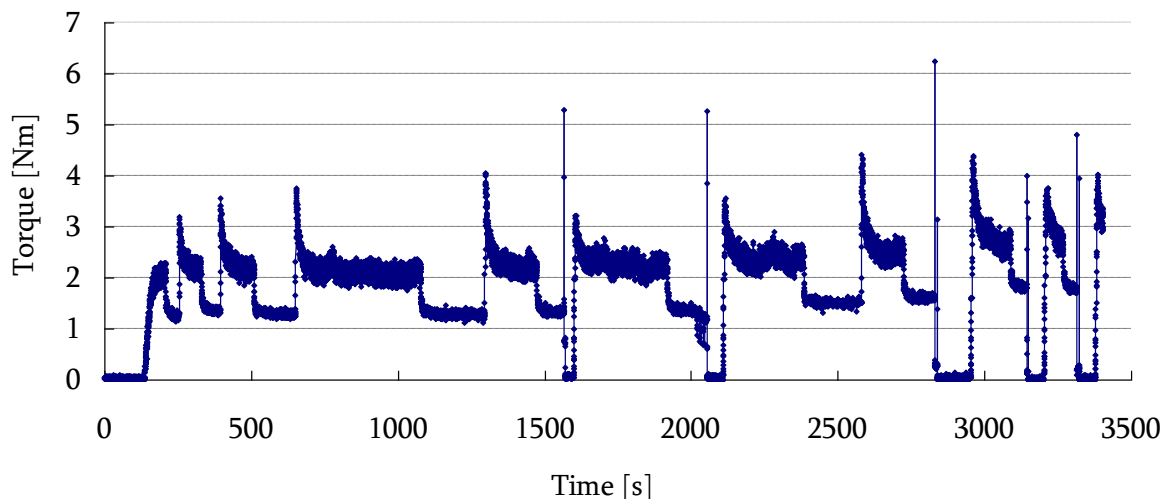
Fig. 18: Torque-time dependence of mixture I at age 83 min on start of measurement
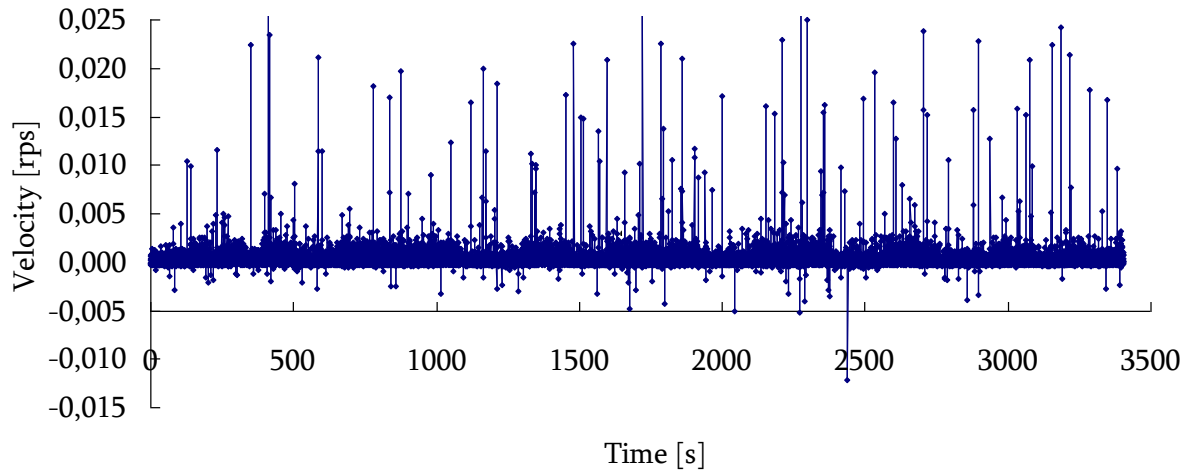

Fig. 19: Velocity profile of measurement

Table 16: Development of yield stresses τ_0 of mixture I

Age of SCC [s]	Age of SCC [min]	τ_0 [Pa]	A_{thix} [Pa/s]
5248	87	334.7	0.064
5295	88	510.1	0.096
5436	91	566.9	0.104
5694	95	601.0	0.106
6339	106	647.6	0.102
6646	111	512.2*	0.077
7155	119	567.8*	0.079
7621	127	703.2	0.092
8001	133	699.1*	0.087
8255	138	600.1*	0.073
8426	140	633.4*	0.075

The yield stress τ_0, which is reached after ,,shaking'' is marked by *.

Table 17: Development of residual stresses τ_{res} of mixture I

Age of SCC [s]	Age of SCC [min]	τ_{res} [Pa]
5293	88	205.1
5432	91	218.3
5690	95	210.9
6335	106	207.1
6599	110	208.9
7040	117	220.4
7618	127	242.2
7865	131	259.3
8180	136	294.0
8353	139	282.3

Table 18: Development of mobilized τ_{mob} and fully mobilized τ_{fully} stresses of mixture I

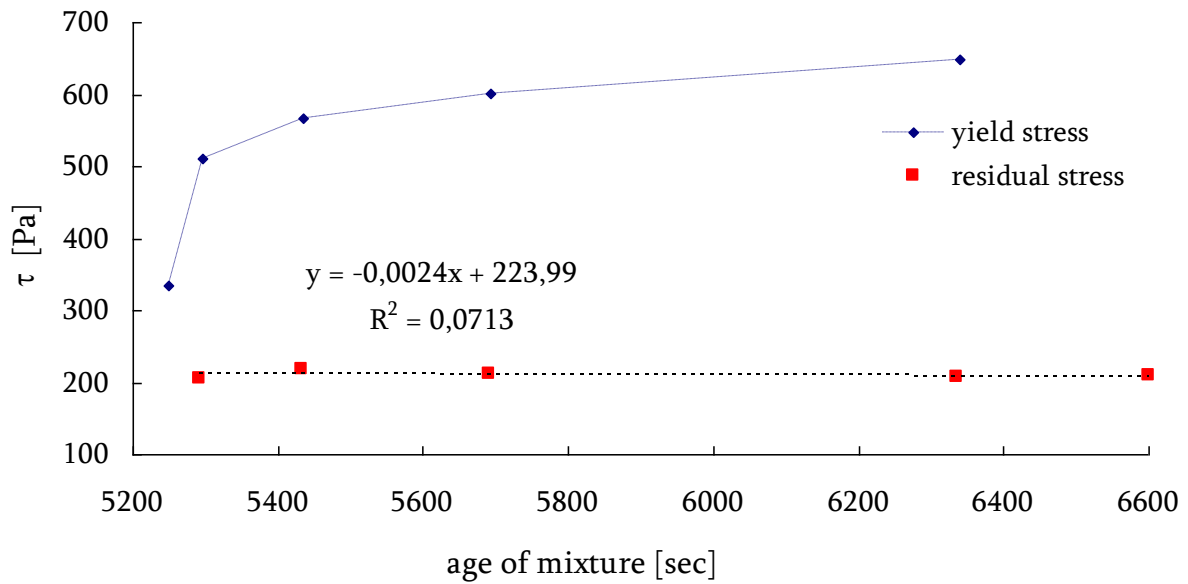| Age of SCC [s]	Age of SCC [min]	τ_{mob} [Pa]	τ_{fully} [Pa]	A_{thix} [Pa/s]
5293	88	305.0	-	0.058
5432	91	348.6	-	0.064
5690	95	390.1	-	0.069
6335	106	440.5	-	0.070
6637	111	-	505.0	0.076
7146	119	-	560.2	0.078
7618	127	461.0	-	0.061
7990	133	-	689.6	0.086
8241	137	-	593.7	0.072
8415	140	-	627.3	0.075

Fig. 20: Development of stresses evaluated from measured point before shaking though including points where stress has been released
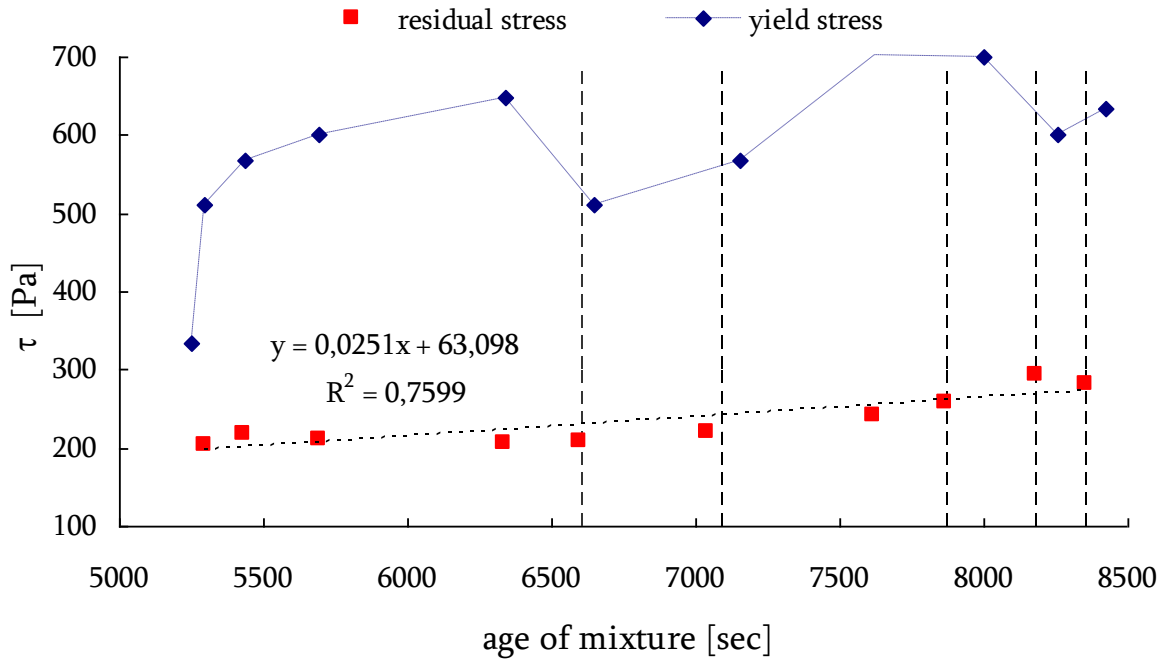
Fig. 21: Development of stresses in mixture I, dashed lines show shaking

The results in tables 10-18 from measurement with the ConTec4 viscometer show similar results of structuration rate (range from 0.06 to 0.15 Pa/s) for the whole torque-time dependency, except for the first testing with confinement, where the obtained structuration rate was almost ten times higher (A_{thix} = 0.389 Pa/s). These results can be comparable with result obtained in Billberg`s work, where structuration rate of micro mortar paste (w/c = 0.34) was equal to 0.13 Pa/s. Again, the result is affected by both age and confinement as well as the hand stirring after the results of Fig. 15 and before Fig. 18.

From Fig. 21 it is obvious that the yield stress, which was reached directly after shaking has a lower value than before. If the measuring is continuously going (without shaking), the yield stress increases. The reason is, that the shaking affects the structure of the mixture in a way destructing some new bonds. This effect is typical for thixotropic materials as cement systems are.

3.3.2   Mixture II

3.3.2.1   First part of measurement – start at age of SCC 32 min

Figures 22 – 30 show the results of an effort to make a more systematical investigation of the yield stress build up with regular intervals of stress release by the "shaking" which presumably released the stress by a slight (less than 1/100th) manual rotation.
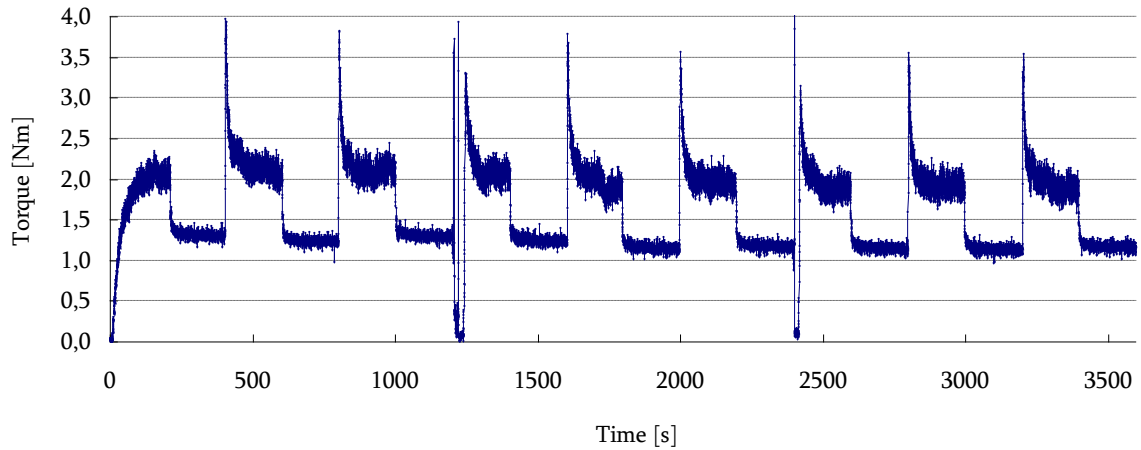
Fig. 22: Torque-time dependence of mixture II at age 32 min on start of measurement

I. procedure of calculation and evaluation

Based on the experience with mix I the evaluation of measured dependence was done more precisely on mixture II. The objective was to translate the torque-time dependence into stress – strain curves, thus evaluating the elastic behaviour at very low deformation. The measured torque-time dependency was divided into 34 steps and for every step the average velocity and corresponding stress was calculated (yield stress, residual stress,...). The range of every step was defined by reaching some important stress values (yield, residual, dynamic stress). First step ends by reaching yield stress (gradual), second by reaching residual stress, third starts and ends by reaching residual stress and third ends by reaching yield stress. The first step is finished in T_{max1} = 2.004 Nm in time 210 sec. All values of velocity (software logged actual velocity 5 times per second during measurement) were used for calculation of the average value of velocity (arithmetical mean) in the given step. The average value of the velocity for the first step is N_{a1} = 0.000538 rps. Then the angular velocity ω [rad·s^{-1}] was calculated, as well as the angle alpha. The following equations were used including a numerical example for the lowest speed:

$$\omega = N_a \cdot 2\pi \tag{10}$$
$$\omega = 0.00054 \cdot 2\pi = 0.00338 \text{rad} \cdot \text{s}^{-1}$$

$$\Delta\alpha = \omega \cdot \Delta t \tag{11}$$
$$\Delta\alpha = 0.00338 \cdot 210,0 = 0.710 \text{rad}$$

Then the angle γ was calculated using eq. 6, where the dimensions of the inner and outer cylinder of the ConTec4 viscometer and angle α were used. Delta γ was calculated for every step. At every step gamma increases because of the contribution of the previous step. After the first step γ is 1.7 rad, after the third step γ is 2.6 rad (=1.7 + 0.9) and so on. Thus the value γ belongs to the time at the end of each step (for example gamma 6.8 rad is reached after 1001 sec). The calculated data for the first 11 steps (part before first shaking) are shown in the following table.

Table 19: Results of values of velocity, alpha and gamma for part of the stress-strain dependency before first shaking

Step	Time [s]			N_a [rps]	ω [rad/s]	$\Delta \alpha$ [rad]	cos γ	$\Delta \gamma$ [rad]	γ [rad]	γ [degree]
	from	to	Δ time							
1	0	210	210	0.00054	0.00338	0.710	-0.102	1.7	1.7	96
2	210	215	5	0.00011	0.00067	0.003	1.000	0.0	1.7	97
3	215	403	187	0.00017	0.00109	0.203	0.607	0.9	2.6	150
4	403	405	3	0.00065	0.00411	0.011	0.998	0.1	2.7	153
5	405	604	199	0.00052	0.00330	0.654	-0.052	1.6	4.3	246
6	604	607	3	0.00004	0.00023	0.001	1.000	0.0	4.3	246
7	607	801	194	0.00015	0.00097	0.188	0.643	0.9	5.2	296
8	801	804	3	0.00045	0.00284	0.010	0.998	0.1	5.2	300
9	804	1001	197	0.00048	0.00302	0.596	0.004	1.6	6.8	389
10	1001	1004	3	0.00010	0.00061	0.002	1.000	0.0	6.8	390
11	1004	1199	195	0.00010	0.00060	0.118	0.820	0.6	7.4	425

N_a – average velocity [rps]
ω – angular velocity [rad/s]

According to the previous table and the above explanation the torque-time dependency was converted to a torque-gamma dependency.
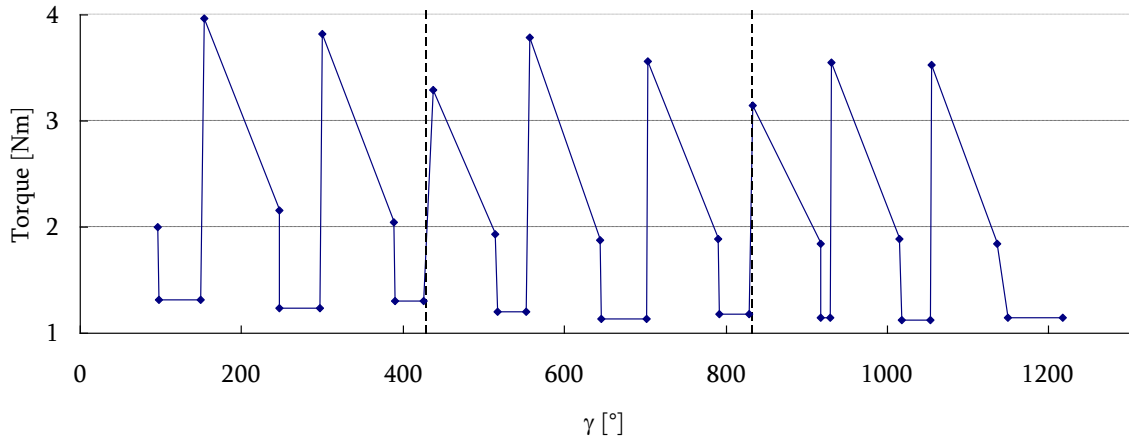

Fig. 23: Torque-gamma dependence evaluated from measured points of mixture II (dashed lines show shaking)

All points of torque-gamma dependence in Fig. 23 were used for calculation of stress according to equation 7 and the obtained dependency is shown in Fig. 24.
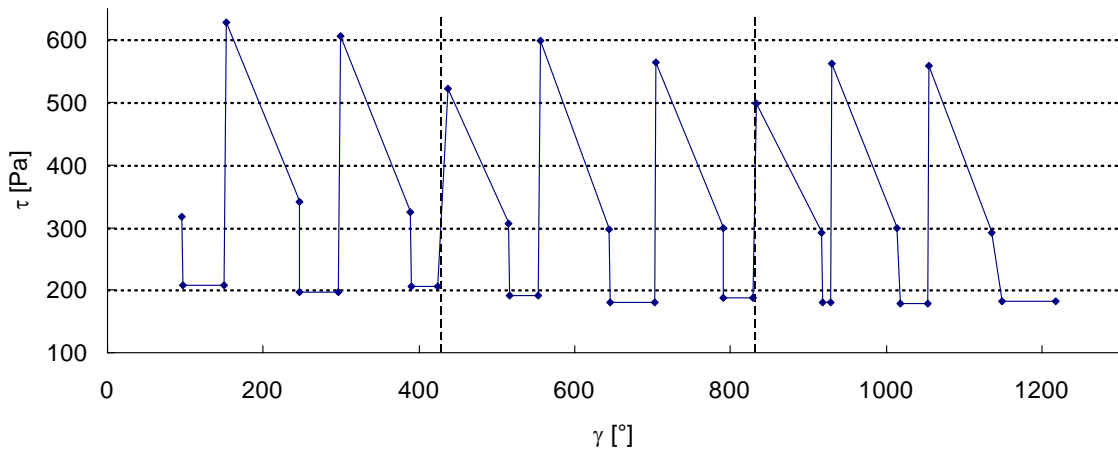
Fig. 24: Shear stress-gamma dependence evaluated from measured points of mixture II (dashed lines show shaking)

The mentioned dependency was analyzed by calculating static yield stress (τ_0), dynamic stress (τ_{dyn}), residual stress(τ_{res}) and mobilized stress (τ_{mob}). All results are shown in following tables (20-22) and Fig. 25 and Fig. 26.

Table 20: Development of yield stresses τ_0 of mixture II

Age of SCC [s]	Age of SCC [min]	τ_0 [Pa]	A_{thix} [Pa/s]	A_{thix} [Pa/s]
2130	35	317.0	0.149	
2325	39	627.9	0.270	
2724	45	605.5	0.222	
3167	53	522.1*	0.165	
3525	59	599.5	0.170	0.163
3919	65	564.4	0.144	
4340	72	498.1*	0.115	
4721	79	562.4	0.119	
5122	85	559.3	0.109	

The yield stress τ_0, which is reached after ,,shaking" is marked by *.

Table 21: Development of residual stresses τ_{res} of mixture II

Age of SCC [s]	Age of SCC [min]	τ_{res} [Pa]
2320	39	202.9
2720	45	198.9
3120	52	206.6
3520	59	190.9
3915	65	180.4
4310	72	187.7
4712	79	180.8
5113	85	178.8
5514	92	181.8

Table 22: Development of mobilized τ_{mob} and fully mobilized τ_{fully} stresses of mixture II

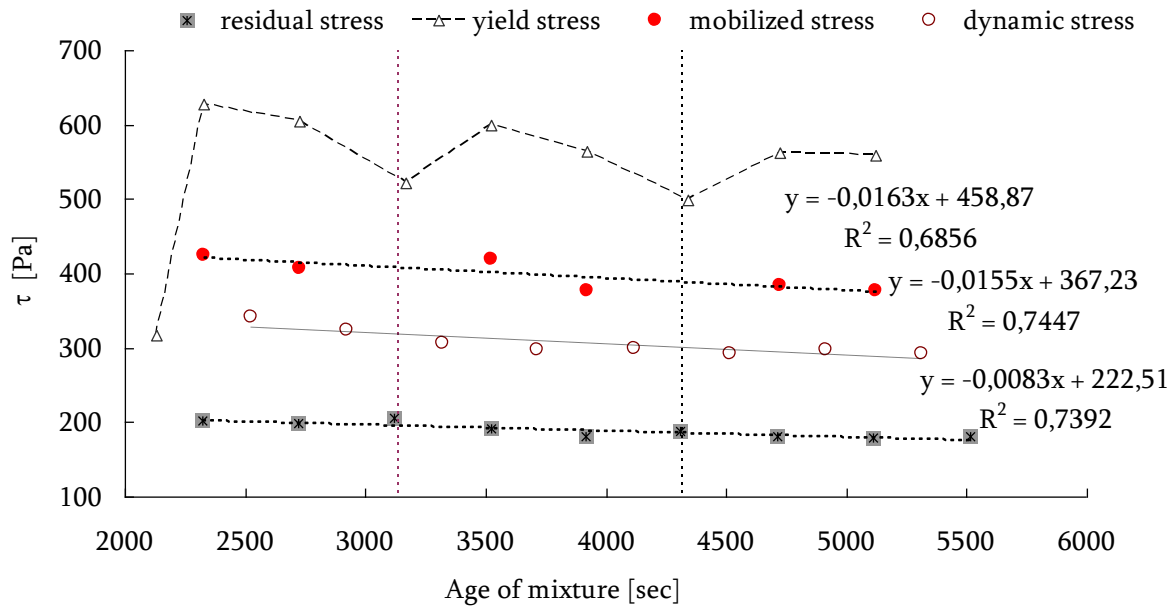| Age of SCC [s]	Age of SCC [min]	τ_{mob} [Pa]	τ_{fully} [Pa]	A_{thix} [Pa/s]	A_{thix} [Pa/s]
2325	39	425.0	-	0.183	
2724	45	406.6	-	0.149	
3159	53	-	508.0	0.161	
3525	59	419.1	-	0.119	0.122
3919	65	376.7	-	0.096	
4331	72	-	485.8	0.112	
4721	79	383.6	-	0.081	
5122	85	377.5	-	0.074	

Fig. 25: Development of stresses in mixture II (dashed lines show shaking)
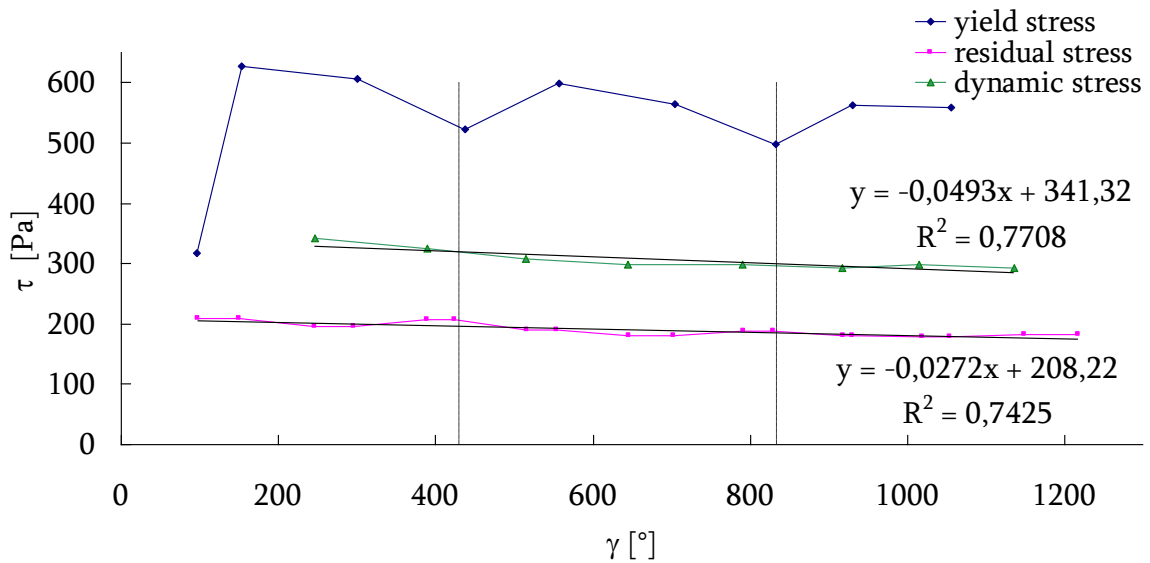

Fig. 26: Shear stress-gamma dependence of mixture II (dashed lines show shaking)

From Fig. 25 and Fig. 26 no clear increase of none of the stresses are seen except for from the first (gradual) to the second (sharp) maximum torque values reached in figure 25. However, between all

values subsequent to the first value no clear increase was seen. Due to this the calculation procedure was reviewed resulting in a modified 2nd procedure of calculation and evaluation of the data.

II. procedure of calculation and evaluation

In this procedure the calculation of gamma was done for every measured point. During measurement the software logged data every 0.2 seconds. Because of very slow rotation of the outer cylinder (0.0015 rps) and the low accuracy of the rotation control of the equipment, a lot of negative values of rotation velocities were logged as seen in figures 10, 12, 14, 16 and 19. Negative values of velocities means counter motion of the outer cylinder, which corresponds to a decrease of gamma. These negative values thus contribute to the growth of gamma due to the cosine function in equation 6, which is used for evaluating gamma. That means that negative value of velocity (for example -0.0015 rps) give negative value of angle alpha (-0.0019 rad in our case), but the value is positive after applying cosine function (cos (-0.0019 rad = 0.999998) and therefore gives the same contribution as the values obtained from positive value of velocity (0.0015 rps).

During the whole measurement 9 steps were made with the motion of the outer cylinder. Every step took 200 seconds that gives 9x200 = 1800 seconds of motion. When we assume the rotation velocity N = 0.0015 rps (0.0015 rps = 0.00942 rad/s), then 0.00942x1800 = 16.956 rad = 972° done during the whole measurement.

Gamma was calculated for every measured point in the modified second procedure of evaluation and the final value of gamma was 63 rad (3628°). It appears from this that the contributions of negative values of velocities on increasing the gamma are so large that this way is not applicable.

Anyway the evaluation of gamma was done in this way too and the results are shown in the following figures 27-29. The shear stress was calculated in the same way as previously, that means using equation 7.
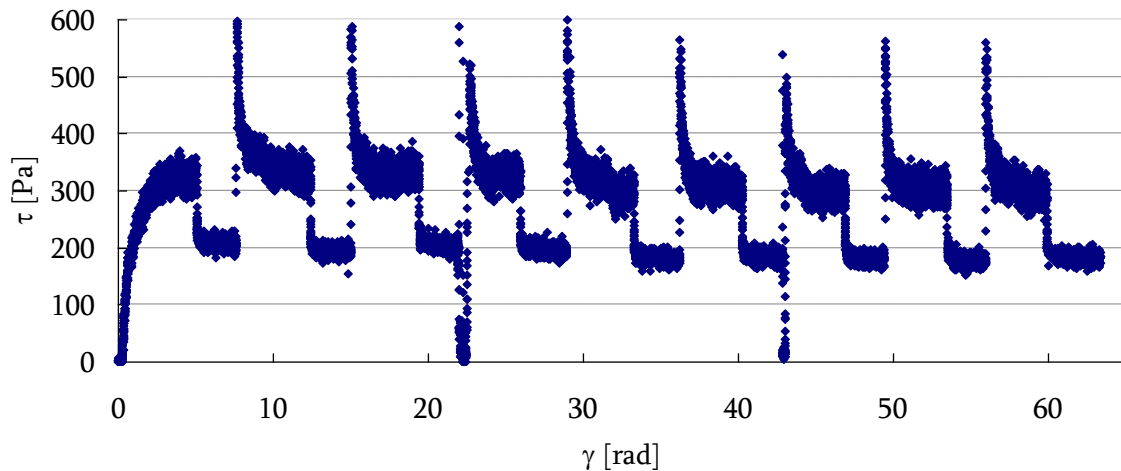

Fig. 27: Calculated dependency measured for mixture II evaluated with procedure 2 (which means calculation of gamma for every measured point) at starting age 32 min
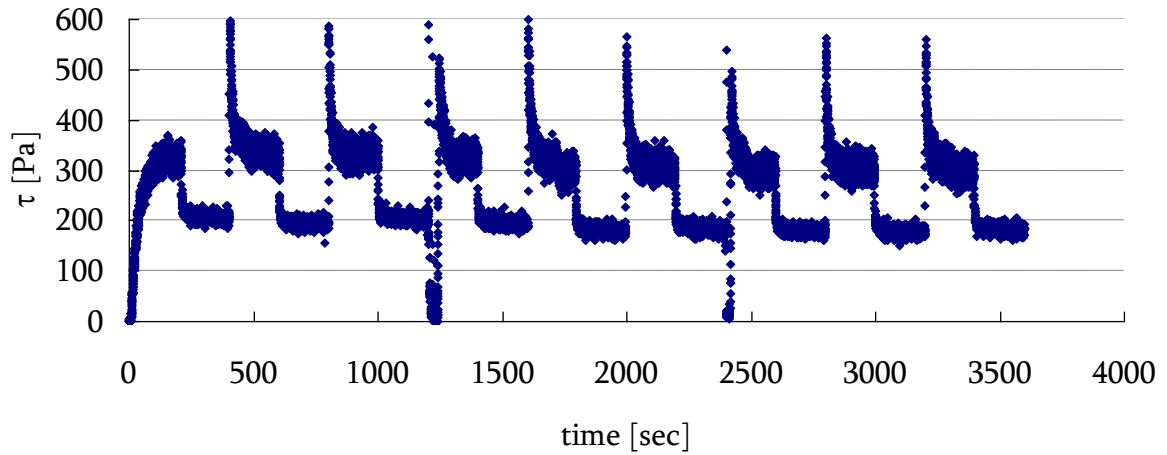
Fig. 28: Calculated dependency for mixture II, where measured torque was converted into stress according to eq. 7

In the plot of stress versus age of mixture dependence (Fig. 29) a linear regression was applied on the linear parts of the curves. This means those parts of the curves when the rotation was applied and torque (stress) suddenly peaked reaching maximum values (the static yield stress). The slopes of these lines represent the rate of increase of stress at the moment of start of rotation (reaching the yield value). These values are proportional to the shear modulus G and are called B [Pa/s] in table 23. G can be obtained by dividing B with the rotational speed (0.0015 s^{-1}). This development of G modulus is shown in Fig. 30 together with the clear increase of the G modulus which was reached immediately after shaking. The increasing trend of G modulus can be found between values which were achieved between the shaking except for the first part of the measurement, that means before first shaking.

Table 23: Obtained data for mixture II

age of mixture [min]	[s]	τ_o [Pa]	A_{thix} [Pa/s]	B [Pa/s]	G [Pa]	G [kPa]
35	2130	317.0	0.149	6.9	4600	4.6
39	2325	627.9	0.270	149.3	99467	99.5
45	2724	605.5	0.222	117.8	78533	78.5
53	3167	522.1*	0.165	60.7	40467	40.5
59	3525	599.5	0.170	134.0	89333	89.3
65	3919	564.4	0.144	140.1	93400	93.4
72	4340	498.1*	0.115	84.4	56267	56.3
79	4721	562.4	0.119	130.6	87067	87.1
85	5122	559.3	0.109	133.0	88667	88.7

The yield stress τ_0, which is reached after ,,shaking" is marked by *.
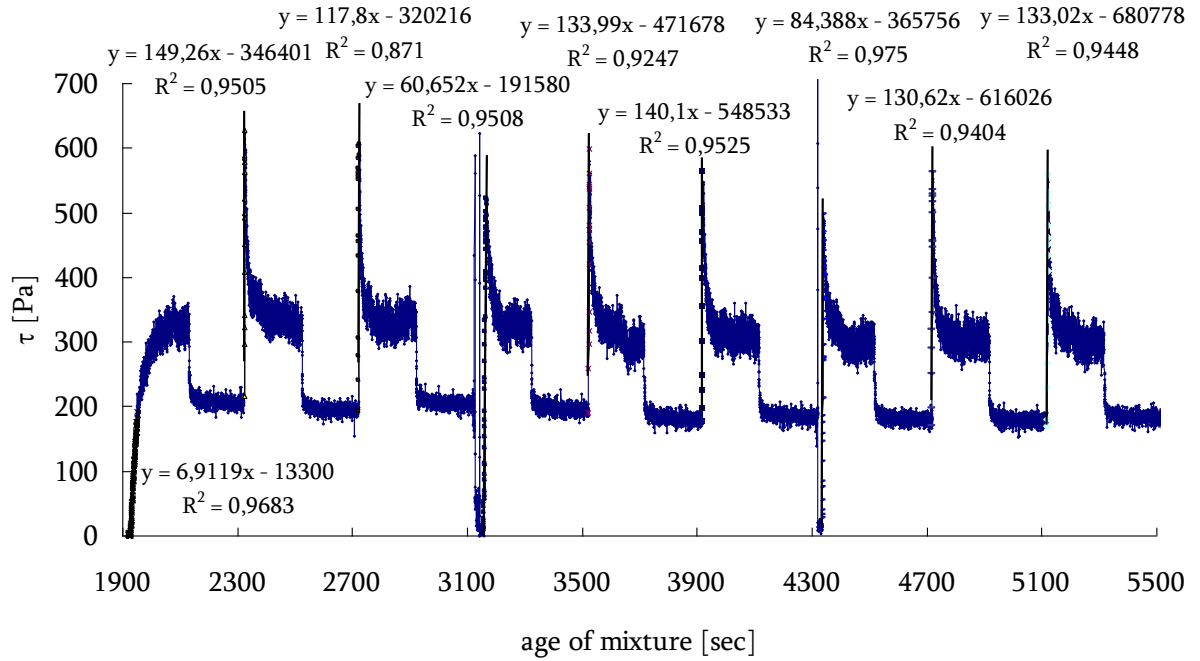
Fig. 29: Calculated time-dependency of stresses for mixture II at age 32 minutes from water addition to start of measurement
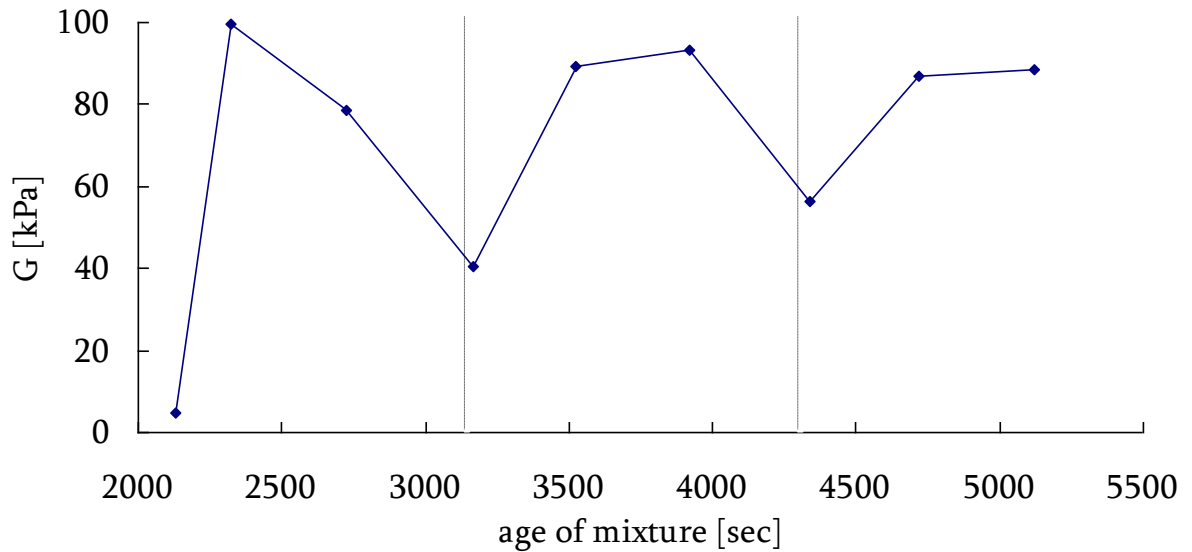

Fig. 30: Development of G modulus of mixture II (dashed lines show shaking)

3.3.2.2   *Second part of measurement – start at age of SCC 94 min*

Figures 31 and 32 show the results of repeating the whole experiment at age 94 minutes with mixture II. Torque-time dependency (Fig. 31) was evaluated in the same way of calculation of stresses as shown in tables 24-26 and Fig. 32.
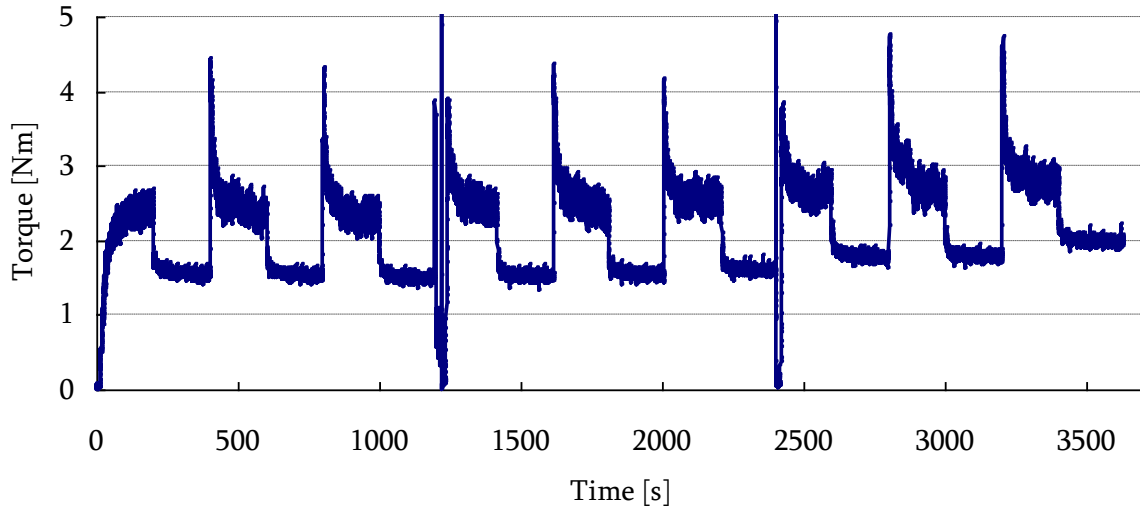
Fig. 31: Torque-time dependence of mixture II at age 94 minutes from water addition to start of measurement

Table 24: Development of yield stresses τ_0 of mixture II

Age of SCC [s]	Age of SCC [min]	τ_0 [Pa]	A_{thix} [Pa/s]	A_{thix} [Pa/s]
5840	97	381.8	0.065	
6045	101	702.6	0.116	
6444	107	685.0	0.106	
6883	115	611.2*	0.089	
7259	121	689.3	0.095	0.090
7647	127	659.1	0.086	
8065	134	603.8*	0.075	
8444	141	752.7	0.089	
8844	147	748.1	0.085	

The yield stress τ_0, which is reached after ,,shaking" is marked by *.

Table 25: Development of residual stresses τ_{res} of mixture

Age of SCC [s]	Age of SCC [min]	τ_{res} [Pa]
6040	101	237.9
6440	107	236.3
6729	112	238.1
7241	121	243.3
7640	127	245.2
8016	134	255.2
8440	141	279.7
8817	147	282.8
9268	154	314.8

Table 26: Development of mobilized τ_{mob} and fully mobilized τ_{fully} stresses of mixture

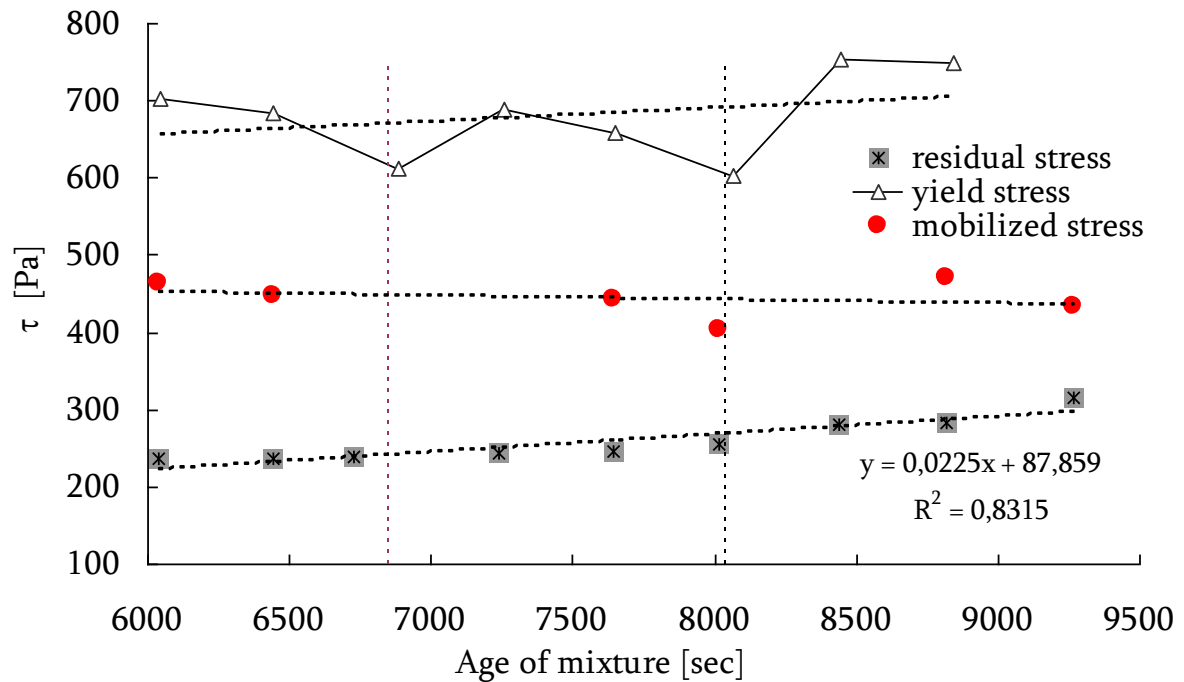| Age of SCC [s]	Age of SCC [min]	τ_{mob} [Pa]	τ_{fully} [Pa]	A_{thix} [Pa/s]
6040	101	464.7	-	0.077
6440	107	448.8	-	0.070
6866	114	-	591.3	0.086
7640	127	444.1	-	0.058
8016	134	403.9	-	0.050
8047	134	-	598.5	0.074
8817	147	469.9	-	0.053
9268	154	433.3	-	0.047

Fig. 32: Development of stresses evaluated for mixture II

Figure 32 shows more tendency of structural build-up over the period of the experiment than does Fig. 25. However, compared to figures 17 and 21 the time dependency is less clear. The structuration rate ranges from 0.16 Pa/s which is an average obtained in the first part of the measurement to 0.09 Pa/s which is an average of the second part. This indicates a slowing structural build-up of mixture. Again, the results are affected by age and confinement as well as motion up and down with inner cylinder before second testing. According to Roussel´s classification (table 6) the mixtures II belongs to thixotropic SCC.

According to procedure 2, where every measured point was used for calculation of the yield stress value, the following dependency was obtained (Fig. 33). The linear regression was applied on the linear part of curves and B as well as G modulus was obtained in same way as mentioned before (Table 27).
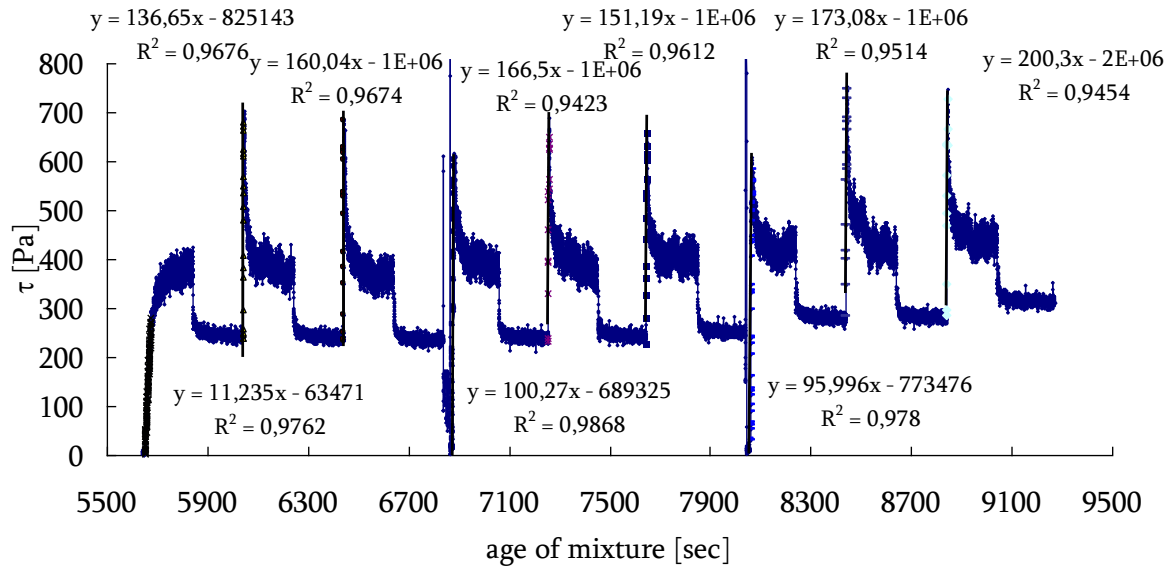
Fig. 33: Calculated time-dependency of stresses for mixture II at age 94 minutes from water addition to start of measurement

Table 27: Obtained data for mixture II

age of mixture		τ_o [Pa]	A_{thix} [Pa/s]	B [Pa/s]	G [Pa]	G [kPa]
[min]	[s]					
97	5840	381.8	0.065	11.2	7467	7,5
101	6045	702.6	0.116	136.7	91133	91,1
107	6444	685.0	0.106	160.0	106667	106,7
115	6883	611.2*	0.089	100.3	66867	66,9
121	7259	689.3	0.095	166.5	111000	111,0
127	7647	659.1	0.086	151.2	100800	100,8
134	8065	603.8*	0.075	96.0	64000	64,0
141	8444	752.7	0.089	173.1	115400	115,4
147	8844	748.1	0.085	200.3	133533	133,5

The yield stress τ_0, which is reached after ,,shaking'' is marked by *.

Development of G modulus is shown in Fig. 34, where an obvious increase of the G modulus before first and after second shaking can be deduced. The G moduli obtained during the second part of the measurement (Fig. 34) are higher than G moduli from the first part of the measurement (Fig. 30) due to the aging of the mortar.
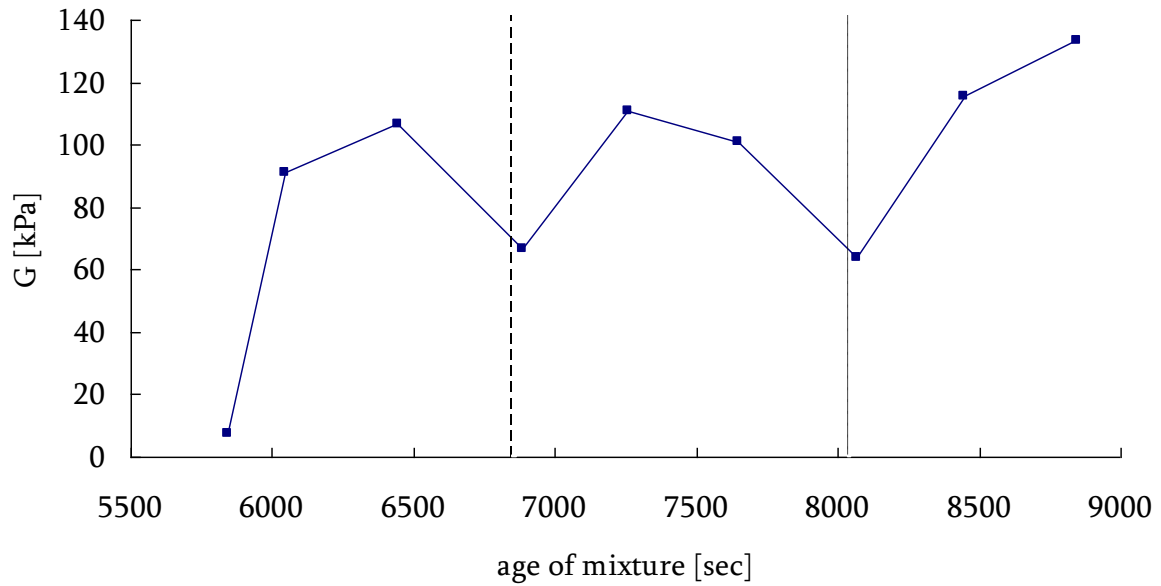
Fig. 34: Development of G modulus of mixture II (dashed lines show shaking)

3.4 Plate test

The result from the plate test gives the time-dependency of yield stress. The structuration rate A_{thix} was obtained from linear regression. These gave the values 0.021 Pa/s for the first mixture and 0.014 Pa/s for the second mixture (Fig. 35 and Fig. 36).

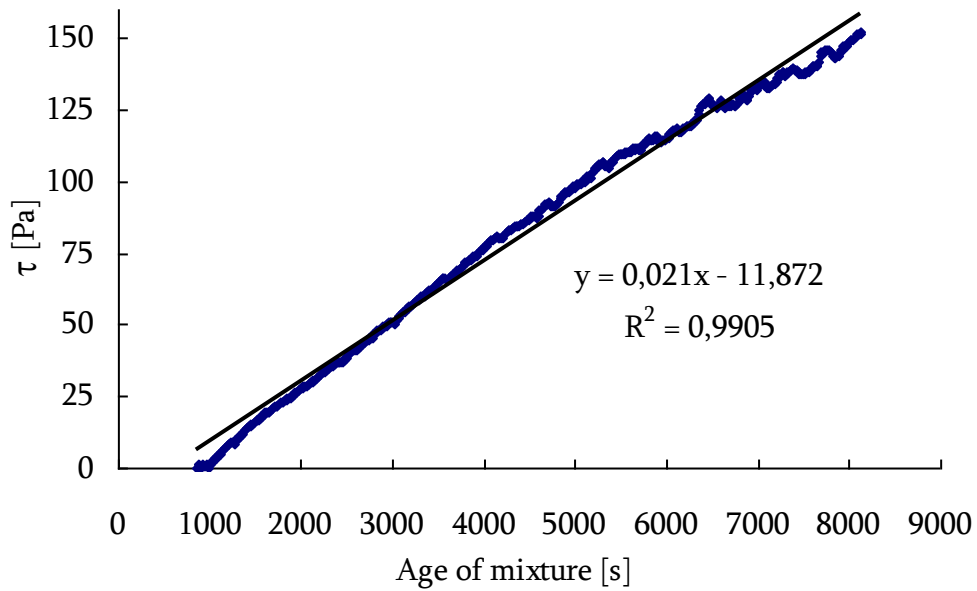$$y = 0{,}021x - 11{,}872$$
$$R^2 = 0{,}9905$$

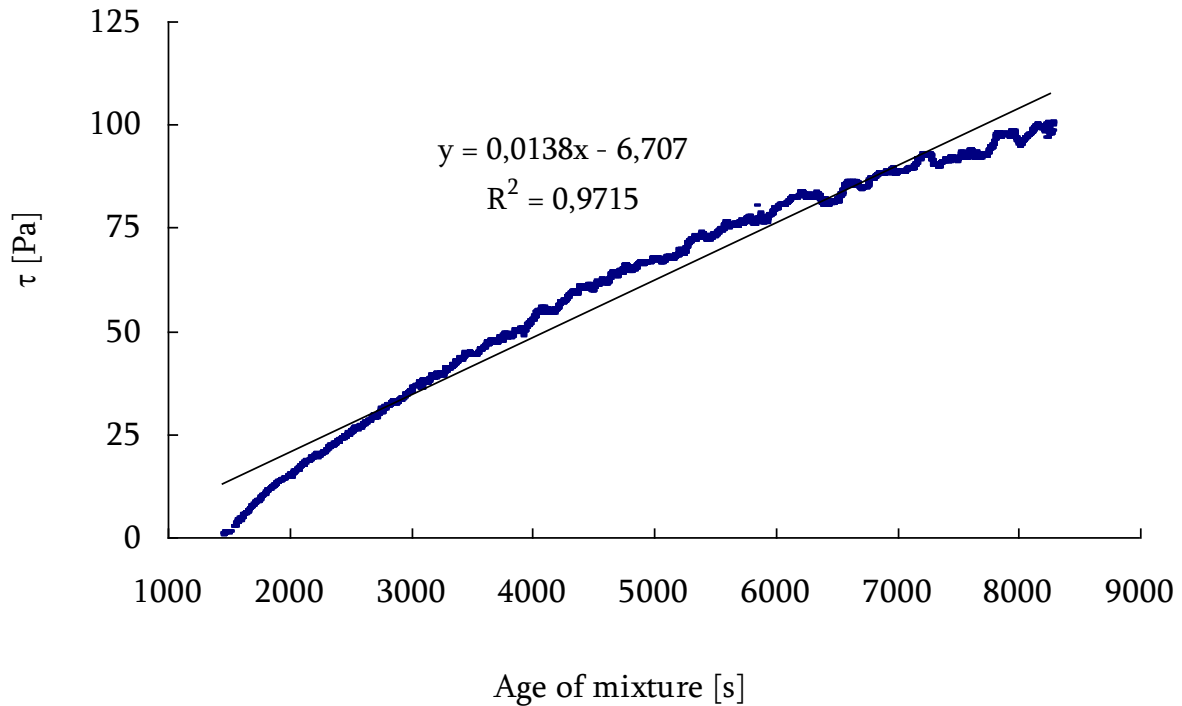Fig. 35: Obtained curve from plate test for mixture I

Fig. 36: Obtained curve from plate test for mixture II

Clearly this method gives very low increase of yield stress values compared to the viscometer values given in tables 10, 13, 15, 16, 18, 20, 22, 23, 24, 26 and 27. It should be noted that the plate test we used was mainly developed for cement paste. Possibly the roughness of the sandpaper on the plate (Fig. 6), which was approximately 0.2 mm, will not reflect the same yield as the rougher surface of the core of the viscometer which has larger knifes (Fig. 4). According Roussel`s classification (Table 6) the tested mixtures belongs to non-thixotropic SCC.

3.5   Conclusions Mortar in ConTec4 and plate test

An investigation on the time-dependant development of yield stress in two similar self-compacting mortars using slowly rotating ConTec4 viscometer and a newly developed plate test was made. The results from the ConTec4 revealed that both the static yield stress and structuration rate depend on the confinement conditions. A much higher static yield stress was obtained with a residual stress in the confined mortar in the viscometer gap compared to yield stress developing in unconfined state at start or after a release of the residual stress by a shaking movement of the viscometer. Also very clear peaks of static yield stress were detected during slow rotation. The absence of these peaks in certain experiments (after stirring, after stress release and possibly during other conditions) needs further investigation. One interesting feature in figure 17 is that the rate of increase of static yield stress seems to be the same with and without confinement.

A more detailed analysis based on data filtration of negative rotation values showed structuration rate of similar magnitude and also allowed to evaluate the shear modulus G which also showed a very clear increase with time.

Finally, measurements with the plate test showed much lower absolute values of yield and lower structural build-up rate, possibly due to the low plate roughness designed for paste tests as opposed to the larger vanes of the viscometer core. Also the deformation conditions around the plate and the viscometer core are very different.

3.6 Results from measurement with parallel plate rheometer

3.6.1 Test I

In this test the effects of various shear rates were investigated. The different sequences used are explained in section 2.2.1.1. Fig. 37 shows the measured curves obtained during sequence 3 and gel strengths are shown in Table 28. Fig. 38, Fig. 39 and Fig. 40 show measured curves obtained during testing with constant shear rate to reach the static yield stresses. The results from these figures are shown in Table 29, Table 30 and Table 31, where the static yield stress and G moduli are evaluated. Fig. 41 shows the obtained flow curves with evaluation of Bingham's parameters that are given in Table 32. Table 33 summarizes test I.
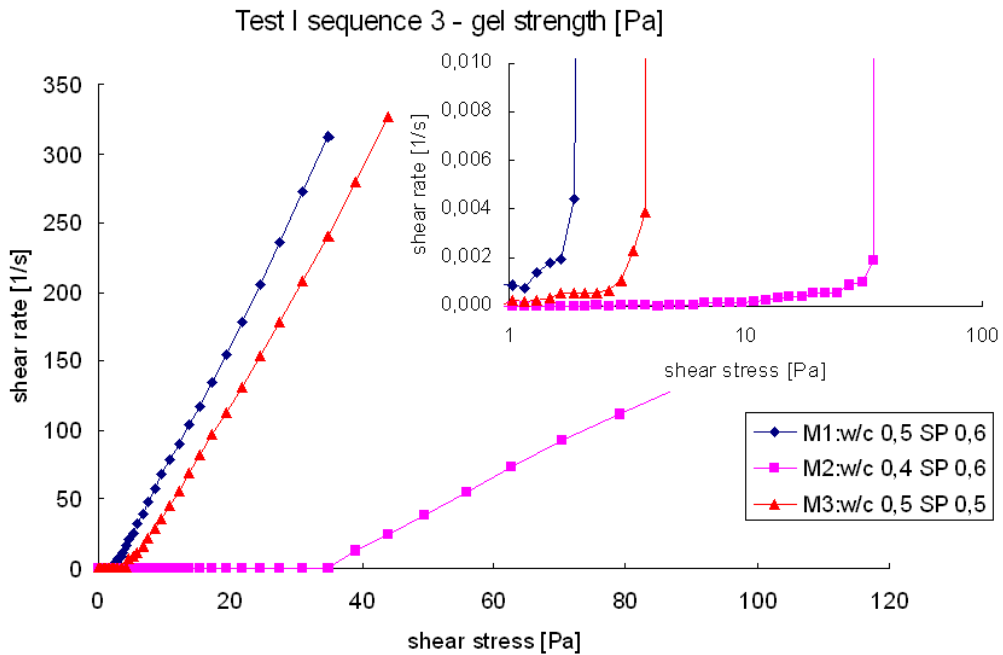

Fig. 37: Gel strength with logarithmic stress sweep of tested matrixes (age of matrixes on start of measurement 11.5 min)

Table 28: Resulting gel strength of matrixes

Matrix	Gel strength [Pa]	Age [min]
M1 w/c=0.5,SP=0.6	2.1	11.5
M2 w/c=0.4,SP=0.6	34.9	11.5
M3 w/c=0.5,SP=0.5	3.8	11.5

The gel strength of the first matrix M1 (corresponding with the mortars tested in previous tests) was 2.1 Pa. A decrease of SP content led to a little bit higher value of gel strength: 3.8 Pa. There was a much larger effect on gel strength on decrease of w/c ratio for matrix M2 with gel strength 34.9 Pa. The obtained curves from the next sequences of test I are the following:
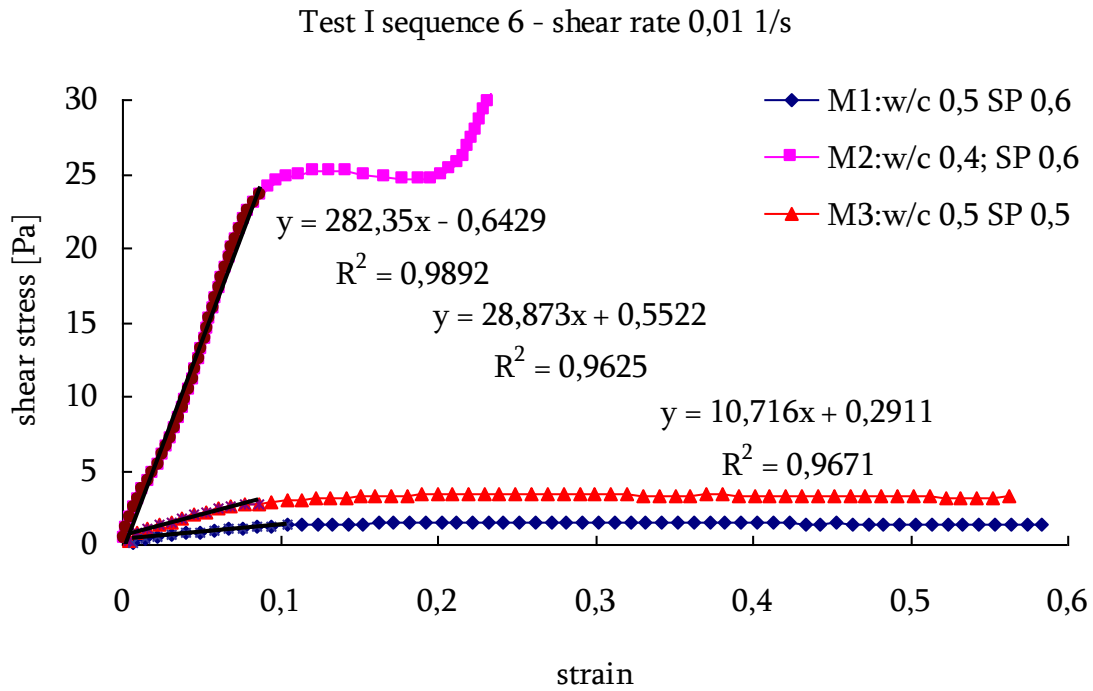
Test I sequence 6 - shear rate 0,01 1/s

Fig. 38: Stress-strain curves obtained from test I sequence 6 for all matrixes (age of matrixes on start of measurement 18 min)

Table 29: Resulting G moduli and static yield stress of matrixes from sequence 6

Matrix	Age [min]	G modulus [Pa]	Static yield stress [Pa]
M1	18.0	10.7	1.5
M2	18.0	282.4	25.2
M3	18.0	28.9	3.4

The highest G modulus was observed for matrix M2 with the lowest w/c ratio: 282.4 Pa. The curve for matrix M2 showed clearest linearity in fig 37 and also the clearest point where the elastic deformation changed to plastic. The value was 25.2 Pa. The end of this curve shows a strange behaviour as shown by rapid increase of shear stress after the plastic behaviour, possibly due to dilatancy at particle rearrangement and change of packing state at interaction at early shear-movement of this most densely packed matrix. Shear stress – strain curves of matrix M1 and M3 have short linear parts before yielding and coming to almost constant stress during increased deformation. The G moduli take the values 10.7 Pa and 28.9 Pa respectively. The static yield stress (evaluated as the maximum value reached during measurement) was 1.5 Pa and 3.4 Pa for M1 and M3 respectively.
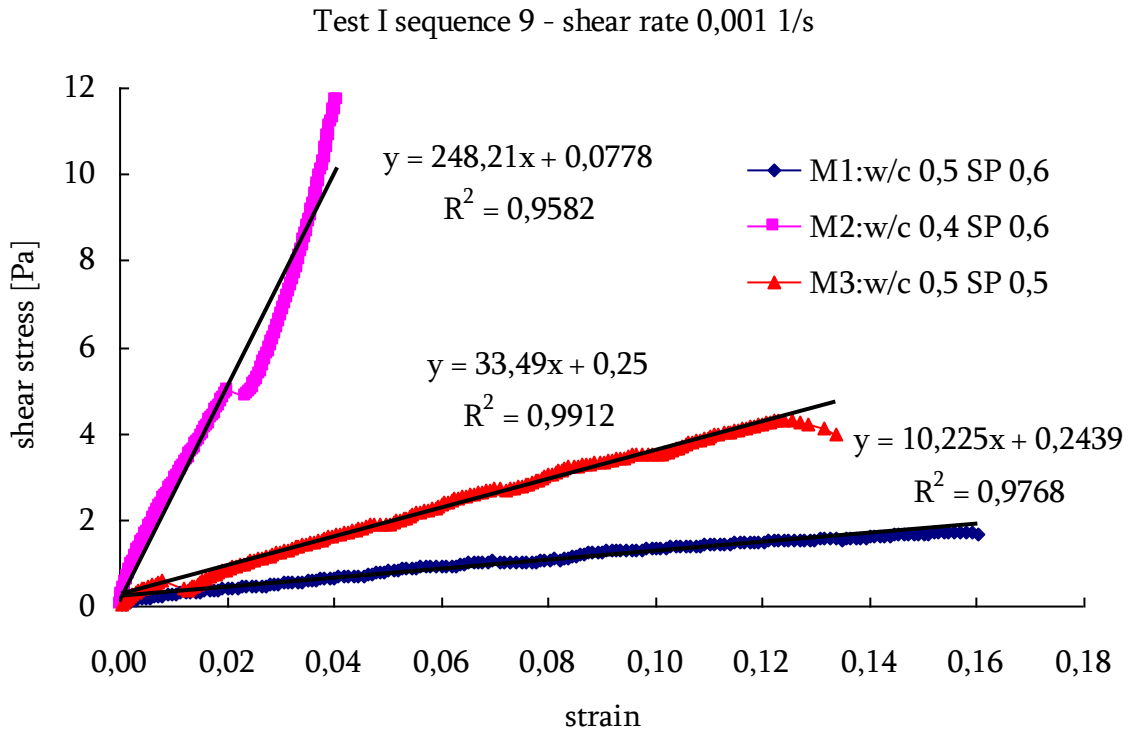
Test I sequence 9 - shear rate 0,001 1/s

Fig. 39: Resulting curves obtained from test I sequence 9 for all matrixes (age of matrixes at start of measurement 20.5 min)

In sequence 9 (shown on fig. 39 and Table 30) the slowest shear rate (0.001 s^{-1}) was used. This very low value of shear rate should give high values of G moduli because of high sensitivity. However, this only seems to be the case for matrix M3 with value of G modulus 33.5 Pa. The G modulus of matrix M1 is practically the same as the value obtained in sequence 6 and it is 10.2 Pa and the G modulus obtained for matrix M2 is a little bit lower compared with previous sequences and reaches the value 248.2 Pa. The static yield stress was caught only for matrix M3, whereas the other matrixes didn't reach the static yield stress because of very low shear rate and not long enough measurement time. The static yield stress of matrix M3 was 4.3 Pa which is a little bit higher value than the value obtained in the previous test sequence (3.4 Pa). This observation is in line with the findings of others [31] observing that applied shear rate strongly affects the static yield stress.

Table 30: Resulting G moduli and static yield stress of matrixes from sequence 9

Matrix	Age [min]	G modulus [Pa]	Static yield stress [Pa]
M1		10.2	-
M2	20.5	248.2	-
M3		33.5	4.3

Test I sequence 12 - shear rate 0,01 1/s

$y = 237{,}27x - 0{,}462$

$R^2 = 0{,}994$

$y = 18{,}713x + 0{,}6147$

$R^2 = 0{,}9596$

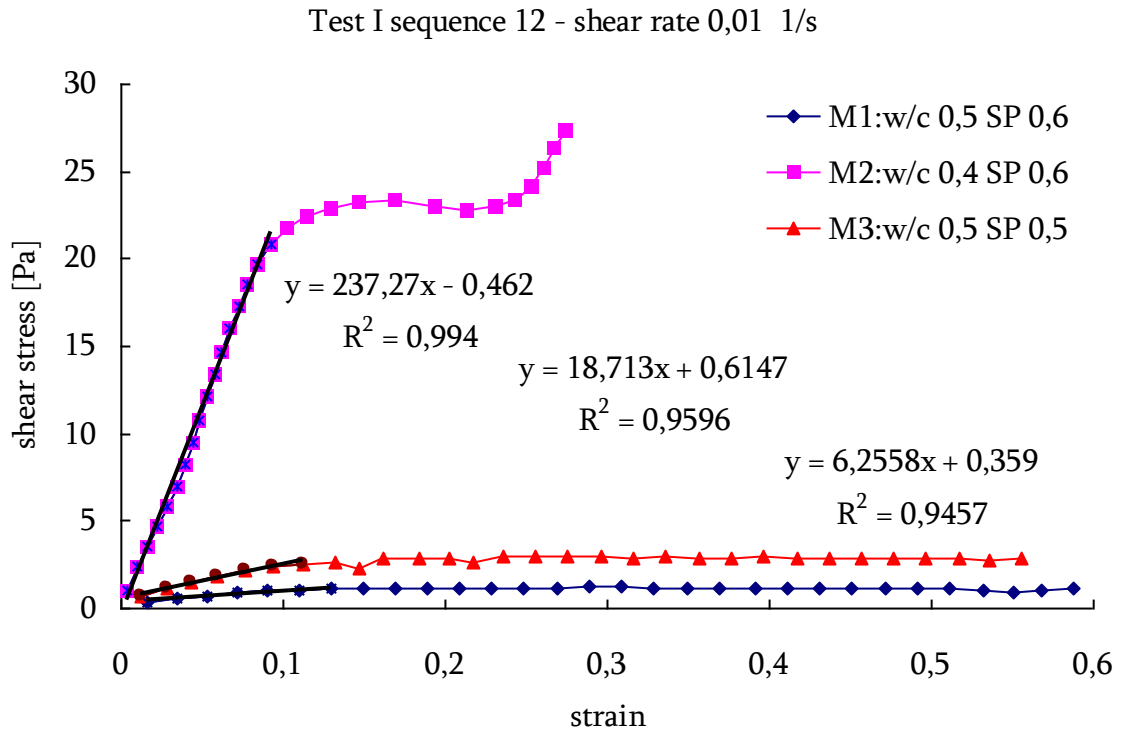$y = 6{,}2558x + 0{,}359$

$R^2 = 0{,}9457$

Fig. 40: Resulting curves obtained from test I sequence 12 for all matrixes (age of matrixes on start of measurement 25 min)

Figure 40 shows sequence 12 which is similar to sequence 6. All obtained values of G moduli are lower compared to the results from sequence 6 and 9. This can be explained by the shear history of the samples (look at the test description) and some breaking of transient bonds in the matrixes during aging (setting). Again the same behaviour is seen for w/c 0.40. All values of G moduli and their change with time are shown in table 31. The ratio dG/dt seems to be more suitable for comparison of results, because these values are almost the same for each sequence (0.01 and 0.01 Pas.s^{-1} for M1; 0.25 and 0.20 Pas.s^{-1} for M2; 0.03 and 0.03 Pas.s^{-1} for M3) except the last sequence (12) where these values are lower because of the shear history of the samples as mentioned. G moduli obtained during test I are summarized in Table 31.

Table 31: Results of G moduli of matrixes obtained by test I

sequence	Age of matrix [min]	Matrix	G modulus [Pa]	dG/dt [Pa/sec]
6	19.0	M1	10.7	0.01
		M2	282.4	0.25
		M3	28.9	0.03
9	20.5	M1	10.2	0.01
		M2	248.2	0.20
		M3	33.5	0.03
12	25.0	M1	6.3	0.00
		M2	237.3	0.16
		M3	18.7	0.01

The last sequence of test I consisted of measuring flow curves of matrixes in shear rate ranging from 0.01 to 60 s^{-1}. The obtained curves are shown in Fig. 41 and the rheological parameters plastic viscosity and yield stress are listed in Table 32. Again we see the possible consequence of dilatancy for w/c = 0.40 in the early part of the flow curve at early particle interaction and rearrangement.
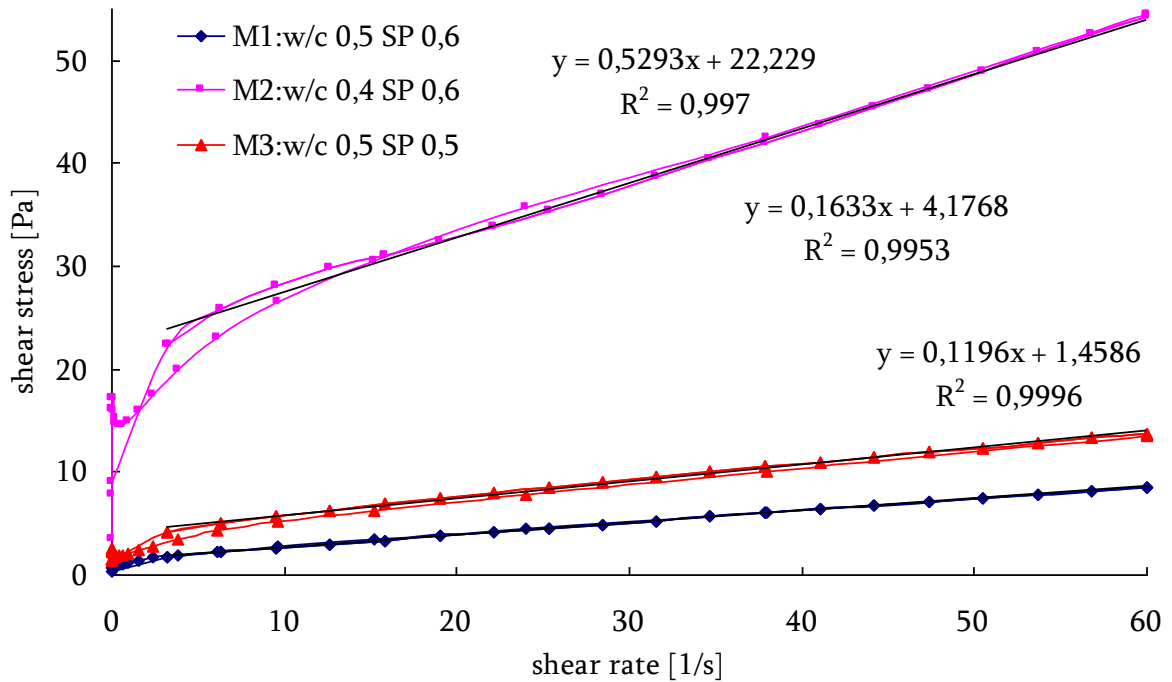
Test I sequence 15,16 - flow curves

Fig. 41: Flow curves of matrixes (age of matrixes on start of measurement 27.5 min and 29.5 min for up-curve and down-curve respectively) with linear regression of down-curves

Table 32: Obtained results from evaluation of flow curve

Matrix	Plastic viscosity [Pa.s]		Dynamic yield stress [Pa]	
	Up-curve	Down-curve	Up-curve	Down-curve
M1	0.12	0.12	1.5 *1.5	1.5
M2	0.61	0.53	19.1 *25.2	22.2
M3	0.17	0.16	3.4 *3.4	4.2
Age [min]	27.5	29.5	27.5	29.5

*the values of the static yield stresses obtained with values from the sequence 6 (table 29)

The Bingham's parameters were evaluated for up and down flow curves. In case of matrix M1 the flow curves were coincident, and therefore also the Bingham's parameters. The flow curves of matrix M2 had different behaviour during very low shear rates and beyond a shear rate of approximately 15 s^{-1} the flow curves became identical. That is the reason for a bit lower plastic viscosity and higher yield stress evaluated from the down-curves compare to the up-curves. The flow curves of matrix M3 show similar tendency. Therefore only yield stress is a little bit higher in case of evaluation from down curves.

The lowest values of plastic viscosity (0.12 Pa.s) and yield stress (1.5 Pa) were found for matrix M1 with the highest water and SP content. As in case of values of gel strength the effect of w/c is more important than SP dosage and led to increasing plastic viscosity to 0.53 Pa.s and yield stress 22.2 Pa (matrix M2). Decreasing SP dosage changed the parameters to 0.16 Pa.s and 4.2 Pa respectively (matrix M3).

Table 33: obtained results from test I for all matrixes

sequence	Test description	Age [min]		M1	M2	M3
3	-	11.5	gel strength	2.1	34.9	3.8
6	shear rate 0.01 s^{-1}	18.0	Static yield stress	1.5	25.2	3.4
			G modulus	10.7	282.4	28.9
9	shear rate 0.001 s^{-1}	20.5	Static yield stress	-	-	4.3
			G modulus	10.2	248.2	33.5
12	shear rate 0.01 s^{-1}	25.0	Static yield stress	1.2	23.4	2.8
			G modulus	6.3	237.3	18.7
15	flow curve-up	27.5	plastic viscosity	0.12	0.61	0.17
			yield stress	1.5	19.1	3.4
16	flow curve-down	29.5	plastic viscosity	0.12	0.52	0.16
			yield stress	1.5	22.6	4.2

All results obtained during the test I are summarized in the Table 33. If the gel strength is compared with the static yield stress of matrixes, in all cases the gel strength achieved higher value. This is connected with quite rapid change of stress (logarithmic sweep) during sequence 3 and more sensitive measurement during sequences where the constant shear rate was used (sequence 6, 9 and 12).

The static yield stresses obtained during sequence 12 (0.01 s^{-1} 2 sec pr point) are a little bit lower than values obtained during sequence 6 (0.01 s^{-1} 1 sec pr point), were the same shear rate was applied. This fact should be connected with breaking new bonds during measurement despite of creating new structure during aging of samples. The static yield stress evaluated for matrix M3 in sequence 9 (the applied shear rate was 0.001 s^{-1}) is higher compared to the stresses obtained in sequence 6 and 12 (the applied shear rate was 0.01 s^{-1}), which is in compliance with [31].

The dynamic yield stress obtained from flow curves is the same as static yield stress in the case of matrix M1. The dynamic yield stress of matrix M2 is lower than the static, which is in compliance with theory [31]. On the other hand, matrix M3 showed the opposite behaviour.

3.6.2   Test II

In this test the behaviour of samples under constant shear rate 0.001 s^{-1} was studied. The obtained curves (Fig. 42) were nearly linear. The lowest regression coefficient 0.92 was found for the last sequence in test II. Results of G moduli and their change with time are shown in the Table 34. G modulus increases with time (from 24 Pa to 31 631 Pa) due to aging (setting) of matrixes. The rate of increase of G (dG/dt) increases almost exponentially as shown on Fig. 43.
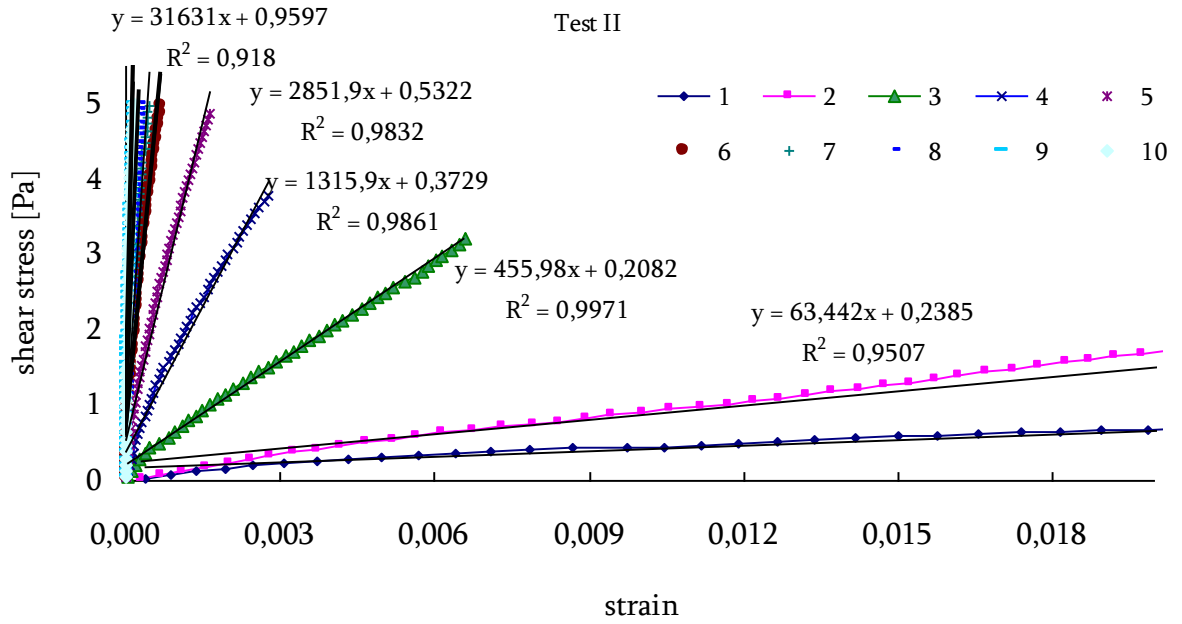
Fig. 42: Measured shear stress- strain curves with linear regressions for evaluation of G moduli (age of matrixes on start of measurement of first curve was 12.0 min and time between individual steps was 5 min)

Table 34: Results from test II

	G [Pa]	age [min]	dG [Pa]	dt [sec]	dG/dt [Pa/sec]
1	24.4	12	24.4	720	0.0
2	63.4	17	39.0	300	0.1
3	456.0	22	392.6	300	1.3
4	1315.9	27	859.9	300	2.9
5	2852.0	32	1536.1	300	5.1
6	6878.7	37	4026.7	300	13.4
7	10479.0	42	3600.3	300	12.0
8	15582.0	47	5103.0	300	17.0
9	27083.0	52	11501.0	300	38.3
10	31631.0	57	4548.0	300	15.2

*age of matrixes on start of measurement of curve

$$y = 0{,}0117x - 14{,}649$$
$$R^2 = 0{,}8409$$

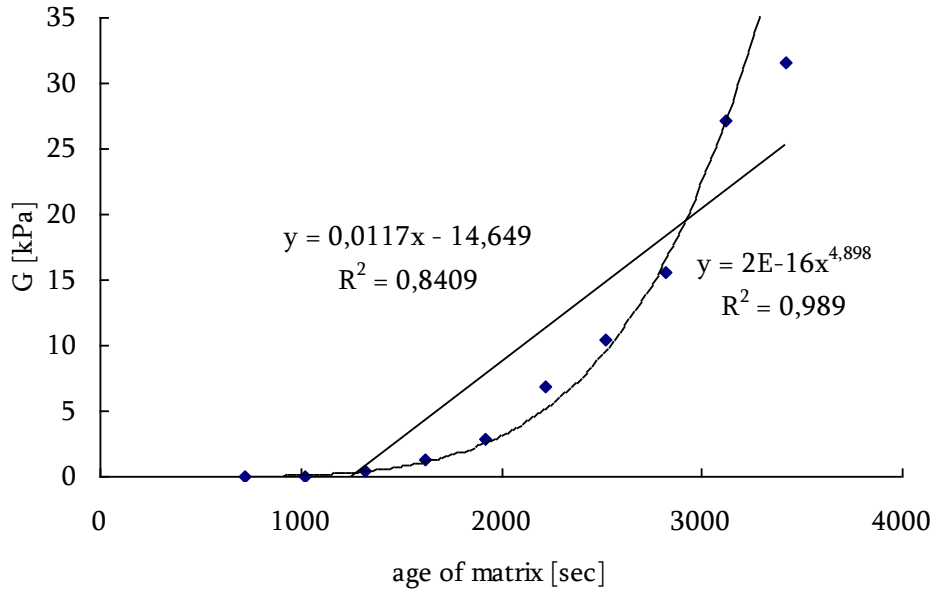$$y = 2E-16x^{4,898}$$
$$R^2 = 0{,}989$$

Fig. 43: Development of G modulus obtained from test II

3.6.3 Test III

The behaviour of the samples was studied in this test under the constant shear rate 0.01 s^{-1}. The lower shear rate compared to the previous test was chosen to reach yield stress in different steps. G moduli were evaluated via linear regression of the initial part before reaching the yield stress (maximum value of shear stress). The first measured curve has no clear yield stress, the stress only slowly increased and then was almost constant, so the static yield stress was evaluated as the highest shear stress reached during measurement. The results of yield stresses, A$_{thix}$, G moduli and their changes are shown in Table 35.
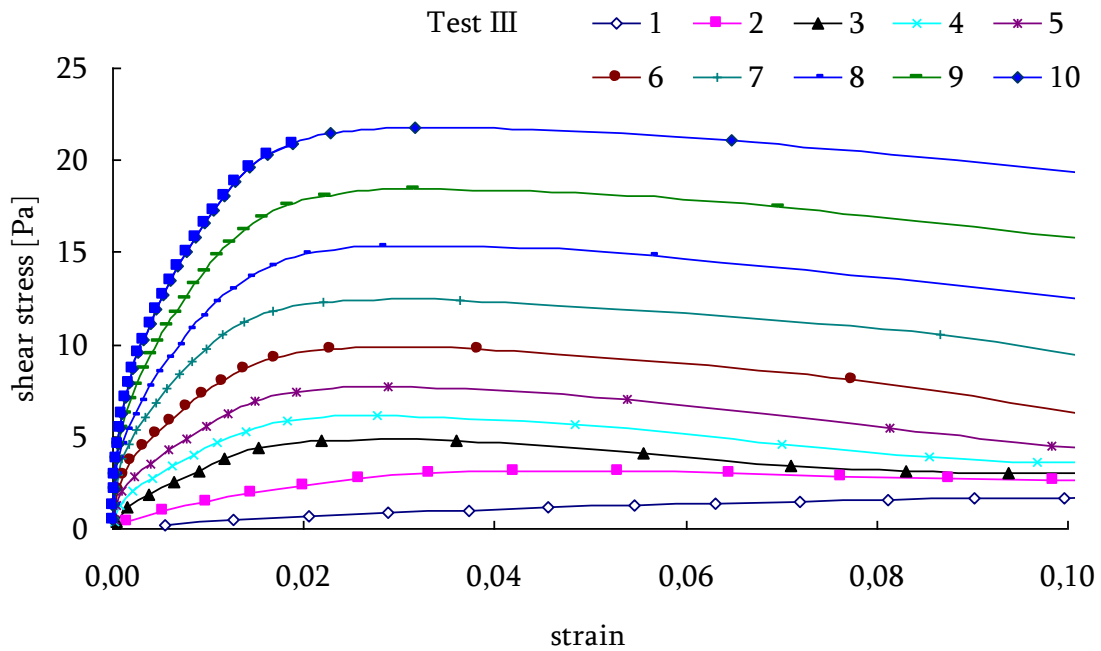

Fig. 44: Measured shear stress - strain curves during test III (age of matrixes on start of measurement of first curve was 12 min and time between individual steps was 5 min)

Table 35: Results from test III

step	age [min]	yield stress [Pa]	A_{thix} [Pa/s]	G [Pa]	dG	dt [sec]	dG/dt
1	12	1.9	0.003	9.8	9.8	720	0.014
2	17	3.2	0.003	80.9	71.1	300	0.237
3	22	4.8	0.004	201.2	120.3	300	0.401
4	27	6.1	0.004	287.4	86.2	300	0.287
5	32	7.7	0.004	403.6	116.2	300	0.387
6	37	9.7	0.004	489.6	86.0	300	0.287
7	42	12.4	0.005	649.3	159.7	300	0.532
8	47	15.3	0.005	792.3	143.0	300	0.477
9	52	18.5	0.006	904.8	112.5	300	0.375
10	57	21.8	0.006	1076.3	171.5	300	0.572
		average	0.005			average	0.357

Graphic representation of time development of yield stresses and G moduli with linear regression are shown on Fig. 45 and Fig. 46. The rate of increase of yield stress and G moduli are 0.008 Pa/s and 0.394 Pa/s respectively.
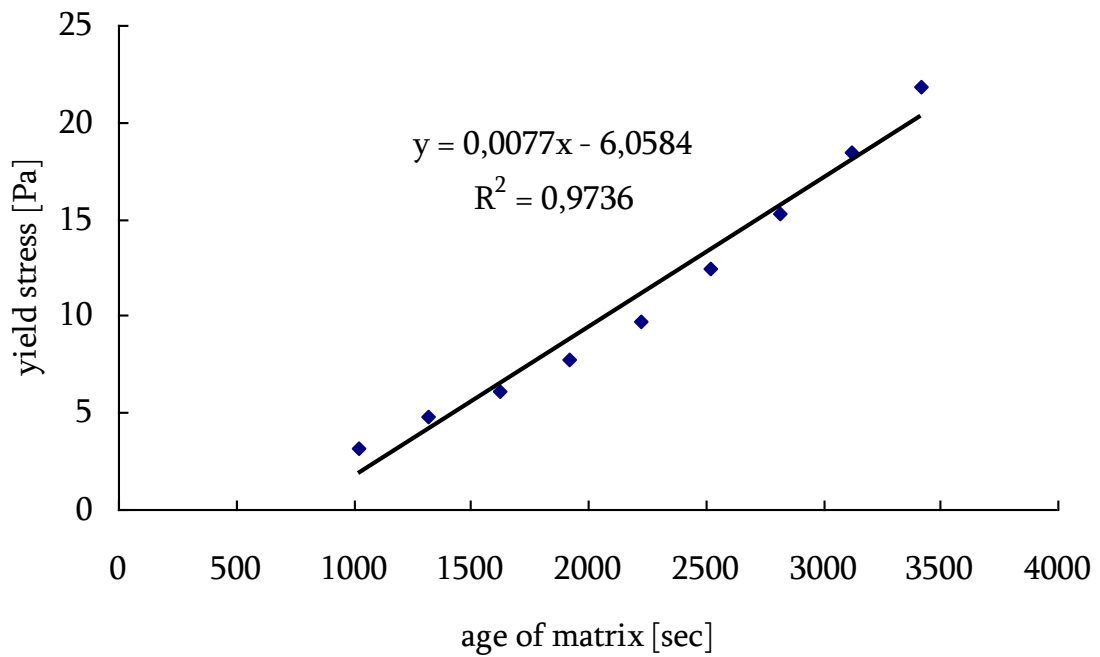

$$y = 0,0077x - 6,0584$$
$$R^2 = 0,9736$$

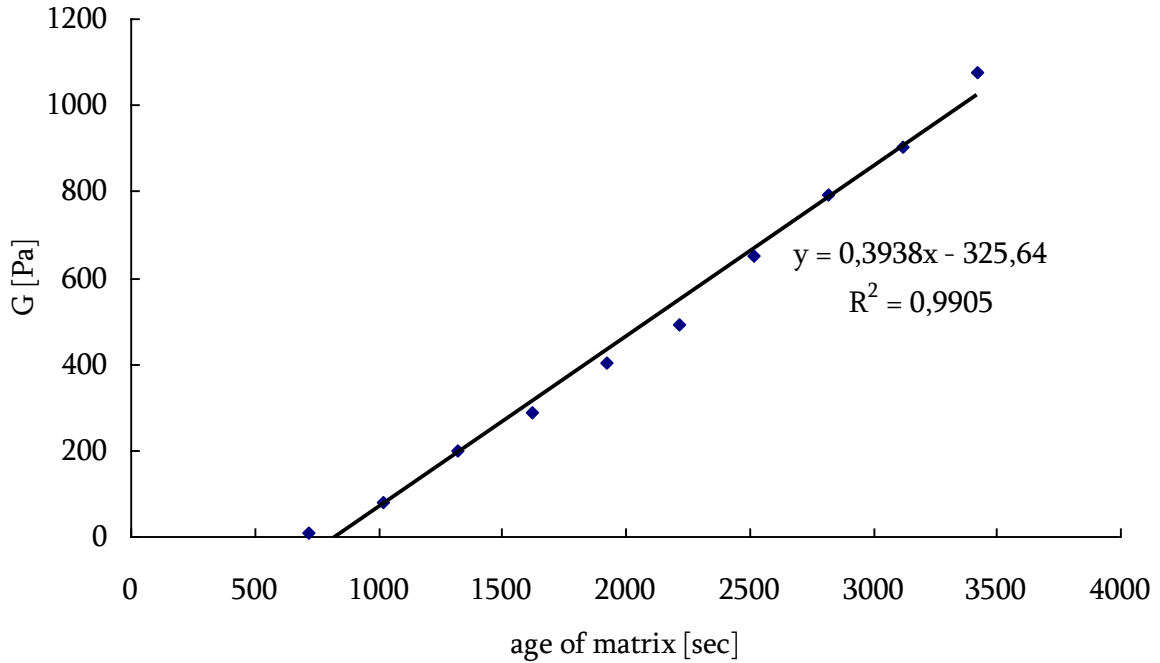Fig. 45: Development of yield stress during aging of matrix

Fig. 46: Development of G modulus during aging of matrix

3.6.4 Conclusion parallel plate rheometer

Measurement with parallel plate rheometer was used for the study of rheological properties of matrixes with fly ash cement and granitic filler from Årdal at w/c = 0.40 and 0.50 and SP = 0.5 and 0.6 % of cement. At first the gel strength was determined for all matrixes and took the value from 2.1 Pa to 34.9 Pa. Flow curves of tested matrixes were evaluated using the Bingham model and plastic viscosity range from 0.12 to 0.52 Pa.s and yield stress from 1.5 to 22 Pa. One can say that all these rheological parameters are much more influenced by w/c ratio than SP dosage.

The static yield stress of the matrices was very shear history dependant and varied very little over time (tables 29, 30) for test I and was very similar to dynamic yield stress (table 32). One reason was the unclear maxima of the constant shear rate tests at 0.01 and 0.001 s^{-1} so that the gel strength test with increasing deformation at exponential stress increase seems better. Shear modulus G seems to give an even safer measure of the structural build-up with clear linear increase of G over time (dG/dt ≈ constant) with R^2 = 0.97 and 0.99 (figures 45 and 46). Then the behaviour of matrixes was studied under constant shear rate and from linear part of obtained curves G moduli were evaluated. G modulus is strongly influenced by magnitude of shear rate which is used for testing. In case of lower shear rate (0.001 s^{-1}) the resulting G moduli will have higher value (24 – 4548 Pa) than moduli obtained in test with higher shear rate (0.01 s^{-1}) (G increased from 10 to 1076 Pa). That is true for yield stress as well.

If the results from matrix's test are compared to the results from mortar tests, the plastic viscosity of mortar is 25.7 Pa.s and matrix was less than 1/100th: 0.12 Pa.s. Yield stress of mortar was determined to be 14.2 Pa and matrix was 1/10th: 1.5 Pa. The structuration rate A$_{thix}$ for mortar was determined to be 0.16 Pa.s for the first part of the measurement and 0.90 Pa.s for the second part. Much lower value of the structuration rate was found for matrixes, only 0.005 Pa.s.

4 Results of part II – summer 2011

4.1 The inclined plane test

Inclined plane tests were carried out to determine static yield stress of SCC and their mortars. The inclined planes were arranged with sandpaper with an average roughness of 200 μm. A small layer of water was sprayed onto the surface of the sandpaper in accordance with the measurement procedure [5]. The measuring cylinder with diameter 62 mm and height 120 mm was filled to 100 mm height for mortar and 120 mm for SCC. The filling time corresponded with time of start of measurement. After filling the cylinder was slowly lifted and the resulting spread was covered with a wide cylindrical container to avoid any evaporation from the mixture during the rest time. After 10 minutes of rest the covering container was removed and the spread was determined. The height of the spread (thickness) was determined by averaging five measurements near the central area. The upper plane was slowly lifted until it started to flow (Fig. 47). The angle of inclination was measured with protractor.
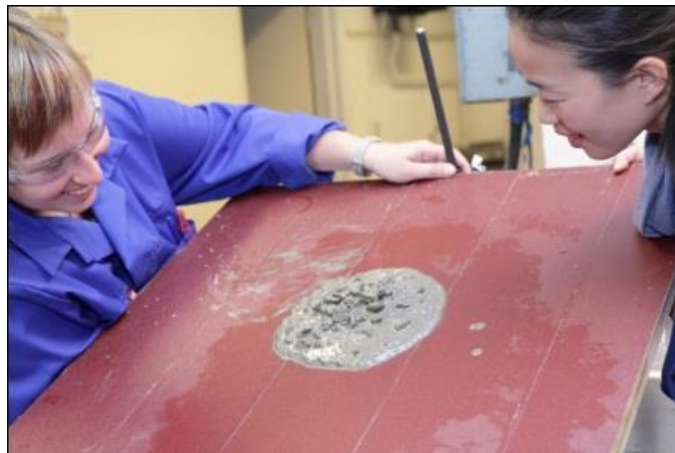

Fig. 47: The inclined plane test with sieved out mortar

The static yield stress was then calculated according to the following formula [5]:

$$\tau_0 = \rho g h \sin \theta \tag{11}$$

where ρ is the density of the sample, g is the gravitational acceleration, h is the thickness of the spread and θ is the angle of inclination of the inclined plane.

4.1.1 Preparing mixtures and proportioning:

The mixtures were prepared according to Table 36 where the proportioning, w/c and SP dosage are shown. The composition of the mortars were proportioned with the same matrix volume as in case of mixture I and II, that means 40 volume %. The used materials were the same too (appendix I). The mixture S1 correspond to the mixture II in first part of the report and mixtures S2 and S3 have different SP dosage. The moisture in the sand was 0.7 %. The volume of prepared mixture was 6 litres.

Table 36: Materials and parameters of mixtures

Materials [kg.m^{-3}]	SI	S2	S3
Norcem Standard FA	432.2	431.7	431.9
Sand	1567.2	1567.2	1567.2
Tau	56.8	56.8	56.8
Water	216.1	215.9	216.0
ResconMapei SP-130	2.6	4.3	3.5
SP %	0.6	1.0	0.8
w/c	0.5	0.5	0.5

4.1.2 The inclined plane test

No angle of inclination was found during the testing of mixture S1, because the flow properties, especially the yield stress of the mixture was too high. Previous testing of this mixture (mixture II) showed a dynamic yield stress value of 14 Pa (from testing with BML viscometer). For the other tests the mixtures with higher SP dosage were used. The results of mixtures S1-S3 are shown in Table 37.

Table 37: Results from plane test

mixture	Age [min]	Density [kg.m^{-3}]	Spread [mm]	h [m]	Angle of inclination [°]	Static yield stress [Pa]	A$_{thix}$ [Pa/s]
S1	19	2247.6	120	0.053	-	-	-
S2	23	2328.1	203	0.014	34	178.8	0.130
S3	18	2265.4	163	0.021	43	318.3	0.295

The static yield stress of mixture S2 was 179 Pa and the structuration rate 0.13 Pa/s which corresponds to thixotropic SCC according Roussel´s classification. The lower dosage of SP in mixture S3 compared to the S2 that reduced SP dosage increases the yield stress.

As already mentioned mixture S1 had too high yield for the inclined plane test with spread 120 mm and height 5.3 cm. Properties measured previously for mixture II (for example slump-flow 565 mm, T500 2.7 sec, structuration rate around 0.1 Pa/s…) may be representative for S1 but were not measured for S1 so its SCC properties are not known.

4.1.3 ConTec4 viscometer

4.1.3.1 mixture S2

Mixture S2 was unstable with bleeding and aggregate separation. During measurement with viscometer segregation could be seen after testing when the sample was poured from the outer cylinder and bigger particles were left at the bottom. Torque-time dependency was not evaluated from Fig. 48 because of the unstability.
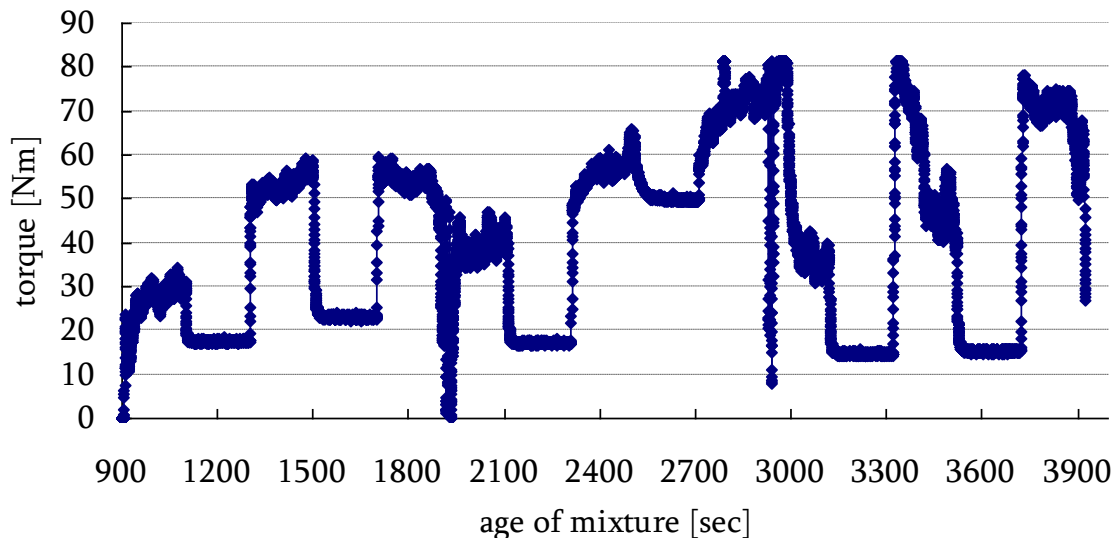

Fig. 48: Torque-time dependence of unstable mixture S2 at age 15 min

4.1.3.2 mixture S3

Mixture S3 was stable, the distribution of coarse particles seemed to be homogeneous and no bleeding was observed. The rheological measurements with the ConTec4 viscometer were carried out to determine plastic viscosity and yield stress by applying decreasing levels of shear rates as shown in Fig. 49. After that the static yield stress was determined as described in part I by measuring torque-

time dependency as very low rotation velocity was applied and stopped every 200 second. During this measurement the inclined plane tests were performed.
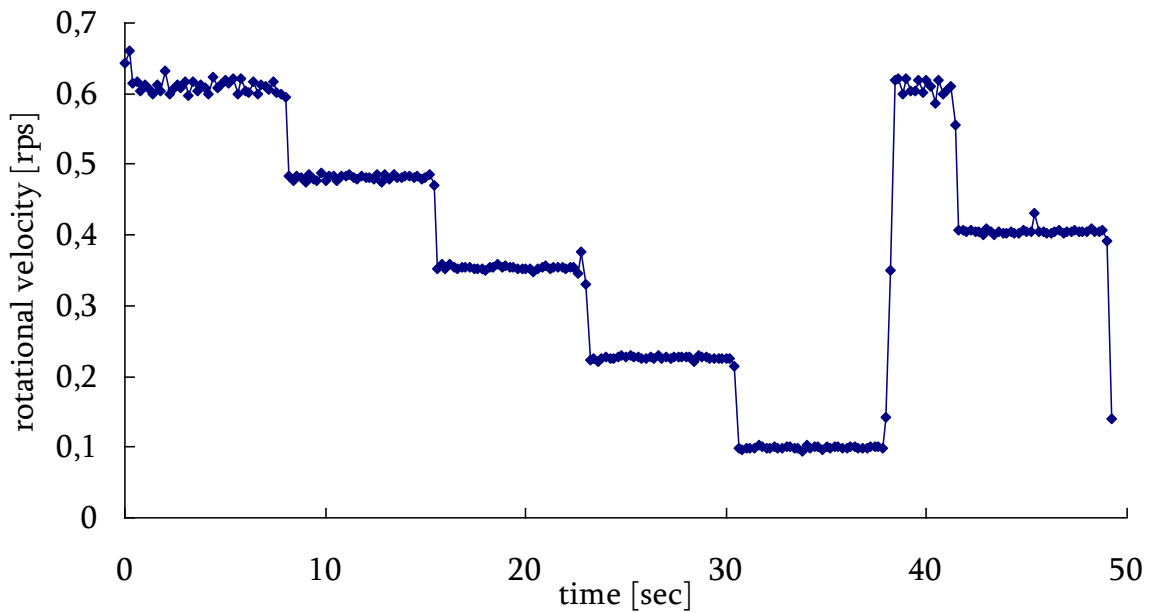

Fig. 49: Rotation history of measurement with ConTec4 – mixture S3

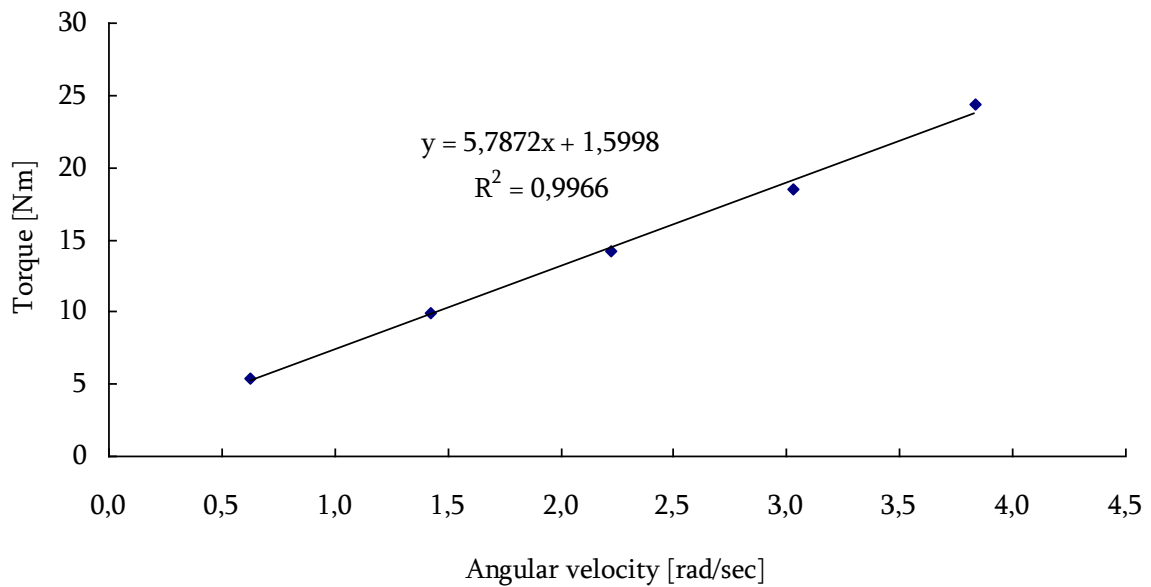$$y = 5{,}7872x + 1{,}5998$$
$$R^2 = 0{,}9966$$

Fig. 50: Resulting curve from measurement with ConTec4 viscometer of mixture S3 at time 14 min after water addition

Table 38: Obtained rheological properties of mixture S3

Time [min]	Dynamic yield stress value [Pa]	Plastic viscosity [Pas]
14	209.0	145.2

The rheological properties of mixture S3 are shown in Table 38. Dynamic yield stress reached 209.0 Pa which seems to be consistent with the value of static yield stress 318.3 Pa. Compared to

mixture II the yield stress and plastic viscosity are ten times higher (yield stress and plastic viscosity of mixture II determined using the larger BML viscometer with much wider gap were 14.2 Pa and 25.7 Pa.s respectively). Mixture S3 has similar proportioning to mixture II, only SP dosage is higher (0.8 % compared to 0.6 %). The viscometer size effect due to the very narrow gap between the torque sensing core and the outer container of the small ConTec4 is the reason for the much higher values of S3.
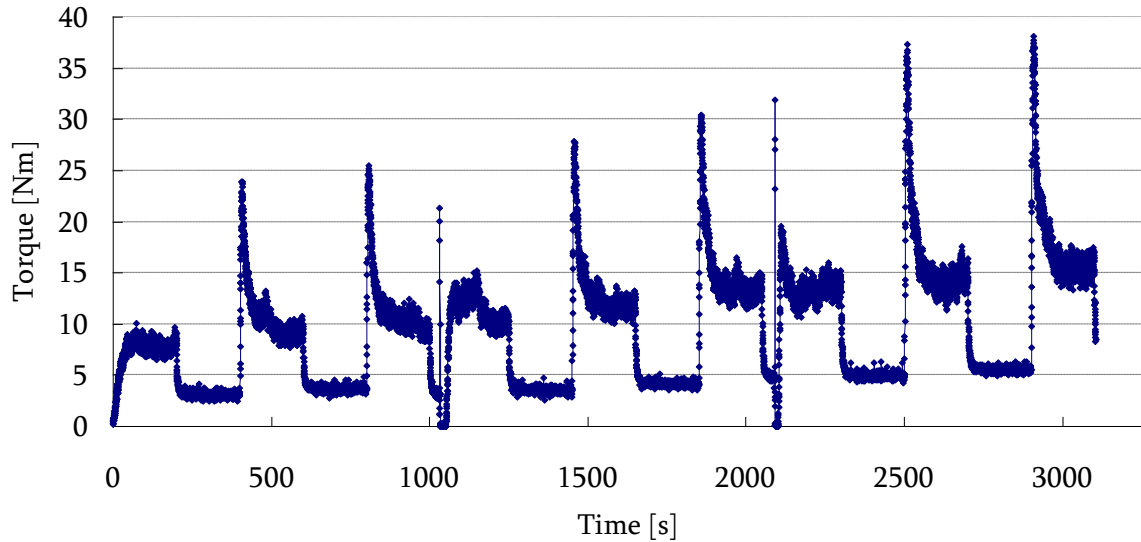

Fig. 51: Torque-time dependency of mixture S3 at age 24 min on start of measurement
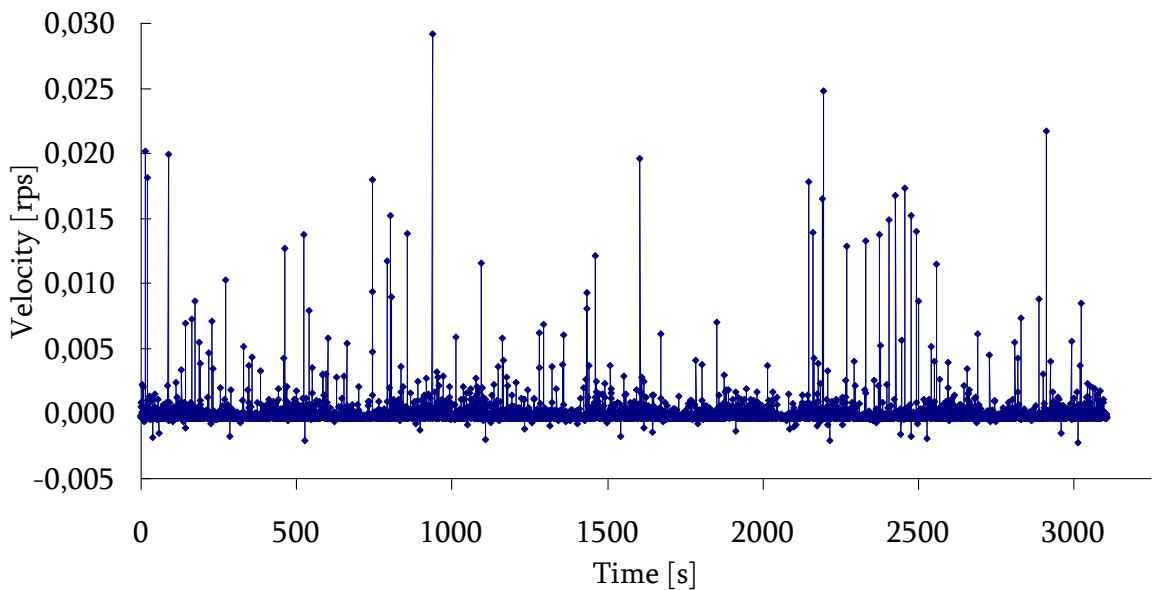

Fig. 52: Velocity profile of measurement

The measured torque-time dependency is shown on Fig. 51 and the velocity profile on Fig. 52. The dependence was evaluated according to procedure 2 with linear regression to evaluate the B and G modulus (Fig. 53). The static yield stresses were evaluated from maximum values of torques which were reached immediately after applying the rotation. The yield stress reached on start of testing and immediately after first shaking show the gradual type of peak, the other stresses show sharp types of peaks as seen earlier and this is most probably due to the effect of confinement by the residual stress on yield stress build-up. Apparently the moderate pressure affects the thixotropic structural build-up, as seen from Fig. 53 and partly for Fig. 18, Fig. 22 and Fig. 31 the peaks after "shaking" are lower

compared to peaks starting from a confined stress state. The results for mixture S3 are summarized in Table 39.
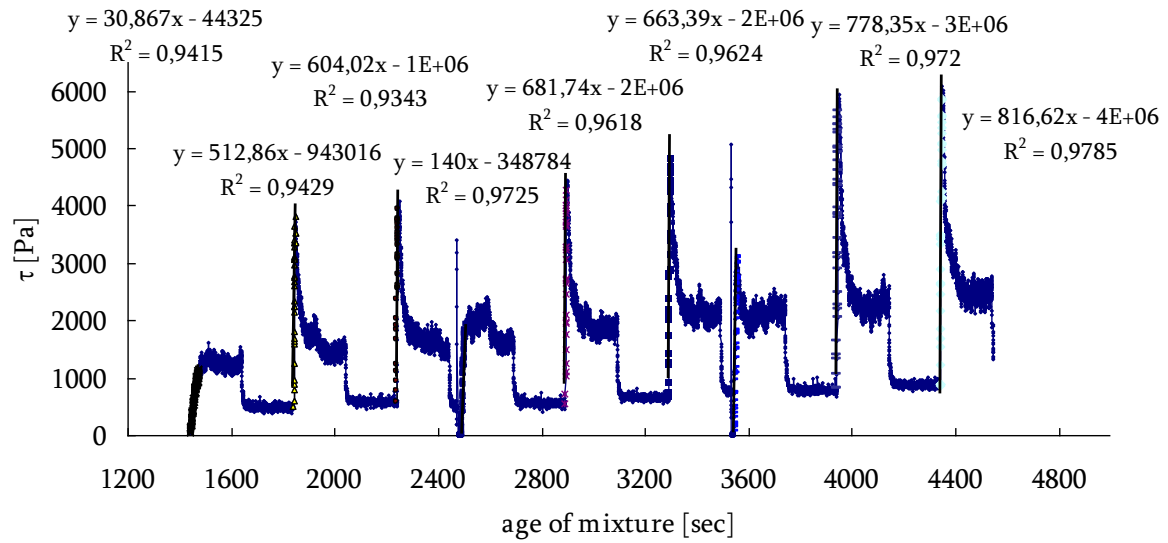

Fig. 53: Calculated time dependency of shear stress for mixture S3 with linear regressions to determine B

Table 39: Obtained data for mixture S3

| age of mixture | | τ_o [Pa] | A_{thix} [Pa/s] | B [Pa/s] | G [Pa] | G [kPa] |
[min]	[s]					
25	1475	1411.4	0.957	30.8	20533	20,5
31	1847	3818.3	2.068	512.9	341933	341,9
37	2249	4072.0	1.811	604.0	402667	402,7
37	2240	2236.1	0.894	140.0	93333	93,3
48	2897	4453.3	1.537	681.7	454467	454,5
55	3299	4852.8	1.471	663.4	442267	442,3
59	3551	3114.9*	0.877	322.2	214800	214,8
66	3949	5954.4	1.508	778.4	518933	518,9
72	4349	6082.5	1.399	816.6	544400	544,4

The yield stress τ_0, which is reached after ,,shaking" is marked by *.

The values of the static yield stresses increase almost linearly ($R^2 = 0.9588$) as shown on Fig. 54, where the first stress and stresses reached immediately after shaking were showed as a crosses with linear increasing tendency.
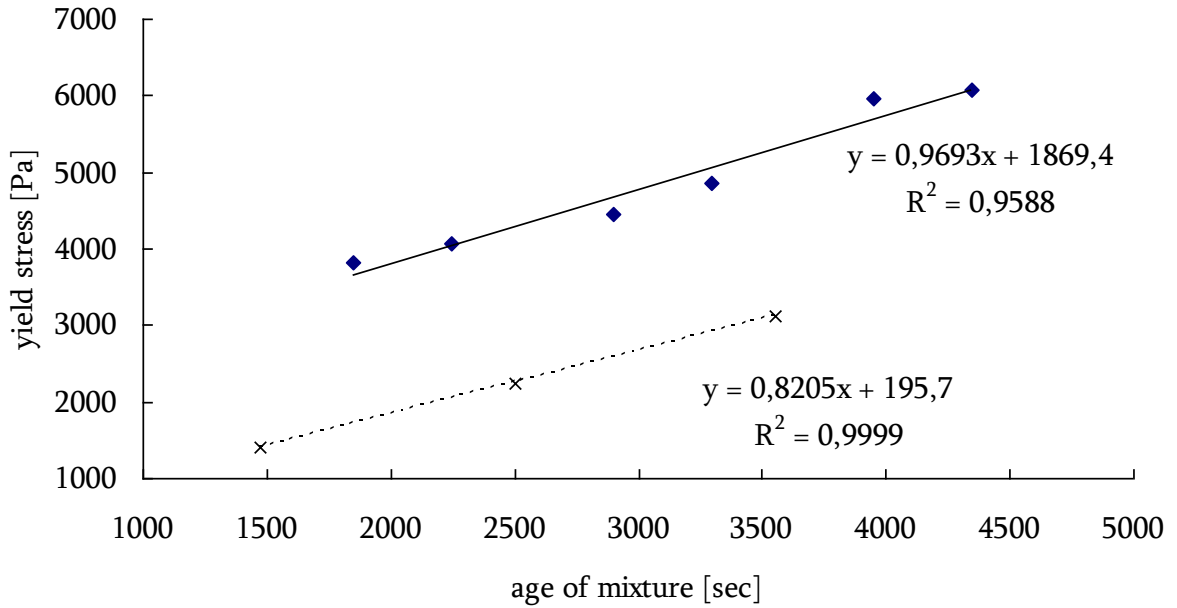
Fig. 54: Development of static yield stresses of mixture S3, lower line shows the unconfined first yield stress and stresses which were reached immediately after shaking and the upper line shows confined yield stress reached during confinement by the residual stress

The obtained values of yield stress are more than ten times higher than dynamic yield stress evaluated from the (Bingham's) flow curve (Table 38). This leads to high structuration rate, which was approximately 1.5 Pa/s. Comparing this value with results for mixture II (the difference between mixture II and S3 was in SP dosage, 0.6 % and 0.8 % for mixture II and S3 respectively) where A_{thix} was approximately 0.2 Pa/s as shown in Table 23 makes it a bit hard to explain the high A_{thix} of S3. However, since mix S2, which separated, had high values too, the S3 results could be related to slight segregation of large particles, though with much less accumulation at bottom than for S2. According to literature [17], the SP dosage should lead to a decrease of the yield values.. Possibly also a slightly more well-dispersed mix and/or slight difference in cement- and/or SP composition over the time period (almost a year) could have contributed to the difference from mixture II.
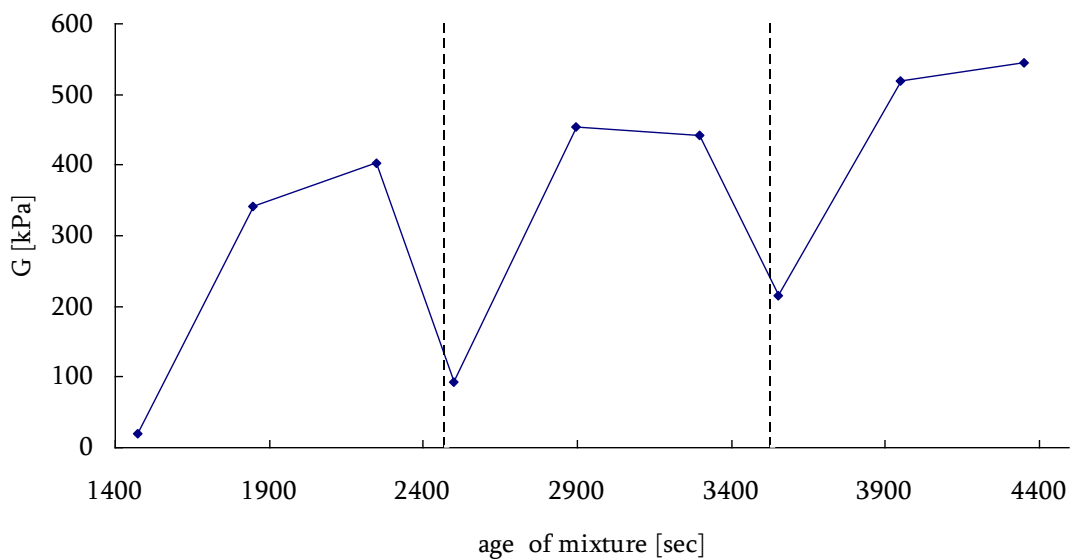

Fig. 55: Development of G modulus of mixture S3 (dashed lines show shaking)

Development of G modulus is shown on Fig. 55, where the increase of G modulus reached immediately after shaking is clearly seen. The G moduli obtained between shaking have increasing tendency. The maximal values of G modulus reached approximately 550 kPa after 72 min, which is ten times higher value compare to the G modulus obtained in case of mixture II (Table 23). Again, since the tests were done on similar, though not identical, materials more than half a year later than mix I and II this could be part of the explanation for differences.. Clearly the static yield stress is a sensitive parameter both in terms of test method, test set-up, test conditions (confinement, shear history, age…) and material composition.

4.2 Testing SCC mixtures from ready-mix concrete plant

After these initial studies of the S- mixes that were similar to the first M-mixes, static yield stress was measured on 3 different SCCs produced at a ready-mix plant and tested in a work of Klaartje de Weerdt in the summer of 2011. There the effect of stabilization on the surface quality of concrete elements was investigated [32]. The proportioning of the mixtures is shown in Table 40 and Table 41.

Table 40: Parameters of the three different ready mix SCCs used

Initial parameters	Filler stabilized	Chemically stabilized	Unstable SCC
w/c	0.678(*)	0.65	0.65
w/p	0.42	0.49	0.49
f/c (limestone filler) [%]	22.5	0.0	0.0
Admixtures	% of C	% of C	% of C
AE	0.65	0.65	0.65
SP	0.71	0.84	0.75
retarder	0.10	0.10	0.10
Stabilizer	0.0	0.75	0.0
Matrix	l/m^3	l/m^3	l/m^3
Matrix volume	332	310	310
Volume cement glue	299	276	276

(*) due to an error in the moisture content of the sand the w/c ratio of the filler stabilized SCC is 0.678 instead of 0.65

Table 41: Weighed in quantities for the production of the different SCCs

Materials [kg/m^3]	Filler stabilized	Chemically stabilized	Unstable SCC
CEM II/A-V 42.5 R	278.2	278.3	278.3
Limestone powder	62.5	0.0	0.0
Free water	177.8	178.2	178.2
0/8 mm Søberg aggregate	1001.2	1035.7	1035.7
8/16 mm Ramlo aggregate	819.2	847.4	847.4
AE	1.81	1.81	1.81
SP	1.98	2.34	2.09
Retarder	0.28	0.28	0.28
Stabilizer	0.0	2.09	0.0

4.2.1 Testing

The fresh concrete was characterized via several tests and some properties like density, air content, slump flow, plastic viscosity and yield stress (dynamic and static) were determined. The concrete was sieved to obtain mortar with all particles smaller than sieve size 6.3 mm. The sieved mortars were characterized by Bingham parameters from flow curves using ConTec4 viscometer and static yield stress and density were determined as well.

4.2.2 Results

The structural build up of sieved mortar was investigated in detail using the ConTec4 viscometer. Testing was performed in the same way as in previous measurement alternating the applied rotation speed. All achieved results concerning the three tested mixtures are published in the work by Klaartje de Weerdt et al. [32]. The measured torque-time dependencies were evaluated according to procedure 2 with linear regression to evaluate the B and G modulus and the static yield stress were evaluated too.

4.2.2.1   Sieved mortar from filler stabilized SCC mixture

Torque-time dependency of filler stabilized mixture is shown on Fig. 56, velocity profile of measurement is shown on Fig. 57 and the calculated yield stress – time dependency on Fig. 58. The yield stress reached at start of testing shows gradual types of peaks, other stresses show sharp type of peak. The results for filler stabilized mixture are summarized in Table 42 and on Fig. 59 and Fig. 60.
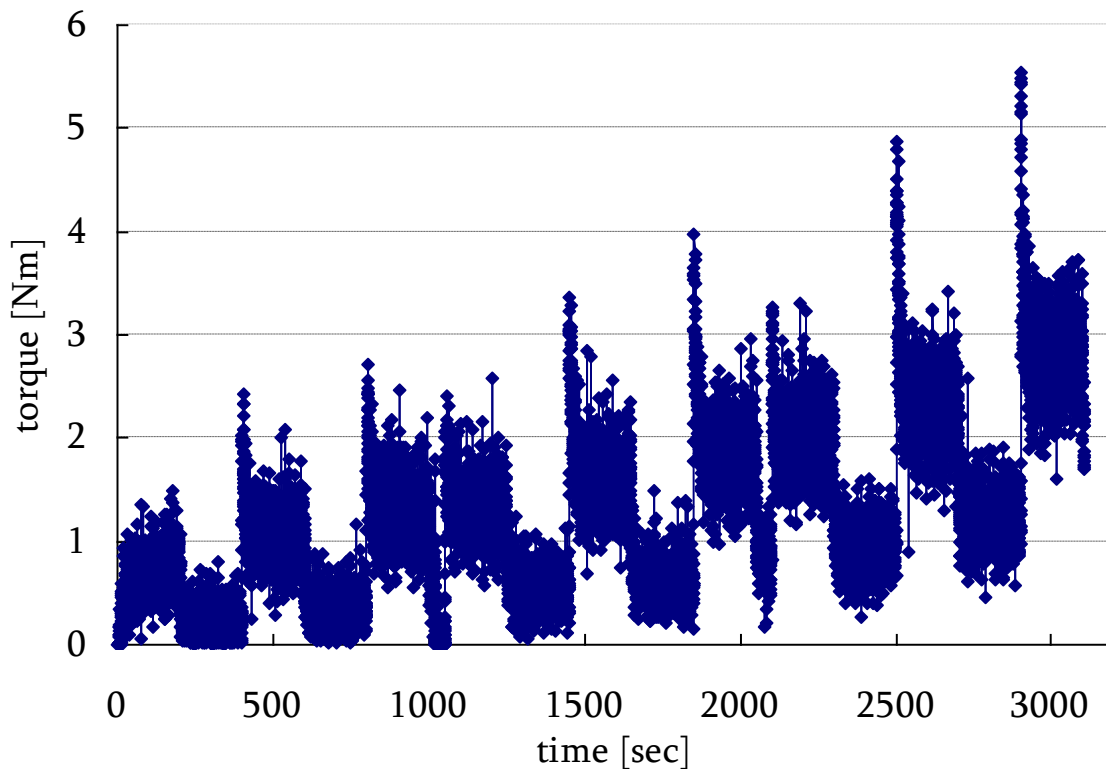

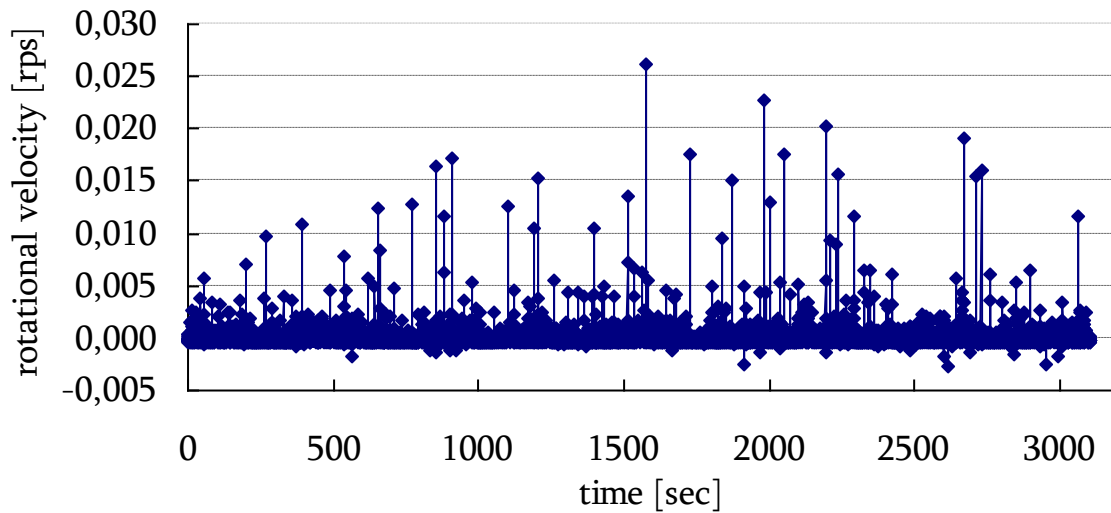Fig. 56: Torque-time dependence of filler stabilized mixture
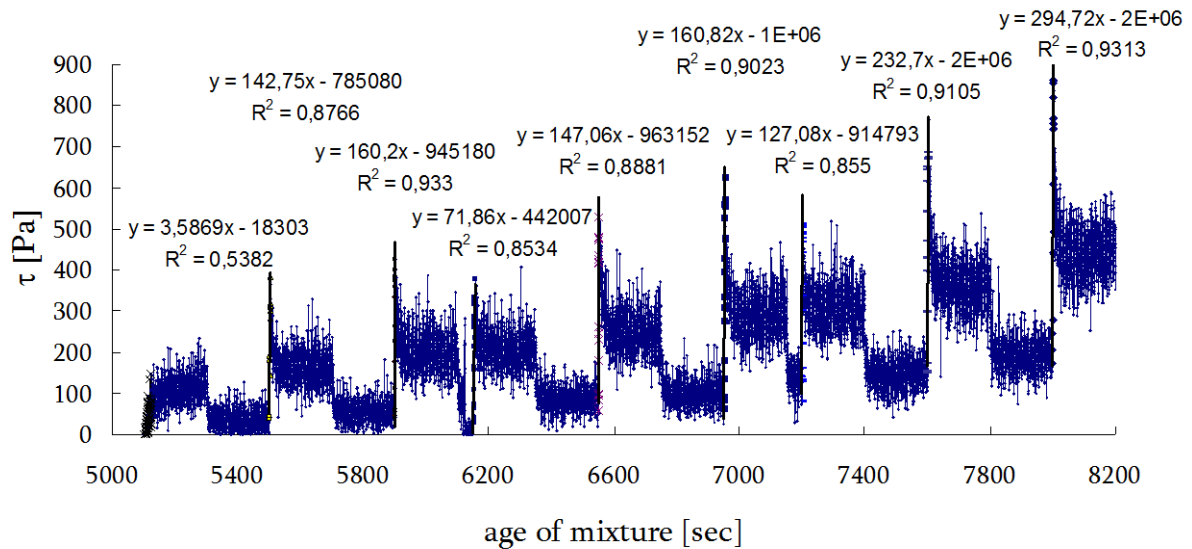
Fig. 57: Velocity profile of measurement

Fig. 58: Calculated time-dependency of stresses (including yield stress) for filler stabilized mortar with linear regressions to determine B

Table 42: Obtained data for filler stabilized mortar

age of mixture		τ_o [Pa]	A_{thix} [Pa/s]	B [Pa/s]	G [Pa]	G [kPa]
[min]	[s]					
88	5300	167.9	0.032	3.6	2400	2.4
92	5503	383.3	0.070	142.8	95200	95.2
98	5903	426.1	0.072	160.2	106800	106.8
103	6156	377.8*	0.061	71.9	47933	47.9
109	6553	527.8	0.081	147.1	98067	98.1
116	6953	626.7	0.090	160.8	107200	107.2
120	7203	513.7*	0.071	127.1	84733	84.7
127	7605	765.7	0.101	232.7	155133	155.1
133	8004	872.9	0.109	294.7	196467	196.5

The yield stress τ_0, which is reached after ,,shaking'' is marked by *.

As shown on Fig. 59 the yield stress has an increasing linear tendency with low decrease immediately after shaking. Nevertheless after that the increase of yield stress is continuing, so the stresses reached immediately after shaking (the first one, i.e. yield stress build-up at un-confined conditions in the ConTec4 after shaking to release the residual stress) are showed as crosses and had linear tendency too. In the end the yield stress reached the value almost 900 Pa. The rate of increase of yield stress slowly increased and reached the value 0.11 Pa/s, which corresponds to a thixotropic mixture according to Roussel´s classification in Table 6. A similar tendency could be seen in the development of G modulus as shown on Fig. 60.

$y = 0,1978x - 735,47$
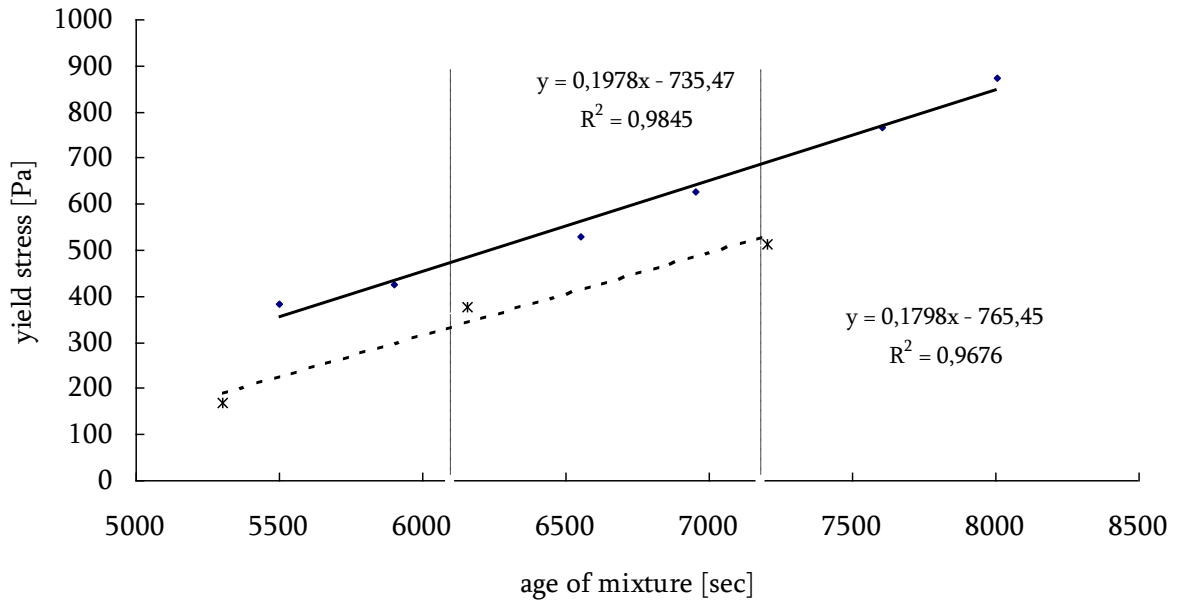$R^2 = 0,9845$

$y = 0,1798x - 765,45$
$R^2 = 0,9676$

Fig. 59: Development of yield stresses of filler stabilized mortar (dashed lower line shows unconfined yield stress and top-curve shows time development of yield stress confined by residual stress in viscometer)
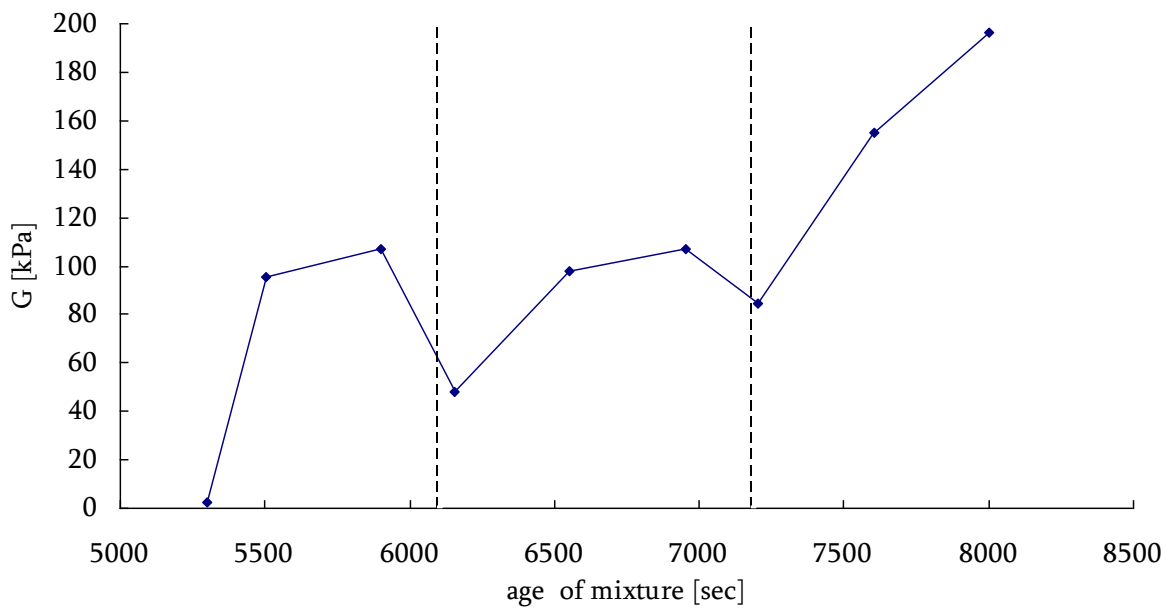

Fig. 60: Development of G modulus of filler stabilized mortar (dashed lines show shaking)

4.2.2.2   Sieved mortar from chemically stabilized SCC mixture
   Torque-time dependency of the chemically stabilized mixture is shown on Fig. 61, velocity profile of measurement is shown on Fig. 62 and calculated time-dependency of stress on Fig. 63. The yield stresses reached in start of testing and immediately after shaking show gradual type of peak, others show sharp type of peak. The results for chemically stabilized mixture are summarized in Table 43 and in Fig. 64 and Fig. 65.
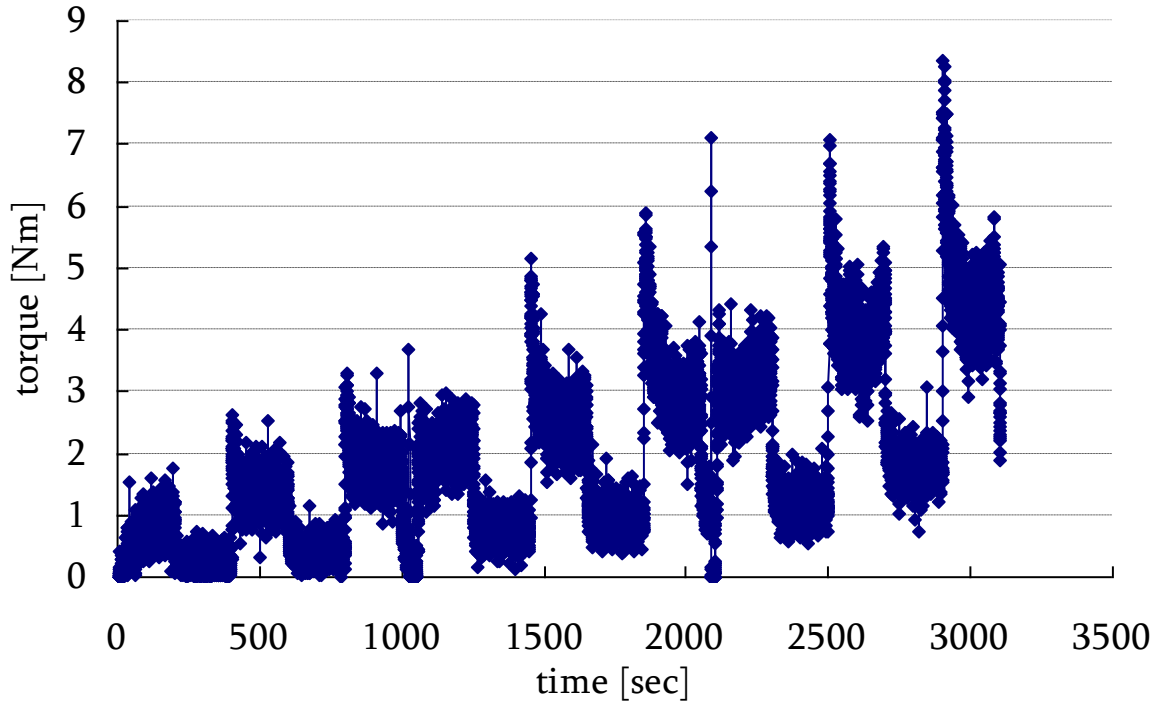

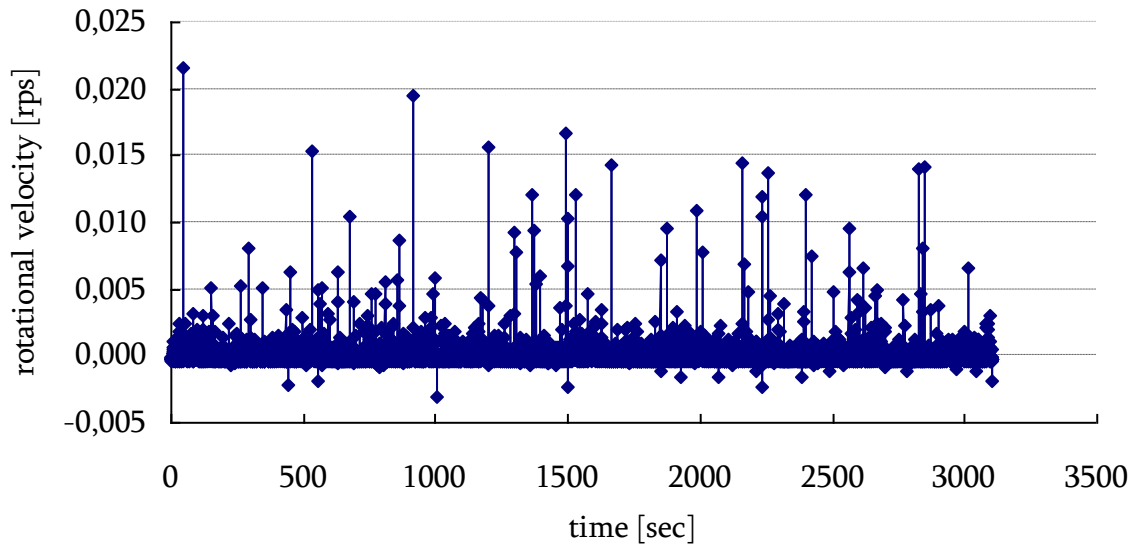Fig. 61: Torque-time dependence of chemically stabilized mixture

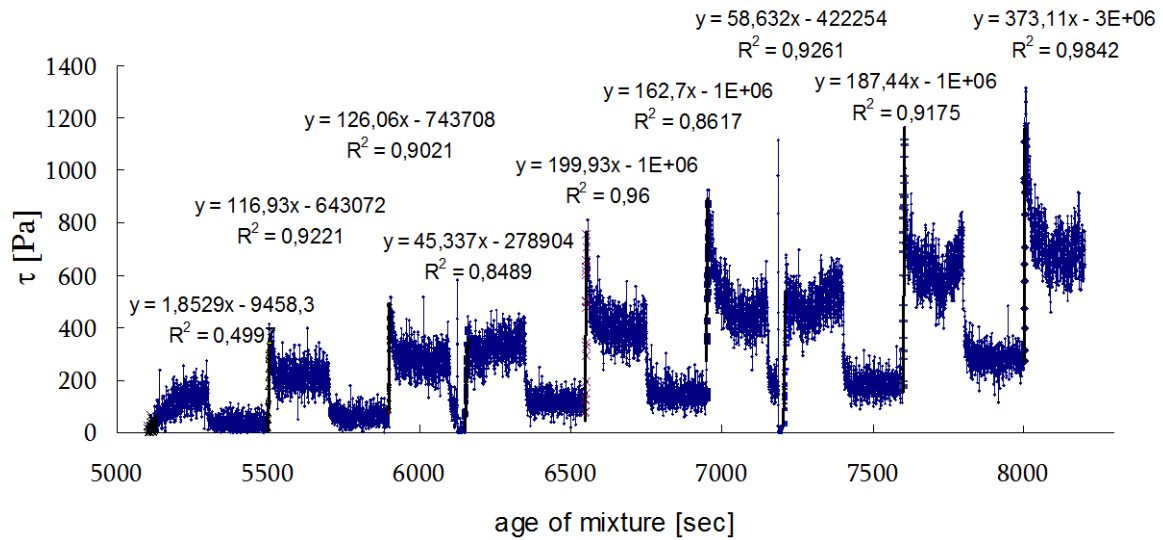Fig. 62: Velocity profile of measurement

Fig. 63: Calculated time-dependency of stresses for chemically stabilized mortar with linear regressions to determine B

Table 43: Obtained data for chemically stabilized mortar

age of mixture		τ_o [Pa]	A_{thix} [Pa/s]	B [Pa/s]	G [Pa]	G [kPa]
[min]	[s]					
88	5298	208.4	0.039	1.9	1267	1.3
92	5506	414.4	0.075	116.9	77933	77.9
98	5906	520.4	0.088	126.1	84067	84.1
103	6162	441.3*	0.072	45.3	30200	30.2
109	6556	810.1	0.124	199.9	133267	133.3
116	6957	927.4	0.133	162.7	108467	108.5
120	7213	679.3*	0.094	58.6	39067	39.1
127	7605	1113.6	0.146	187.4	124933	124.9
133	8005	1315.3	0.164	373.11	248740	248.7

The yield stress τ_0, which is reached after ,,shaking" is marked by *.

The yield stress has increasing linear tendency with low decrease immediately after shaking as shown on Fig. 64. After that the increasing of yield stress is continuing, so the stresses reached immediately after shaking (and first one) are showed as crosses and had linear tendency too. In the end the yield stress reached the value approximately 8000 Pa. The rate of increase of yield stress slowly increased and reached the value 0.16 Pa/s, which correspond to the thixotropic mixture according to Roussel´s classification shown in Table 6, and is similar to the filler stabilized mixture. The tendency of development of G modulus was similar as shown on Fig. 65.

$$y = 0,3558x - 1553,8$$
$$R^2 = 0,9937$$

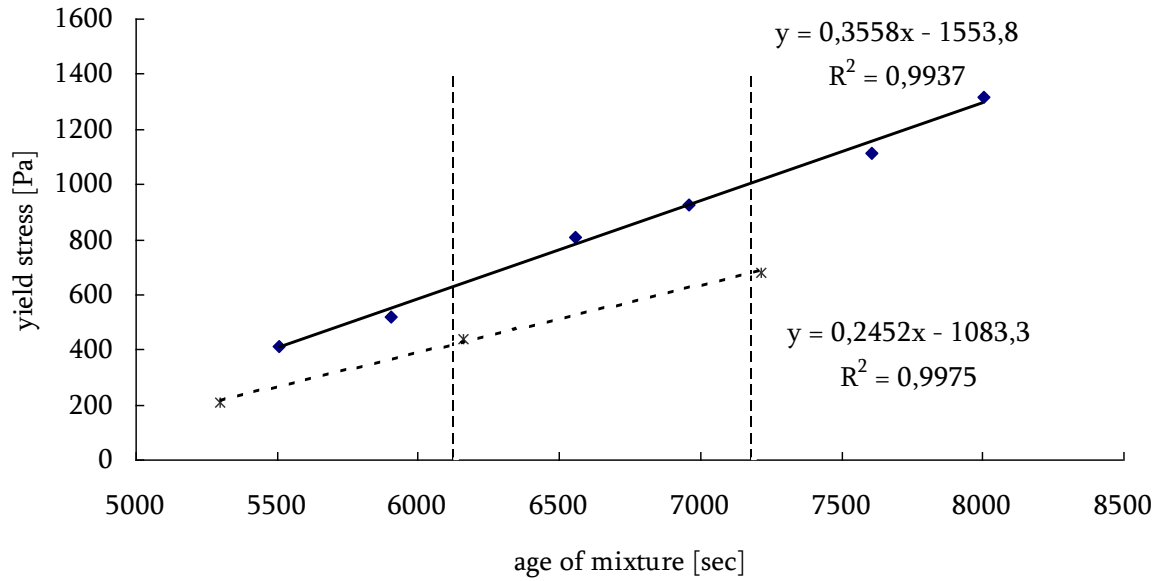$$y = 0,2452x - 1083,3$$
$$R^2 = 0,9975$$

Fig. 64: Development of yield stresses of chemically stabilized mortar (dashed lines show shaking)
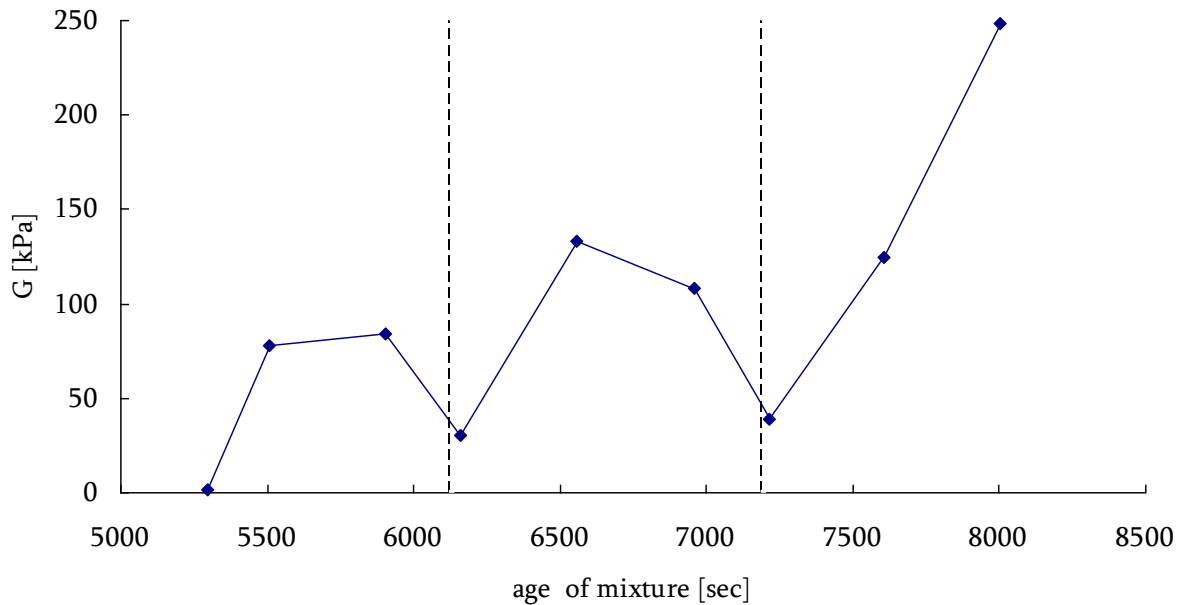
Fig. 65: Development of G modulus of chemically stabilized mortar (dashed lines show shaking)

4.2.2.3   Sieved mortar from unstable SCC mixture

The torque-time dependency of the unstable mixture is shown in Fig. 66 whereas the velocity profile of measurement is shown in Fig. 67 and the calculated time-dependency of stress in Fig. 68. The yield stress shows gradual types of peaks only at start of the measurement (first peak), then the sharp types followed. The results for the unstable mixture are summarized in Table 44 and Fig. 69 and Fig. 70.
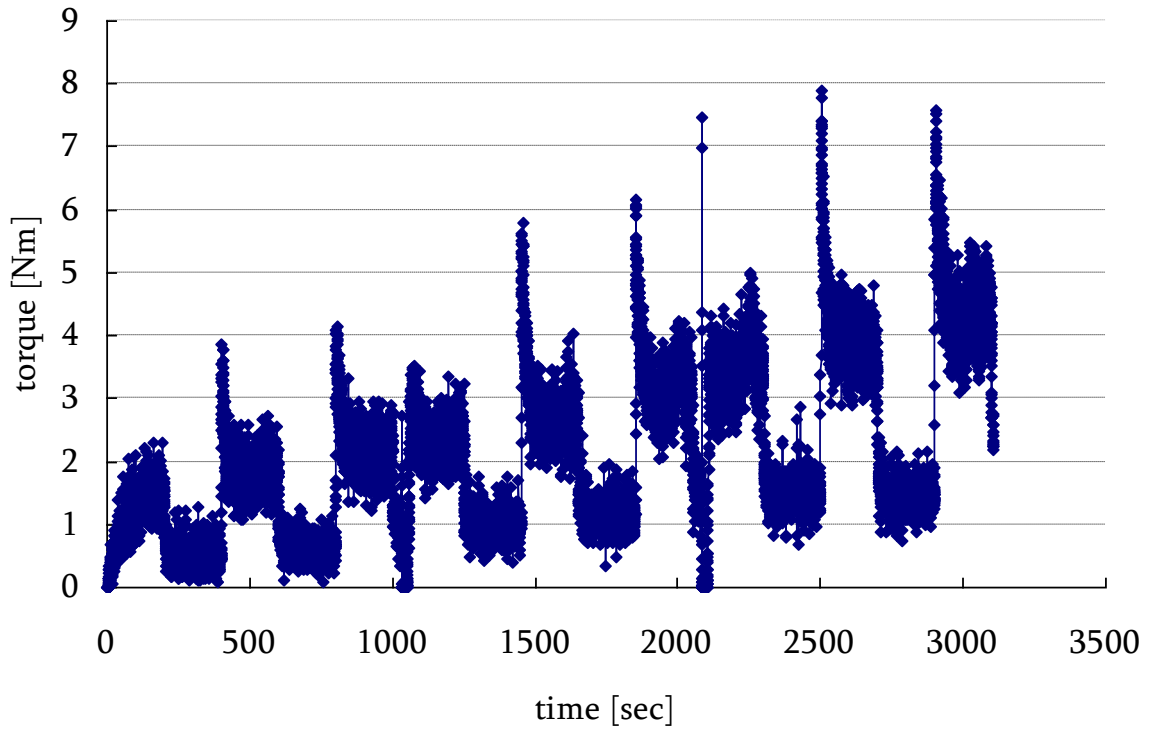
Fig. 66: Torque-time dependence of unstable mixture
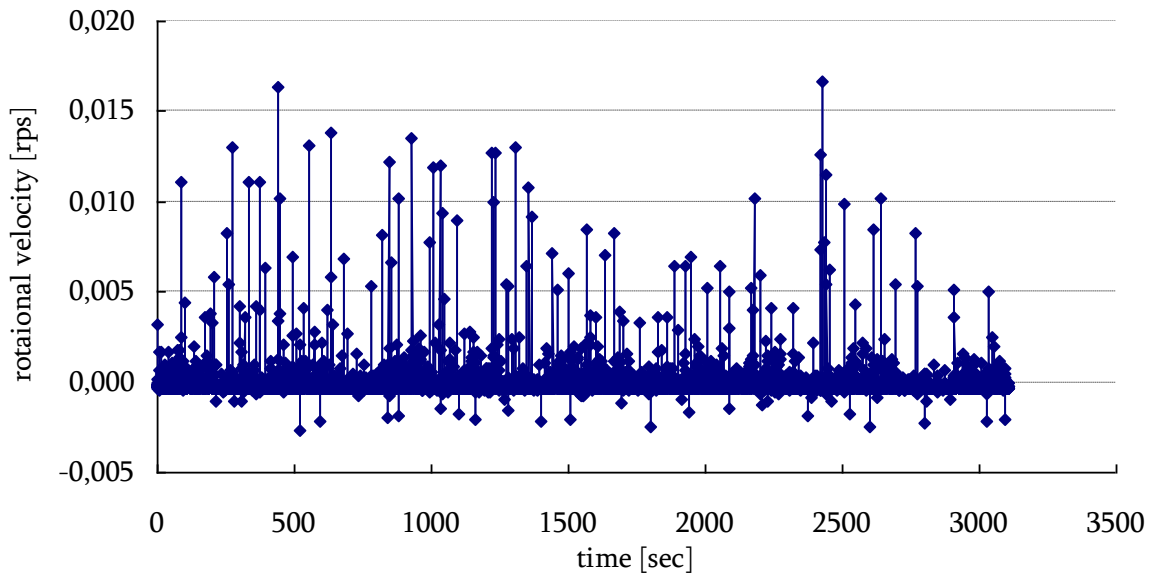
Fig. 67: Velocity profile of measurement
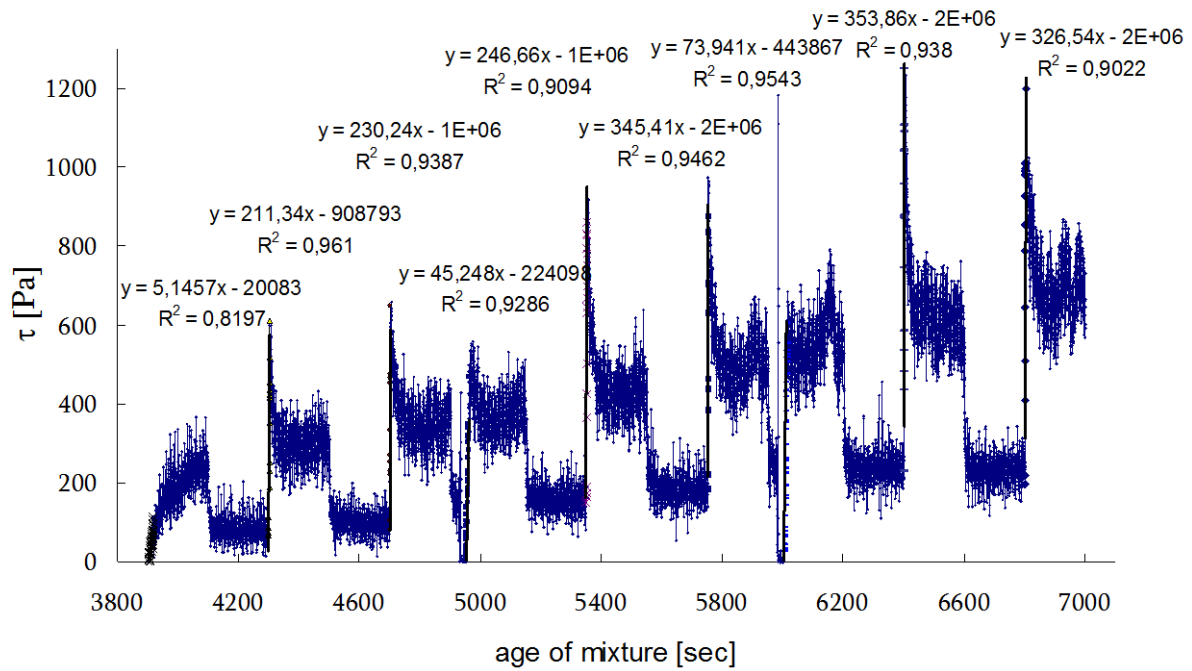
Fig. 68: Calculated time-dependency of stresses for unstable mortar with linear regressions to determine B

Table 44: Obtained data for unstable mortar

age of mixture		τ_o [Pa]	A_{thix} [Pa/s]	B [Pa/s]	G [Pa]	G [kPa]
[min]	[s]					
68	4100	264.4	0.064	5.1	3400	3.4
72	4303	612.8	0.142	211.3	140867	140.9
78	4703	649.6	0.138	230.2	153467	153.5
83	4974	558.2*	0.112	45.2	30133	30.1
89	5356	918.4	0.171	246.7	164467	164.5
96	5753	975.6	0.170	345.41	230273	230.3
100	6028	654.0*	0.108	73.9	49267	49.3
107	6403	1249.9	0.195	353.9	235933	235.9
113	6803	1199.3	0.176	326.5	217667	217.7

The yield stress τ_0, which is reached after ,,shaking'' is marked by *.

As shown in Fig. 69 the development of yield stress was similar to previous mixtures (linear and increasing) and in the end reached the value approximately 1200 Pa. The rate of increase of yield stress slowly increases and reached the value 0.18 Pa/s. This corresponds to thixotropic mixture according Roussel´s classification in Table 6, as for filler and chemically stabilized mixtures. The tendency of development of G modulus was strongly affected by shaking as shown on Fig. 70, where G moduli reached immediately after shaking were several fold lower than others. In case of unstable mixture the increase of the yield stress during aging of the mixture should be affected by segregation. As mentioned above, measurements with viscometers are not suitable for unstable mixtures, so the presented dependency should be assessed with caution.

$y = 0,2698x - 564,32$
$R^2 = 0,9509$

$y = 0,1983x - 505,99$
$R^2 = 0,8891$

Fig. 69: Development of yield stresses of unstable mortar (dashed lines show shaking)

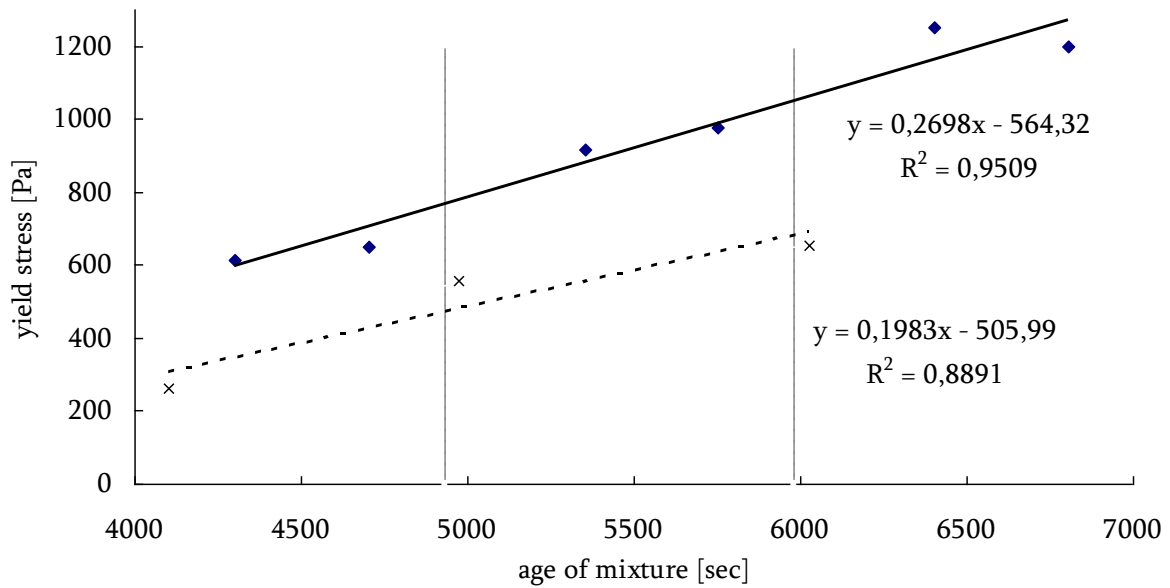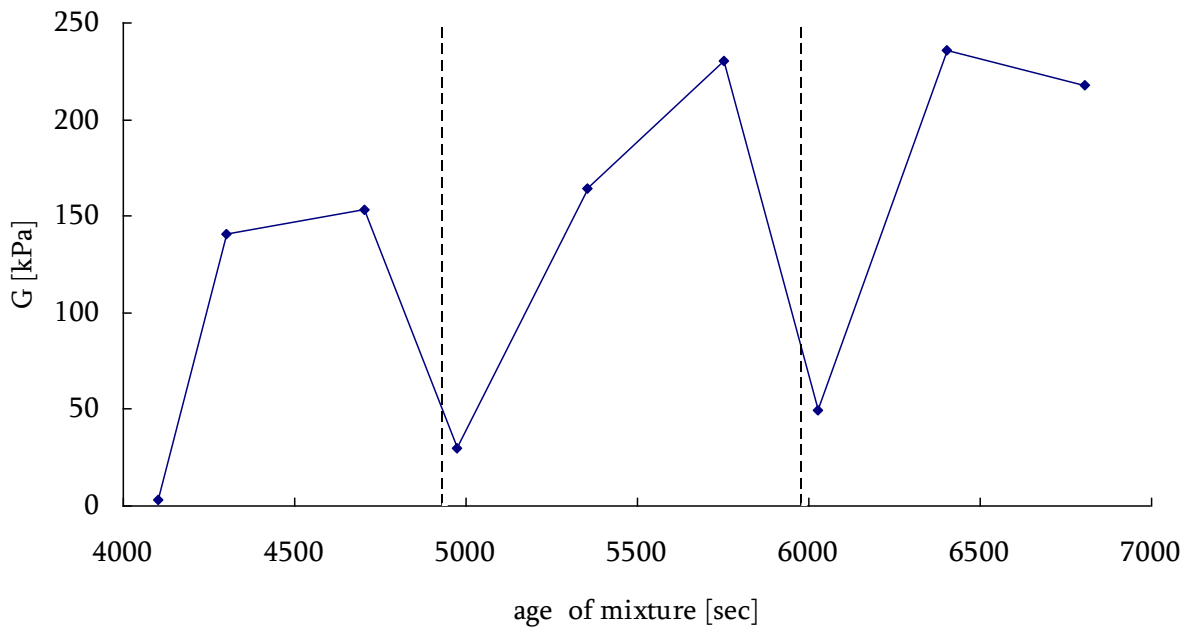Fig. 70: Development of G modulus of unstable mortar (dashed lines show shaking)

4.2.3 Conclusion yield stress of ready mixed SCC

All results for concrete and their sieved mortar are shown in Table 45. Filler stabilized and chemically stabilized mixtures had similar plastic viscosity. Concerning static yield stress value, the filler stabilized mixture had higher yield stress. In the case of the unstable mixture, visible segregation was observed and therefore rheological properties of this mixture are less valid.

Static yield stresses of concrete determined by inclined plane test were always higher than dynamic yield stress and this measurement is more suitable for mortar than for concrete, because the determination of the angle of inclination is more difficult in case of concrete. For concrete movement of coarse aggregate can occur at first (before the mixture starts to flow). So the inclined plane test is strongly dependent on the stability of the mixture. Thus visual observation when conducting the test

rather than the yield stress value itself is possibly an indication of stability. Another factor is the volume of the sample. In this test we are only using small sample volumes (dimensions of cylinder is 62 mm in diameter and 120 mm in height which gives 362 ml) and sampling is tricky and difficult to make representative due to small volume in case of SCC (the worst sampling was in case of unstable SCC). So there is some limitation for samples which are suitable for using the plane test (stability, rheological properties.…).

Testing of mortar gave surprising values of yield stress and plastic viscosity, because these values were higher than in case of unstable and chemically stabilized concrete. The static yield stresses determined in the inclined plane test correspond to the increasing values of yield stresses evaluated from torque-time dependency in the ConTec4 viscometer.

According to the structuration rate all tested mortars are thixotropic mixtures. The structuration rate in all cases increased and the maximum values were found for unstable mixture, apparently because of unstability and collection of coarse aggregate at bottom blocking the viscometer rotation. The B and G modulus was highest in case of chemically stabilized mixture.

Yield stress is higher under confined conditions compared to under non-confined conditions (Fig. 59 and Fig. 64). The rate of increase of static yield stress over time, however, is quite similar as observed from two series of tests made with more than half year in between (Fig. 17 and Fig. 54).

Shear modulus seems to be a more sensitive parameter for structural build up than yield stress and this parameter was investigated in detail for matrix using the Physica Rheometre.

Table 45: Properties of concrete and their mortar

	Unstable SCC	Filler stabilized	Chemically stabilized
Density [kg/m^3]	2427	2368	2408
Air [%]	0.3	1.4	0.7
SF [mm]	685	660	670
T500 [s]	0.66	0.58	1.44
BML			
Yield stress [Pa]	91.7	94.0	54.9
Plastic viscosity [Pa.s]	0.6	6.2	9.0
Inclined plane			
Spread [mm]	148	205	312
Angle [°]	23	26	13
Static yield stress [Pa]	428	295	101
MORTAR			
ConTec4			
Yield stress [Pa]	109.7	63.4	95.9
Plastic viscosity [Pa.s]	24.6	9.8	63.8
A$_{thix}$ [Pa/s]	0.18	0.11	0.16
B [Pa/s]	326.5	294.7	373.1
G kPa	217.7	196.5	248.7
Inclined plane			
Density [kg/m^3]	2360	2241	2356
Spread [mm]	200	228	261
Angle [°]	17	15	11
Static yield stress [Pa]	102	68	31

The A$_{thix}$, B and G are shown only for the closing part of measurement and correspond with the highest values, which were obtained

4.3   Summary of measurements

Table 46: static yield stress ($\tau_{0,s}$) and time dependent increase ($d\tau_{0,s}/dt$, or $A_{thix}= \tau_{0,s}/t$)

Test	Mix	$\tau_{0,s}$, $d\tau_{0,s}/dt$ (Pa, Pa/s)		Fig./Tab.
		$\tau_{0,s}$ at t=0, linear fit,	Individual values (age), $A_{thix}= \tau_{0,s}/t$	
ConTech	I	0 (conf), 0.41	380-703 (63-140 min), 0.06-0.15	T16, F17
	II	-	317-753 (35 – 147min), 0.07-0.27	T20,24,27
	S3 *	196 (unc), 0.82	1411-6083 (25-72 min), 0-96-2.07	F54,T39
		1870 (conf), 0.97		
	RM fi	0 (unc.), 0.18	168-873 (88-133 min), 0.02-0.1	F59, T42
		0 (conf.), 0.20		
	RM VMA	0 (unc.), 0.25	208-1315 (88-133 min), 0.04-0.16	F64, T43
		0 (conf.), 0.36		
	RM unst.	0 (unc.), 0.2	264-1250 (88-133 min), 0.06-0.2	F69, T44
		0 (conf.), 0.27		
Plate	I	0, 0.021		F35
	I	0, 0.014		F36
Inclined plane	S2		179 (18 min), 0.13	T37
	S3		318 (23 min), 0.3	
Matrix	M1			T33,T35
	M2		Variation: 0.005-0.008 Pa/s	F45
	M3			

*: very high values for unclear reason, should be discarded

5   CONCLUSIONS

The rate of increase of static yield stress of SCC and mortar varied in the range 0.014 – 0.25 Pa/s in unconfined tests lasting a bit more than 2 hours. This is a large range of variation (and then the very high results for S3 in ConTech have been excluded). In confined tests it is 0.2 – 0.41 P/s, which is better. The only values at t = 0 are by linear regression and extrapolation, often giving values less than zero indicating some kind of non-linearity at early age although the increase after app 30 minutes seems linear both for unconfined an confined tests.

The test principles in the four tests were: coaxial viscometer for mortar, static plate with continuous development, inclined plane and parallel plate for paste or matrix. The differences between the measurements, briefly, concern both the type of materials that can be used (SCC vs matrix) and the test principles and stress conditions during testing. Our materials were mortar with w/b ≈ 0.50, 40 volume % matrix and 8 mm maximum aggregate size, as well as matrix with similar composition as in the mortar.

Apparently $\tau_{0,s}$ is very sensitive to both test method and how it is calculated. The confinement conditions in the coaxial viscometer seem to give higher values than in the plate- and inclined plane tests. From the above table it is seen that the rate of change, or thixotropic structuration rate, can vary by more than a factor of 10 x for one concrete depending on how it is measured and calculated.

Based on this limited experience it is hard to give a definite answer but the confinement in the ConTech viscometer is possibly a good thing for simulation of concrete confined in a narrow tall wall. This is the geometry where static yield stress build up is of interest for formwork pressure. The

inclined plane showed some weaknesses with larger aggregate particles loosening from the surface but might relate to aggregate segregation. The plate test also has its weaknesses with small roughness on the surface and should perhaps have been exchanged for a geometry with vanes of some kind normal to the plate to get similar "grip" as the vanes of the viscometer. At present it is hard to use these experiences to recommend any of these tests. It should be mentioned that we were not able to get a sensitive vane-tool and we should like to include that in a later study. Clearly more work is needed to obtain a test. Possibly different tests are needed for yield stress for different purposes: related to formwork pressure, to casting joints and to stability of aggregate particle sinking.

Acknowledgement

Thanks to laboratory engineers at NTNU Dept of Structural Engineering Trond Auestad, Ove Loraas and Steinar Seehus for valuable asisstance with the Viscometer programming in Natinal Instruments LabView and plate test set up adapting the Balance link software, to PhD Student Rolands Cepuritis for assistance with the mix design of the Self Compacting Mortar and to Post Doc Klaartje de Weerdt for help with the Physica Rheometer experiments.**.**

References

[1]   WALLEVIK O.H. and WALLEVIK J.E.: Rheology as a tool in concrete science: The use of rheograpsh and workability boxes, *Cement and Concrete Research 41,* 2011, 1279-1288

[2]   BILLBERG P.: Form Pressure Generated by Self-Compacting Concrete – Influence of Thixotropy and Structural Behaviour at Rest; Doctoral Thesis in Concrete Structures. Stockholm, Sweden 2006

[3]   AMZIANE S.. PERROT A.. LECOMPTE T.: A novel settling and structural build-up measurement method, Measurement Science and Technology 19, 2008, 105702

[4]   SMEPLASS S.. MØRTSELL E.: The applicability of the particle matrix model to self compacting concrete (SCC), *Nordic Concrete Research* no. 26-6, 2001, 13p

[5]   KHAYAT K.H. OMRAN A.F. and PAVATE T.V.: Inclined Plane Test to Evaluate Structural Build up at Rest of Self-Consolidating Concrete, ACI Materials Journal, V. 107. No 5, 2010

[6]   *OKAMURA. H.: Self-compacting high-performance concrete,* Concrete International. *1997 vol. 19, no. 7, pp 50–54*

[7]   *KHAYAT. K.:* 'Workability. testing and performance of self-consolidating concrete'. ACI materials journal, 1999, vol. 96, no. 3, pp 346–353

[8]   *GAIMSTER R. and DIXON N.: Institute of Concrete Technology Yearbook 2002-200*

[9]   Okamura H. and Ouchi M: Self-Compacting Concrete, Journal of Advanced Concrete Technology Vol. 1, No. 1, 2003, 5-15

[10]   *The Self-Compacting Concrete European Project Group:* The European Guidelines for Self-Compacting Concrete- Specification, Production and Use; May 2005

[11]   BOUVET A., GHORBEL E. and BENNACER R.: The mini-conical slump flow test: Analysis and numerical study, *Cement and Concrete Research 40,* 2010, 1517-1523

[12]   ROUSSEL N., STEFANI C. and LEROY R.: From mini-cone test to Abrams cone test: measurement of cement-based materials yield stress using slump tests, *Cement and Concrete Research 35,* 2005, 817-822

[13]   ROUSSEL N. and COUSSOT P.: Fifty-cent rheometer" for yield stress measurements : from slump to spreading flow, *Journal of Rheology, Vol. 49*, N°3, 2005, 705-718

[14]   *CHIDIAC S.E. and MAHMOODZADEH F.: Plastic viscosity of fresh concrete – A critical review of predictions methods,* Cement and Concrete Composites 31, 2009, 535-544

[15]   FERRARIS F., BROWER L.E.: Comparison of Concrete Rheometers: International Tests at LCPC (Nantes, France) in October 2000 (NISTIR 6819), National Institute of Standard and Technology, Gaithersburg, USA, 2001

[16]   TATTERSALL G.H.. BANFILL. P.F.G.: The rheology of fresh concrete, Pitman, 1983, ISBN 0273085581, 356pp

[17]   NEWMAN J., CHOO B.S.: Advanced Concrete Technology, Concrete properties, Elsevier Ltd. 2003, 349 s., ISBN 0 7506 5104 0

[18]   ROUSSEL N.: A theoretical frame to study stability of fresh concrete, RILEM Materials and Structutes, Vol. 39, 75-83, 2006

[19]   FEYS D., Verhoeven R. and De Schutter G.: Fresh self compacting concrete, a shear thickening material, *Cement and Concrete Research 38,* 2008, 920-929

[20]   GEIKER M. R. et al.: The effect of measuring procedure on the apparent rheological properties of self-compacting concrete, *Cement and Concrete Research 32,* 2002, 1791-1795

[21]   BARNES H.A.: An Introduction to Rheology, Elsevier 1998, 199 s, ISBN 0-444-87469-0

[22]   FEYS D., VERHOEVEN R. AND DE SCHUTTER G.: Why is fresh self-compacting concrete shear thickening? *Cement and Concrete Research 39,* 2009, 510-523

[23]   BILLBERG P.: Time-dependent Growth of Static and Dynamic Yield Stress of SCC, *RILEM Materials and Structures Journal,* 2006

[24]   BARNES H.A.: Thixotropy – a rewiew, *J. Non-Newtonian Fluid Mech. 70*, 1997, 1-33

[25]   WALLEVIK J.E.: Rheological properties of cement paste: Thixotropic behavior and structural breakdown, *Cement and Concrete Research 39,* 2009, 14-29

[26]   ROUSSEL N.: A thixotropy model for fresh fluid concretes: Theory, validation and applications. *Cement and Concrete Research* 36, 2006, 1797-1806

[27]   CEPURITIS R, JACOBSEN S., de WEERDT et al.: Rheology of Matrix and SCC with Different Mineral Fillers and Admixture, COIN report.....

[28]   WALLEVIK J.E: Rheology of particle suspensions – Fresh concrete. mortar and cement paste with various types of lignosulfonates, Department of Structural Engineering. Norwegian University of Science and Technology, PhD thesis, Norway, 2003

[29]   PERROT A.. AMZIANE S.. OVARLEZ G.. ROUSSEL N.: SCC formwork pressure: Influence of steel rebars, *Cement and Concrete Research* 39, 2009, 524-528

[30]   TCHAMBA J.C.. AMZIANE S.. OVARLEZ G.. ROUSSEL N.: Lateral stress exert by fresh cement paste on formwork: Laboratory experiments, *Cement and Concrete Research* 38, 2008, 459-466

[31]   STEFFE J. F: Rheological methods in food process engineesing, Freeman Press, Secon edition, 1992, ISBN 9632036

[32]   DE WEERDT K.. EIDE M.B. and SMEPLAS S.: The effect of stabilization with either filler or chemical stabilizer on the surface quality of concrete elements

1 APPENDIX: MATERIAL DATA SHEETS

Portland cement of type CEM II/A-V from *Norcem AS*
The test report of the cement batch used for the study is presented on Figure A1.

PRØVNINGSRAPPORT

Oppdragsgiver: KOK
Prøven merket: STD FA sement fra Rescon Mapei

Prøve kode: AZ15-11   Ref: 71-11

KJEMISK ANALYSE EN 196-2			FYSIKALSK PRØVNING EN 196		
Glødetap		2.04 %	**FINHET**		
Fri kalk		1.26 %	Partikkelanalyse	+90my	0.1 %
Flyveaske		18.20 %	" "	+64my	1 %
Svovel trioksyd	(SO_3)	3.41 %	" "	-24my	77.6 %
Silika	(SiO_2)	25.57 %	" "	-30 my	85.1 %
Aluminiumoksyd	(Al_2O_3)	8.40 %	Spesifikk overflate; Blaine		503 m^2/kg
Jemoksyd	(Fe_2O_3)	4.06 %			
Kalsiumoksyd	(CaO)	52.32 %			
Magnesiumoksyd	(MgO)	2.45 %	**NORMAL KONSISTENS**		
Fosfor pentoksyd	(P2O5)	0.27 %	Vannbehov	-	%
Kaliumoksyd	(K_2O)	1.11 %			
Natriumoksyd	(Na_2O)	0.56 %	**VOLUMBESTANDIGHET**		
Alkali		1.29 %	Le Chatelier	-	mm

BINDETIDER
Størkning begynt   -   min.

TRYKKFASTHET

1 døgn	-	MPa
2 døgn	-	MPa
7 døgn	-	MPa
28 døgn	-	MPa

Norcem A.S Brevik, Sement- og betonglaboratoriet, 4. july 2011
ae.

_____
Laboratoriesjef

Fig. A1**:** Test report of the cement batch used for the study

Sand

Natural "low-filler" sand 0/8 mm from Årdal quarry (NorStone AS)
Particle density: 2650 kg/m^3
Saturated-surface-dry water absorption: 0.3 %
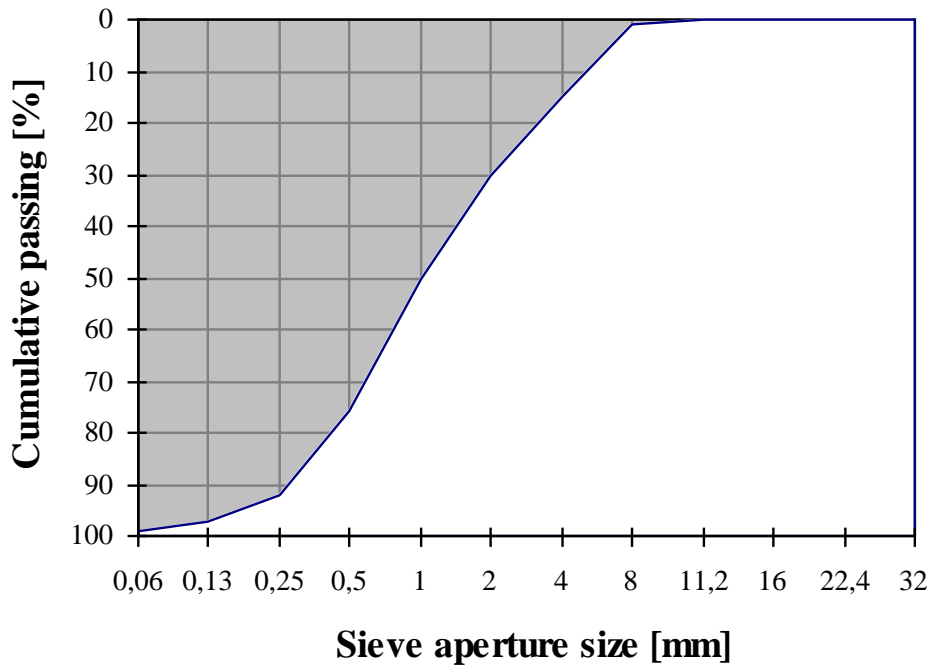Please see following figure for particle size distribution of the aggregate.

Fig. A2: particle size distribution of send

Tau

NorStone Tau
Density: 2780 kg/m^3
Saturated-surface-dry water absorption: 0.3%
rock type: quartz diorite
All particles are lower than 0.13 mm.

Superplasticizer Dynamon SR-N from Rescon Mapei AS

Dynamon SP-130 is a high performance superplasticizing admixture based on modified acrylic polymers. Please see following figure (A3) for technical specifications.

TECHNICAL SPECIFICATIONS	
Form:	Liquid
Colour:	Yellowish brown
Viscosity (Brookfield Viscometer DV-1, LV1, 100rpm at 20±2°C):	Low viscosity;<30 cP
Dry solids content, %:	19.5 ± 1.0
Density, g/cm³:	1.05 ± 0.02
pH-value:	6.5 ± 1
Chloride content,%:	< 0.01
Alkali content (equiv. Na_2O) %:	< 2.0

CHARACRERISTICS OF CONCRETE CONTAINING DYNAMON SR-N		
As water reducing admixture		
Quantity of cement kg/m³ (CEM I- 42.5R):	350	350
Admixture dosage (% by weight of cement)	0	1,1
Mass ratio (w/c ratio):	0.5	0.41
Compressive strength (N/mm²):		
1 day	26	37
7 days	43	56
28 days	52	66

CHARACTERISTICS OF CONCRETE CONTAINING DYNAMON SR-N		
As superplasticising admixture		
Quanity of cement, kg/m³ (CEM I-42.5R):	350	350
Admixture dosage (in % of cement weight):	0	1.1
Mass ratio (w/c ratio):	0.49	0.49
Air content:	2.4	1.9
Workability, mm:		
- slump, 5 min	40	200
- slump, 30 min	30	200
- slump, 60 min	20	210
- slump, 90 min	20	180
- slump flow, 5 min	200	430
- slump flow, 30 min	200	340
- slump flow, 60 min	200	330
- slump flow, 90 min	200	320

Fig.A3: Technical specifications of Dynamon SP-130 from Rescon Mapei AS